Advancing Inertial Sensors for Performance Quantification: Applications in Balance Rehabilitation and Distance Running

by

Jamie Ferris

A dissertation submitted in partial fulfillment
of the requirements for the degree of
Doctor of Philosophy
(Mechanical Engineering)
in The University of Michigan
2023

Doctoral Committee:

Professor Emeritus Noel C. Perkins, Co-Chair
Professor Kathleen H. Sienko, Co-Chair
Assistant Professor Cristine Agresta, University of Washington
Assistant Professor Xun Huan
Associate Professor Leia Stirling

Jamie Ferris

jcferris@umich.edu

ORCID iD: 0000-0002-6122-1304

Table of Contents

List of Tables

List of Figures

List of Abbreviations

Abd/Add: Abduction/adduction

AIC: Akaike information criteria

AP: Anterior-posterior

BW: Body weight

CGM: Conventional gait model

COP: Center of pressure

D/P: Dorsiflexion/plantarflexion

EA: Elliptical area

ECG: Electrocardiogram

EMG: Electromyography

ErKF: Error-state Kalman filter

ES: Early stance

F/E: Flexion/extension

FS: Feeling Scale

FSS: Flow Short Scale

ICC: Intraclass correlation coefficient

IMU: Inertial measurement unit

In/Ev: Inversion/eversion

Int/Ext: Internal/external rotation

LME: Linear mixed-effects regression

LS: Late stance

MAD: Mean absolute difference

ML: Medial-lateral

MS: Mid stance

MV: Mean sway velocity

NRMSD: Normalized root mean square difference

OPTIC: Marker-based optical motion capture

PACES: Physical Activity Enjoyment Scale

PHA: Peak head acceleration

PiG: Plug-in-gait

PL: Path length

PPA: Peak pelvic acceleration

PT: Physical therapist

PTA: Peak tibial acceleration

RMS: Room mean square

RMSD: Root mean squared difference

ROM: Range of motion

rRMSD: Relative root mean square difference

R^2: Coefficient of determination

STA: Soft tissue artifact

TS: Terminal swing

ZUPT: Zero-velocity update

Abstract

Wearable sensors in the form of inertial measurement units (IMUs) enable the unobtrusive quantification of human movement during daily life. As a result, IMUs ubiquitously appear in smart devices such as phones and watches. Substantial research has explored the use of inertial data in performance assessment and feedback systems with applications spanning from biomedical monitoring to athlete training. However, the algorithms required to generate useful insights vary between movement types and user populations. Continued work is required to fully leverage these wearable devices for their potential benefits to human health and performance. This dissertation advances the use of inertial data in two application areas, balance rehabilitation and distance running.

Part I of this dissertation advances IMU-driven feedback systems for use during remote balance rehabilitation programs. Balance rehabilitation is traditionally performed in a clinical setting with the instruction of a physical therapist. However, cost and availability limit access to balance therapy. Technologies improving balance telerehabilitation may therefore improve access to quality care. Inertial sensors can be used to support balance telerehabilitation; training effects can be monitored via automated clinical balance tests, training programs can be automatically or remotely optimized via performance assessments, and the efficacy of training can be improved via feedback.

Two studies herein advance the use of IMUs to support remote balance rehabilitation. In the first study, the effects of IMU-driven terminal (i.e., post-task) visual feedback on sway

magnitude and velocity were found to be comparable to those of established concurrent (i.e., real-time) feedback methods during a single session of training. Because IMU-based terminal feedback is possible via a single smartphone, it may further support simple, affordable, and accessible balance training devices. In the second study, self-assessments and IMU-driven kinematic measurements were significantly but imperfectly correlated with expert physical therapist intensity assessments. They may therefore be useful during telerehabilitation when expert visual assessment is difficult. Together, these studies on balance rehabilitation suggest that IMU-based systems may support high-quality home-based care.

Part II of this dissertation advances the use of IMUs for "real-world" distance running assessment. While analyses of running gait have traditionally been performed in a laboratory, running biomechanics, physiology, and psychology all differ between laboratory and "real-world" settings. IMU-based assessments of "real-world" distance running may therefore capture "real-world" performance determinants, injury etiology, and training or intervention effects. Additionally, IMU-based systems may be less expensive and more accessible than traditional laboratory-based systems. However, additional research is required to expand the set of metrics available via IMUs and to establish relationships between inertial data and important aspects of running performance.

Two studies in the dissertation advance the use of IMUs to assess "real-world" distance running. In the first study, an error-state Kalman filter (ErKF) algorithm for the estimation of three-dimensional lower-body running kinematics resulted in joint angle estimates of comparable accuracies to existing methods. ErKF algorithms may also support adaptation to experimental design (e.g., speed, running surface) and should therefore be further advanced for kinematic estimation during "real-world" running. In the second study, numerous biomechanical measures

including peak acceleration attenuation and stability were associated with positive running experiences during long, outdoor training runs. These relationships should be additionally explored as means of supporting positive running experiences. Together, these studies on distance running demonstrate that wearable sensors can provide meaningful measures of performance during "real-world" running.

Chapter 1 Introduction and Background

Wearable sensors offer the opportunity to unobtrusively quantify biophysical signals during daily life. While many wearable sensors have been developed in recent years, inertial sensors are one of the most widely used. Inertial sensors capture movement of a rigid body by measuring its acceleration and angular rate at a single point. Collectively, we refer to these measurands as inertial sensor data. With recent advancements in microelectromechanical systems (MEMS) fabrication methods, inertial sensors in the form of inertial measurement units (IMUs) have become small, lightweight, and relatively affordable, leading to their ubiquitous use. IMUs are now commonly found in automobiles, satellites, smart phones, smart watches, and more where they are used to support everything from autonomous control to human machine interaction and human movement quantification.

Substantial research has explored the benefits of quantifying human movement via IMUs, with frequent focus on accessibility and/or use in "real-world" settings. Consequently, advancements have been made in a variety of application areas including worker training and safety [1,2], biomedical monitoring and rehabilitation [3–5], physical task training and execution (e.g., astronauts [6,7] and emergency responders [7]), and athlete training [8–10]. Within each of these application areas, inertial data has been used to support both data-driven assessments and wearable feedback systems with common goals including fatigue and workload monitoring [11–18], injury prevention [8,18–24], and performance optimization [4,24–27]. For example, a

wearable system developed by Seshadri et al. monitors internal and external athlete workload and provides coaches and athletes with actionable insights into training load [28].

While many applications have been explored and numerous benefits have been documented, both the algorithms required to generate useful insights and the feedback systems needed to affect change vary between tasks, populations, use contexts, and more. As a result, continued work is required in order to more fully leverage wearable inertial sensors for their potential benefits to human health and performance.

1.1 Objectives in performance quantification

Across various activities, inertial sensors can be used to support performance quantification through three primary objectives: the calculation of accurate and interpretable performance metrics, the association of sensor data with immediate and longitudinal outcomes, and the delivery of information back to the user via feedback (see Figure 1.1).

Figure 1.1: The primary objectives in quantifying human performance via inertial sensors, and their applications to balance rehabilitation and distance running. Left image downloaded from https://swordhealth.com/solutions/digital-therapy in August 2023.

1.1.1 Calculation of accurate and interpretable metrics

Time series IMU data are often summarized by calculating task-specific and meaningful metrics. These metrics can be as simple as the signal maximum or as complicated as the Lyapunov exponent, and they may span both the time and frequency domains [29–32]. Often, a suite of complementary metrics is used to examine various interrelated movements or aspects of a task. For example, in the study of standing balance, both sway magnitude and sway speed can assist in understanding the postural control activity [29,33–35]. These metrics can then be used to identify differences between time points, conditions, or groups and to assess training or intervention effects. During research where metrics are interpreted by highly trained staff, the metrics may be chosen primarily to optimize insight into the movement pattern. However, metrics may also be used by various groups including practitioners, patients, coaches, and athletes. In these cases, familiar and easily interpretable metrics should be chosen when possible [36]. Common metrics for standing balance and distance running are further discussed in sections 1.4.1.3 and 1.5.1.2.

1.1.2 Association of metrics with immediate and longitudinal outcomes

IMU-based metrics can also be related to various performance (e.g., race times), injury, and perceptual outcomes of interest. These relationships may illuminate performance determinants [31,37] and injury risk and etiology [32,38,39]. They may therefore support deeper and more meaningful interpretation of intervention effects. For example, knowledge of the relationship between peak tibial acceleration and stress fracture risk would enable evaluations of the effects of gait retraining not only on peak tibial acceleration but also on stress fracture risk, a meaning outcome for runners.

1.1.3 Delivery of information via feedback

IMU data can further be used to support feedback systems that effect longitudinal improvement by providing relevant and interpretable information back to the user. Feedback can be divided into two primary types: knowledge of results and knowledge of performance. Knowledge of results systems provide information about movement outcomes such as walking speed, race time, or throwing accuracy, while knowledge of performance systems provide information about movement parameters such as joint angles, impact forces, or stride regularity [40,41]. Both can be effective in supporting motor learning, although effects vary by task, skill level, age, height, physical readiness, psychological state, etc. [42]. Feedback systems should therefore be designed and assessed within specific user populations and contexts.

As such, feedback can take a variety of forms, including monitors [25,43], alerts and warnings [44–46], and augmented feedback systems [1,4,24,26]. For example, daily workload and performance metrics may be available upon request so that an athlete or coach can assess changes in training or fitness level over time and subsequently adjust training. Alternatively, the coach could be alerted every time an athlete's fatigue level or daily workload surpassed a threshold so that they may terminate or modify training. The athlete could also be provided augmented feedback pertaining to their performance (e.g., speed) or mechanics (e.g., stride length) so that they may adjust their behavior from moment to moment in order to accelerate performance improvement.

1.1.4 Augmented feedback systems

While all feedback systems require that the feedback be carefully designed in order to affect change, the effects of augmented feedback on performance and motor (re-)learning are particularly sensitive and depend on a number of design decisions [1,3,47–49].

Augmented feedback supplements intrinsic feedback arising from one's own sensory systems with externally provided feedback (see Figure 1.2). Augmented feedback may be provided via a number of modalities including visual, auditory, haptic, or multimodal sensory augmentation [47]. In addition to influencing the required equipment (e.g., tactors, screens), the modality may influence the types of information that can be easily and intuitively conveyed. For example, visual feedback can easily encode both spatial and temporal information [50]. Practical considerations related to the task (e.g., balance exercises requiring the eyes to be closed), user (e.g., people with impaired hearing or vision), and context (e.g., use while moving throughout a building or along a trail) may also limit which modalities are available for use.

Feedback efficacy is also reliant on timing and frequency [1,3,47–49]. Feedback can be provided throughout the task (i.e., real-time or concurrent feedback) or at its conclusion (i.e., terminal feedback). Feedback can also be provided after every repetition, on a set schedule, or at the user's discretion. Because the optimal timing and frequency of feedback varies depending on the task complexity and user[47], assorted options should be evaluated for any given use case.
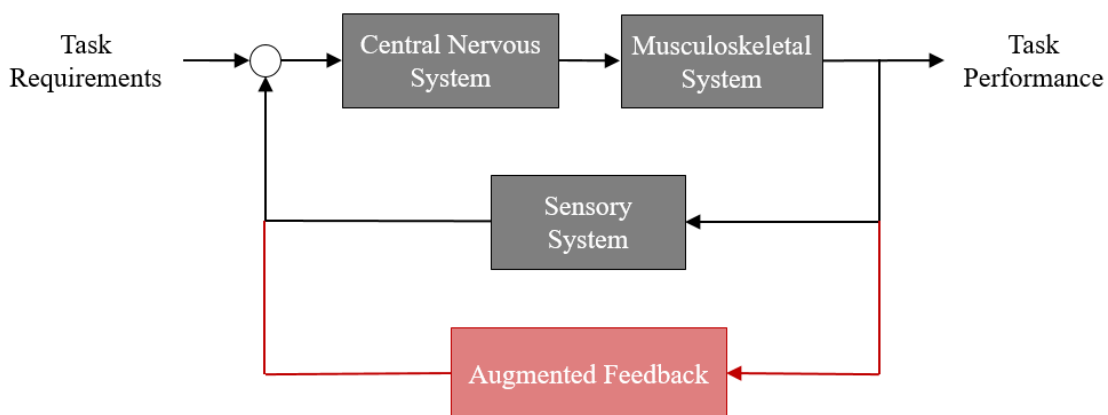
Figure 1.2: Augmented feedback introduces an additional feedback loop to the human control system.

1.1.5 Applications in balance rehabilitation and distance running

In this dissertation, four studies examine IMU-driven assessment and feedback systems with applications in balance rehabilitation and distance running (see Figure 1.3). Because prior work has established IMU-based metrics for standing balance quantification, the studies of standing balance advance the association of metrics with outcomes and the delivery of feedback during balance rehabilitation. In contrast, running is a complex motion with only a relatively small number of established and reliable IMU-based metrics. As a result, the studies of distance running contribute to the calculation of interpretable metrics and their association with outcomes of interest.
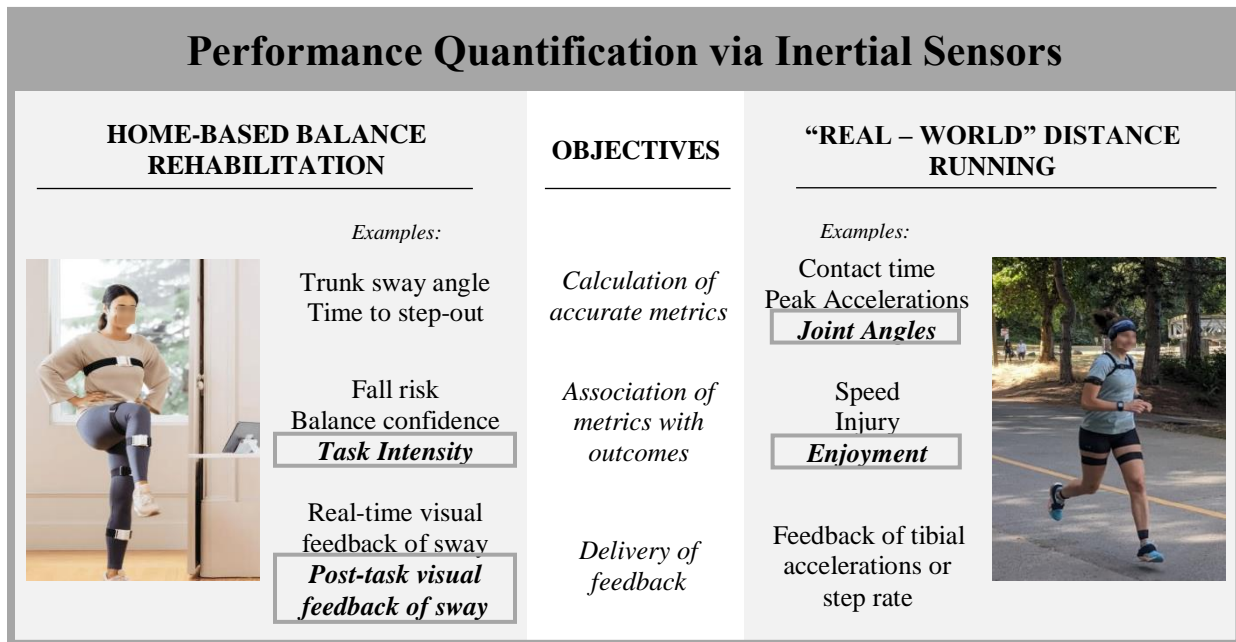
Figure 1.3: The four studies in this dissertation span the primary objectives in the study of human performance via inertial sensors, with applications in balance rehabilitation and distance running. Left image downloaded from https://swordhealth.com/solutions/digital-therapy in August 2023.

All four studies rely on using inertial sensors to quantify human movement and then statistical analyses to assess key measures and relationships. We highlight below some common methods and challenges in deploying inertial sensors and statistical analyses in the study of human movement. We then provide additional background specific to balance rehabilitation and distance running, and we overview each study (i.e., the subsequent chapters of this dissertation).

1.2 Common methods when using inertial sensors for human movement quantification

IMUs combine triaxial accelerometers, gyroscopes and, in some cases, magnetometers or GPS units. An IMU attached to a rigid body therefore measures, at minimum, the angular velocity of the body and the specific acceleration at the location of the accelerometer. With the right algorithms, these measurands can also predict the orientation and position of the body. As a result, IMUs have been used to measure many aspects of human movement and performance including body sway during balance [4,51–53], step rate during running [31,32,54], movement of various sporting equipment such as balls and bats [55–59], and fall occurrences during daily life [46,60–62]. IMUs can also be small and lightweight, helping to limit their impact on human movement and perception. As a result, IMUs are extremely useful for human movement quantification.

The use of inertial data requires signal processing that differs substantially from that of traditional (i.e., marker-based) motion capture data. The primary differences result from (1) differing reference frames, and (2) differing measurands.

While traditional motion capture data are recorded in the global, lab-fixed reference frame, IMU data are recorded in the sensor-fixed reference frame (see Figure 1.4). As long as the sensor is securely attached to the body segment, the relationship between the IMU sense frame and the segment anatomical frame is approximately constant. The rigid transformation can be

7

estimated using a variety of sensor-to-segment alignment methods including assumed alignment, functional alignment, and augmented data methods [63]. During assumed alignment, sensors are carefully attached such that the sensor axes approximately align with anatomical axes. In contrast, functional alignment methods use sensor measurements during prescribed movements to identify anatomical axes in the IMU sense frame. For example, the gravitational acceleration vector during static standing is often assumed to approximately align with the anatomical long axis. Finally, augmented data methods avoid such assumptions but require the use of additional sensors. Optical motion capture, for example, can be used to determine the orientation of both the anatomical and IMU sense frames and the transformation between them.
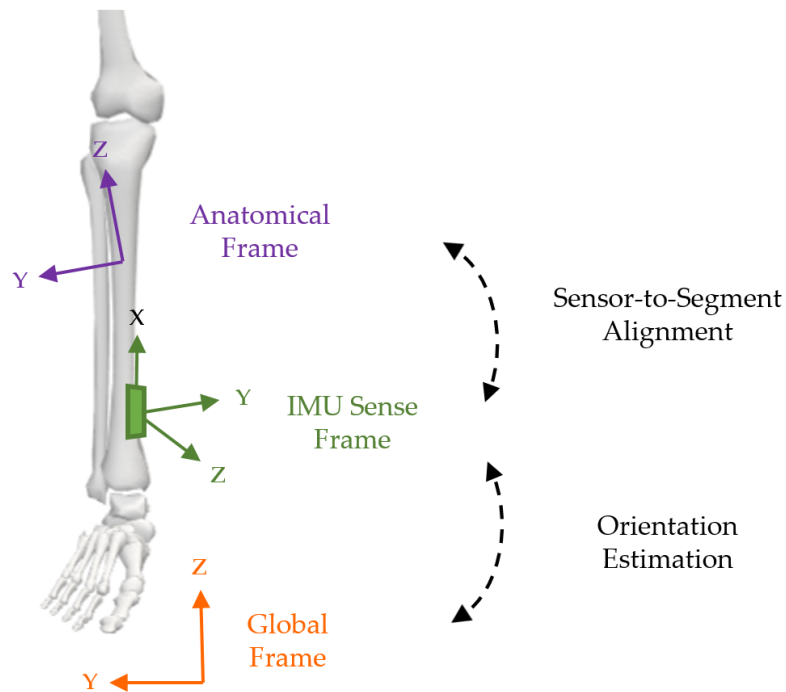
Figure 1.4: Reference frames of concern in the use of IMUs.

The transformation between the IMU sense and global frames is not constant and instead defines the orientation of the IMU. When estimating position information (i.e., orientation and

8

position) from IMU data, drift and other errors arising from several sources including measurement noise, soft tissue artifacts, sensor-to-segment misalignment, and finite sampling rates can accumulate, resulting in increasingly poor estimates over time. For example, drift errors due to fixed biases compound linearly when the gyroscope signal is integrated once to obtain angular position (i.e., orientation) and quadratically when the accelerometer signal is integrated twice to obtain linear position. Sensor fusion algorithms such as complementary or extended Kalman filters can be used to combat the accumulation of such errors.

Sensor fusion algorithms often leverage task-specific information to correct for drift in orientation and position estimates. The most common of these correction methods are gravitational and zero-velocity update (ZUPT) methods. In the gravitational method, the orientation estimate during periods of low dynamics (i.e., acceleration magnitude close to gravity, angular rate close to zero, and angular acceleration close to zero) is adjusted so that the acceleration vector is aligned with the gravitational vector (i.e., global vertical) [64]. In the ZUPT method, the foot is assumed to have zero velocity during each stance phase of gait. The foot's estimated linear velocity is adjusted to be zero during these times [65]. Additional correction methods may assume limited ranges of motion, level ground conditions, and constraints between connected body segments.

While IMUs measure acceleration and angular rate in the sensor-fixed reference frame, specialized signal processing methods including sensor-to-segment alignment and algorithms for position-domain information are used throughout this dissertation to generate interpretable kinematic measures.

1.3 Common statistical methods for the analysis of human subjects data

When studying human movement as in this dissertation, it is often beneficial to analyze repeated measurements for study participants. Recording multiple repetitions can reduce the effects of inter-trial or inter-session variability and increase the power of subsequent analyses. In addition, recording multiple samples over time allows for evaluations of duration, adaptation, habituation, or learning. However, many statistical tools (e.g., paired t-tests) cannot be used in repeated measures designs due to assumptions of independence between each measurement. Fortunately, methods such as linear mixed effects models (LMEs) exist for this purpose.

The LMEs subsequently used in this dissertation are an extension of linear regression models that accommodate both fixed and random effects and as a result do not require strict independence [66]. Fixed effects do not vary and as such are the same for every participant, while random effects differ between individuals or groups. LMEs can therefore assess group effects while accommodating individual differences. For example, an LME can evaluate the average rate of improvement due to strength training while accommodating differing baseline fitness levels. It can also quantify variation in the improvement rate (see Figure 1.5).
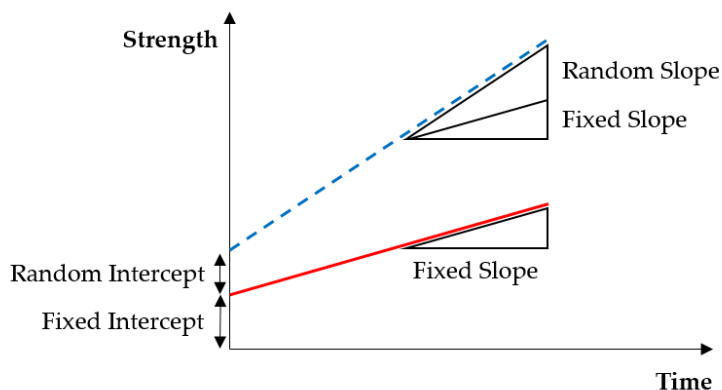
Figure 1.5: An example linear mixed effects model of strength changes over time where the red solid line represents the average strength trajectory and the blue dashed line represents an individual's response.

An LME can be expressed in standard form as

$$y = X\beta + Zb + \varepsilon$$

where y is the response vector, X is the fixed-effects design matrix, β is the fixed-effects vector, Z is the random-effects design matrix, b is the random-effects vector, and ε is the observation error vector. The random-effects (b) and observation error (ε) vectors are each assumed to be normally distributed with mean zero, and they are assumed to be independent of one another. In addition to determining the resulting coefficients, the fitted model can also be used to calculate various summary measures such as correlation coefficients. LMEs will be used throughout this dissertation to quantify training effects, assess inter- and intra-rater reliability, and calculate correlation.

Next, we provide an additional task-specific background and study overviews for each application area explored in this dissertation, starting with balance rehabilitation.

1.4 An overview of Part I: Advancing inertial sensors for use during home-based balance rehabilitation

1.4.1 Context, motivation, and potential impact

Part I consists of two studies forming Chapters 2 and 3 that advance IMU-driven assessment feedback systems for use during remote balance rehabilitation programs. Below we highlight the context, motivation and potential impact of these two studies.

1.4.1.1 Balance impairments and their treatment

When studying standing balance, it is necessary to understand the sensory, neurologic, and muscular systems that contribute to the complex task of balance as well as the disorders that impact these systems and consequently balance control.

Standing balance requires stabilization of the body's center of mass (COM) despite humans being inherently unstable systems when standing upright [67]. In order to do so, the visual, somatosensory, and vestibular sensory systems provide myriad information about the body's movement in space. The visual system consists of light receptors in the retina of the eye which respond to visual stimuli. The somatosensory system consists of afferent neurons in the muscles, joints, skin, and fascia which respond to position, effort, movement, touch, and temperature, which results in proprioception and kinesthesia. Finally, the vestibular system consists of otolith organs and semicircular canals in the inner ear which respond to linear and angular accelerations of the head. These signals are integrated and interpreted in the limbic system and frontal cortex, resulting in a complex muscular response aimed at maintaining balance [68].

Because many systems are involved in balance control, balance impairments are common and result from a number of causes. During aging, sensory acuity, cognitive ability, and musculoskeletal function decline, resulting in compensatory mechanisms and reduced postural stability [68,69]. Various sensory or neurologic disorders also impair balance including peripheral sensory loss [70,71], vestibular disorder [71–73], multiple sclerosis [74–76], cerebrovascular accident [77], traumatic brain injury [78,79], and Parkinson's disease [80,81]. Many of these disorders are most prevalent in aging populations [68], further compounding the effects of age on balance control.

Balance impairments are traditionally assessed and treated by trained physical therapists through a series of in-person visits. Balance ability is typically assessed using standardized clinical balance tests (e.g., the Berg Balance Scale) that include various static and dynamic balance tasks. Alternatively, balance ability may be assessed using quantitative posturography in

which sway is quantified via force or inertial sensors. The physical therapist will then use their

expertise to design a customized balance training program that includes a variety of balance

exercises at the appropriate difficulty. Patients are asked to perform these exercises regularly in

between visits and may be given a tool for logging their sessions. As the patient progresses, the

physical therapist will assign new exercises in order to optimize progress. Periodically, the

patient's balance ability will be re-assessed in order to quantify any changes. When their balance

has been restored or, as is more often the case, when they no longer have access to physical

therapy (e.g., insurance will not cover more visits), patients are often instructed to continue a set

of exercises at home for the foreseeable future.

1.4.1.2 Opportunities for inertial sensors in balance rehabilitation

While balance rehabilitation performed in a clinical setting with the instruction of a

physical therapist has been shown to improve balance performance [4,82,83], the cost and

availability of balance therapy [84,85] limits access to balance training. It is predicted that by

2030, the United States alone will have a shortage of 140,000 physical therapists, resulting in the

majority of patients having difficulty accessing necessary physical therapy services [84]. Balance

training technologies designed to be used outside of clinical settings may increase access to

preventative and therapeutic care. However, balance training without a physical therapist's

supervision has been shown to be less effective than supervised training [86,87]. This

shortcoming may be due to challenges in remotely monitoring training dosage as well as a lack

of performance feedback (which would usually be provided by physical therapists). These

factors may be addressed by the use of wearable sensors during balance training. As a result,

inertial sensors have been used in both automated balance assessment and balance performance

feedback.

Over the past 30 years, sensor-based feedback systems have been used as both real-time balance aids and as tools to augment balance training programs [3]. Feedback systems can effectively improve real-time standing balance [88–96], and some studies have shown additional benefits of training with feedback compared to training without feedback [4,97–99]. Visual [97,98], haptic [100–103], and multimodal [104,105] feedback have all been studied; however, there have not been any large-scale randomized controlled trials reported to date and the impact of the improvements on fall rates have not been assessed [99]. Further, many of these training systems require specialized equipment (e.g., vibrating actuators), which may limit access for prospective users. Chapter 2 examines an alternative feedback method (terminal visual feedback) which may require only ubiquitous technology (e.g., a smart phone).

Wearable systems for balance assessment have historically received less attention. Prior work has centered upon the automating the evaluation of clinical balance tests such as the Tinetti Test [106,107], Berg Balance Scale [108,109], Mini Balance Evaluation Systems Test [109], and Timed Up & Go Test [108,110]. These tests provide high-level insights into balance ability, and automated evaluation is useful for longitudinal monitoring. This high-level information may guide approximate exercise difficulty when assigning training exercises. However, they stop short of determining specific exercise assignment as they do not assess the intensity of any specific balance task. Recent studies have examined balance task intensity, showing that trunk sway is correlated with self-assessments of intensity [111,112], suggesting that wearable sensor data may useful in modulating training dosage; however, the relationship between trunk sway and the current standard of care (PT expert assessment) is poorly understood. Chapter 3 investigates this relationship, informing the use of inertial sensors and self-assessments for intensity assessment and consequently dosage regulation during home-based balance training.

1.4.1.3 Measuring standing balance performance

As done in Chapters 2 and 3, quiet standing balance can be modeled as an inverted pendulum where bending can occur at both the ankle and hip. However, during only moderately challenging balance tasks where ankle strategies are sufficient, hip movement is minimal. The pendulum model can therefore be simplified to allow rotation only at the ankle [113]. The sway of this pendulum can be measured using either wearable or non-wearable sensors. Non-wearable sensors include optical motion capture and force plates, which are usually found only in laboratory and specialized clinical settings. Optical motion capture can be used to record the location of reflective markers that are placed on bony landmarks and consequently the location of key body segments (e.g., torso, feet). Force plates can record the center of pressure (COP), reflecting the cumulative effects of all body movements. Alternatively, wearable IMUs placed on the lumbar spine can record movement of the center of mass (COM).

Sway measurements are often summarized by first decomposing the sway into anterior-posterior (AP; i.e., sagittal plane) and medial-lateral (ML; i.e., frontal plane) components (see Figure 1.6) and then calculating a variety of time-, velocity-, and frequency-domain measures including root mean square sway angle (RMS sway), path length (PL), elliptical fit area (EA), and mean angular velocity (MV) [29,91,108,114–117]. These measures differ between populations, are associated with fall risk, and are correlated with clinical balance test scores. For example, the RMS sway in older adults standing on a foam surface is significantly correlated with fall risk and clinical test scores [108]. Similarly, MV differs between young and elderly adults during both eyes-open and eyes-closed balance tasks [29]. By evaluating a complementary collection of metrics, the key aspects of standing balance performance can be assessed.
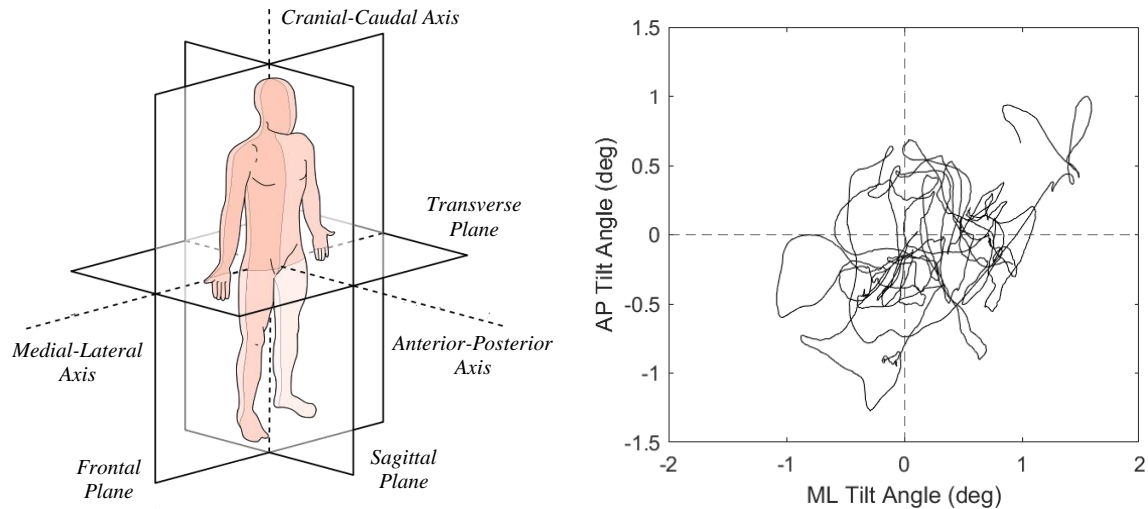
Figure 1.6: Body sway is often decomposed into medial-lateral (ML) and anterior-posterior (AP) components such that sway angles can be depicted on a 2-dimensional stabilogram. Left image downloaded from https://commons.wikimedia.org/wiki/File:Anatomical_Planes-en.svg in August 2023 and modified to include different text.

1.4.2 Overviews of Chapters 2 and 3

Part I includes two studies that further the use of wearable sensors during balance rehabilitation. The first, constituting Chapter 2, is a comparison of the effects of concurrent (i.e., real-time) and terminal (i.e., post-exercise) visual feedback on standing balance in older adults. This study was motivated by a desire to reduce the technology (and cost) required to support remote balance training using sensor feedback. While concurrent visual feedback has been shown to yield benefits compared to training without feedback [97,118], it also requires an appropriately placed screen and technology capable of processing and displaying kinematic data in real-time. In contrast, terminal feedback can be achieved with only a single smartphone, secured to the torso during the balance exercise and viewed between exercises. By comparing terminal visual feedback to concurrent visual feedback, we aimed to assess whether terminal feedback is a viable alternative to concurrent visual feedback. The findings of this study suggest that terminal visual feedback should be further investigated for use in simple, affordable, and accessible balance training devices.

The second study, constituting Chapter 3, is an analysis of the differences between various balance task intensity assessment methods. This study aimed to lay the foundation for improved remote balance exercise assignment, a process which requires accurate evaluation and adjustment of training dosage. Because dosage depends on training frequency, task intensity, training duration, and exercise type, accurate assessments of intensity are necessary. However, traditional intensity assessment methods are only partially complete (as is the case with exercise timing [119]), require the presence of a physical therapist (as is the case with expert visual assessment [120,121]), or require specialized equipment (as is the case with computerized dynamic posturography [100,111,122–125]). As a result, self-assessments and sensor-based sway kinematics have been proposed as alternative forms of balance intensity evaluation. We aimed to compare these alternative methods to traditional physical therapist expert assessment. The findings suggest that self-assessments and kinematic measurements may support PT intensity assessments during contexts in which visual assessment is difficult (e.g., during telerehabilitation).

1.5 An overview of Part II: Advancing inertial sensors for use during real-world running

1.5.1 Context, motivation, and potential impact

Part II consists of two studies forming Chapters 4 and 5 that advance the use of wearable sensors for assessment and monitoring of "real-world" distance running. Below we highlight the context, motivation and potential impact of these two studies.

1.5.1.1 Opportunities for wearable sensors in the assessment of running gait

Prior to the development of various wearable sensors, assessments of running gait were necessarily conducted in a laboratory where 'gold-standard' biomechanical and physiological

17

equipment such as optical motion capture systems, embedded force plates, and high-quality respirometers are available [38,126]. However, these methods are relatively expensive, require time-consuming setup, need highly trained staff to operate, and can be obtrusive [127,128]. As a result, studies of running performance have been restricted to well-funded academic and industrial research groups, and running gait assessments have been available only to elite or financially well-off athletes. Perhaps as a result, the majority of research have focused on optimizing performance (e.g., race times) or minimizing injury risk [129–131].

These methods have been used to build the foundation of our understanding of running gait; however, they also severely limit the running environments that can be studied. Running in a laboratory is usually restricted to treadmill or short overground runs, usually indoors, by oneself, and with the observation of a researcher. However, both running biomechanics (e.g., contact time, peak propulsive force) and physiology (e.g., blood lactate concentration, heart rate) differ between treadmill and overground running [132,133]. Surface and surface regularity as well as real-world race environments may also affect running biomechanics [134–137]. Similarly, various perceptual and psychological responses differ between indoor and outdoor exercise including differences in perceived exertion, anxiety, affect (i.e., emotion, mood), and attentional focus [138–144]. Finally, continuous observation may influence perceived exertion, hormone levels, and anxiety [145].

The ability to study running outside of laboratory settings using wearable sensors presents a valuable opportunity to examine various "real-world" running contexts. As wearable sensors are already widely accessible and are used regularly by over 75% of runners [146], they may also make gait assessment, longitudinal monitoring, and gait modification (i.e., retraining) accessible to athletes without regular access to highly specialized laboratories. However, limited

research has been conducted in real-world running contexts [31,146,147]. Additional research is needed to expand the set of metrics readily available via wearable sensors and to further identify robust relationships between wearable sensor data and important aspects of running performance.

1.5.1.2 Quantifying running performance

Analyses of running gait require that time series biomechanical data are first segmented into strides and then further decomposed into the key gait phases (see Figure 1.7). The stance phase of running is approximately 40% of the gait cycle, beginning when the foot first comes into contact with the ground (i.e., initial contact) and lasting through toe-off. The first part of the stance phase is characterized by braking and shock absorption, while the second part is responsible for propulsion of the body forward and into flight. The flight phase then lasts the remaining 60% of the gait cycle and includes a short float phase (~ 15% of the gait cycle), a moderate swing phase (~ 30% of the gait cycle), and finally another short float phase (~ 15% of the gait cycle), ending with ground contact [148]. Many metrics can then be calculated including contact time (i.e., duration of the stance phase), flight time, stride length, ankle range of motion, and more.
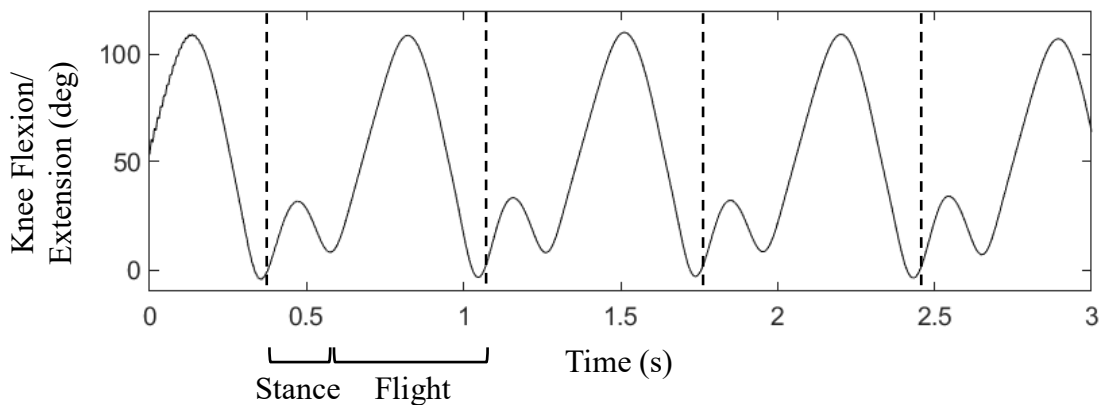
Figure 1.7: Running gait is often decomposed into stance and flight phases.

1.5.2 Overview of Chapters 4 and 5

Part II of this dissertation includes two studies that advance the assessment of "real-world" distance running through the use of wearable sensors. The first study, constituting Chapter 4, extends and evaluates an algorithm for lower-body kinematic estimation originally developed for walking to running. While various temporal and acceleration-based measures (e.g., stride time, peak tibial acceleration) are available during "real-world" running via IMUs, few algorithms exist for the estimation of position-domain measures (e.g., joint angles, stride width) from inertial data. Many of the existing algorithms produce only sagittal plane joint angle estimates, preventing the assessment of important frontal and transverse plane motions such as ankle inversion or hip adduction. In addition, the most accurate existing algorithms employ machine learning methods. However, filter-based algorithms such as Kalman filters, which have shown success in walking gait [64,149,150], may yield estimates of similar or potentially greater accuracy. If accurate, such algorithms are advantageous as they generally require smaller datasets for development relative to current machine learning algorithms [151] and can allow for intentional adaptation between experiments with varying sensor noise characteristics or placement, running surfaces and inclines, etc. This study extended and evaluated an error-state Kalman filter (ErKF) algorithm originally developed for walking for the estimation of 3-dimensional lower-body joint angles, stride length, and step width during distance running. The findings suggest that ErKF algorithms may yield 3D lower-body kinematic estimates during running which are comparable in accuracy to existing optical motion capture and machine learning-based inertial motion capture methods while offering the additional benefits outlined above such as easy adaptation to experimental design (e.g., speed, running surface, etc.).

The second study explored the associations between positive experience and running biomechanics during "real-world" training runs. Running performance (i.e., speed) is influenced by both physical factors (i.e., physiology and biomechanics) [152,153] and runner psychology [154], suggesting that physical and psychological states do not occur independently of one another. Prior work has identified associations between affective valence (i.e., pleasure, enjoyment) and running biomechanics [155,156]. However, these studies were conducted in treadmill or track-based environments, potentially affecting both biomechanics and psychology and limiting the translation to real-world running. This study examined the relationships between positive running experiences and running biomechanics during long, outdoor training runs. The findings suggest that there may be significant associations between positive experiences and running biomechanics, and that the associations may differ between facets of positive experience.

Part I:

Advancing Inertial Sensors for Use During Home-Based Balance Rehabilitation

Chapter 2 A Pilot Study Comparing the Effects of Concurrent and Terminal Visual Feedback on Standing Balance in Older Adults

2.1 Abstract

While balance training with concurrent feedback has been shown to improve real-time balance in older adults, terminal feedback may simplify implementation outside of clinical settings. Similarly, visual feedback is particularly well-suited for use outside the clinic as it is relatively easily understood and accessible via ubiquitous mobile devices (e.g., smartphones) with little additional peripheral equipment. However, differences in the effects of concurrent and terminal visual feedback are not yet well understood. We performed a pilot study that directly compared the immediate effects of concurrent and terminal visual feedback as a first and necessary step in the future design of visual feedback technologies for balance training outside of clinical settings. Nineteen healthy older adults participated in a single balance training session during which they performed 38 trials of a single balance exercise including trials with concurrent, terminal or no visual feedback. Analysis of trunk angular position and velocity features recorded via an inertial measurement unit indicated that sway angles decreased with training regardless of feedback type, but sway velocity increased with concurrent feedback and

decreased with terminal feedback. After removing feedback, training with either feedback type yielded decreased mean velocity, but only terminal feedback yielded decreased sway angles. Consequently, this study suggests that, for older adults, terminal visual feedback may be a viable alternative to concurrent visual feedback for short duration single-task balance training. Terminal feedback provided using ubiquitous devices should be further explored for balance training outside of clinical settings.

2.2 Introduction

Balance ability deteriorates with age, leading to increased fall risk and fall prevalence in healthy older adults [157]. Poor balance confidence and fear of falling are also associated with increased anxiety [158–160], depression [158,159], and institutionalization [160,161], and with decreased activity [159,162,163], social participation [163,164], and quality of life [159,163].

Balance training, which is traditionally performed in a clinical setting with the instruction of a physical therapist, has been shown to improve balance performance for older adults as measured by clinical tests of balance (e.g., Berg Balance Scale) and sway metrics (e.g., center of mass displacements) [4,82,83]. However, the cost and availability of balance therapy [84,85], for either therapeutic or preventative use, limits access to balance training. For example, it is predicted that by 2030, the United States alone will have a shortage of 140,000 physical therapists, resulting in the majority of patients having difficulty accessing necessary physical therapy services [84].

Balance training technologies designed to be used outside of clinical settings may increase access to preventative and therapeutic balance training. However, balance training without a physical therapist's supervision has been shown to be less effective than supervised training [86,87]. This shortcoming may be mitigated by providing feedback during balance training. Feedback systems typically comprise a combination of sensors and displays [47]. Previous studies have explored the use of accelerometers or inertial measurement units (IMUs) [4,5,88,89,98,100,165,166], plantar pressure [4,5,99] or force sensors [5,29,89,97–99,167,168], cameras [98,104,105,167,169], or electromyography (EMG) [99] to measure kinematics, kinetics, or muscle activity information about postural sway and gait dynamics, while feedback has been provided via visual, tactile, auditory, and multimodal displays [4,47,99].

Feedback devices have been used as real-time balance aids and as tools to augment balance training programs [3]. Over the past 30 years, numerous studies have shown that feedback is effective at improving real-time quiet and perturbed standing balance, i.e., balance while the feedback is being provided [88–96]. More recently, a limited number of studies have compared the effects of balance training programs with and without feedback, with a subset of such studies showing additional benefits of training with feedback. In a 2018 review, Gordt et al. examined eight studies assessing the effects of wearable sensor-based feedback during single- or multi-day balance and gait training for individuals with various balance disorders and found evidence of greater reductions in postural sway after training with feedback than after conventional balance training [4]. Alhasan et al. reviewed five studies conducting multiple sessions of standing balance training with visual feedback among older adults and concluded that training with visual feedback is likely to lead to greater improvements in clinical outcome measures and/or trunk sway compared to balance training without feedback or no intervention [97]. Similarly, Mak et al. examined 17 studies on the same topic and found there to be benefits of visual feedback on clinical balance measures and/or trunk sway, with seven out of eight studies finding training with visual feedback to yield greater improvements than no intervention, and three out of three studies finding training with visual feedback to yield greater improvements than placebo interventions [98]. In an examination of vibrotactile feedback, Bao et al. reported improved clinical outcome measures in older adults following an eight-week home-based balance training program using a smartphone-based vibrotactile feedback system, and the improvements were significantly greater for a subset of the clinical metrics assessed compared to improvements for a control group completing the same training without feedback [100]. Similarly, uncontrolled studies by Basta et al. and Rossi-Izquierdo et al. reported reduced trunk

sway and improved clinical outcome measures after two weeks of balance training with vibrotactile feedback in people with various balance disorders or Parkinson's disease, respectively, and a controlled study by Brugnera et al. reported improved clinical outcome measures after two weeks of training with vibrotactile feedback and no improvement after two weeks of training without feedback in people with Parkinson's disease [101–103]. Finally, studies examining balance exergaming with multimodal (auditory and visual) feedback enabled by the Xbox® Kinect have shown that balance training with feedback is more effective than conventional training at improving clinical outcome measures and measures of postural sway [104,105]. However, there have not been any large-scale randomized controlled trials reported to date, and the impact of the improvements on fall rates have not been assessed [99].

While numerous feedback modalities have yielded benefits during balance training, some training systems require specialized equipment (e.g., vibrating actuators), which may limit access for certain prospective users. Visual feedback offers the benefits of being relatively easily understood [99], able to encode both spatial and temporal information (e.g., sway position and velocity) [50], and immediately available via ubiquitous mobile devices (e.g., smartphones, tablets) with little additional peripheral equipment. Terminal visual feedback specifically (i.e., feedback provided after the balance exercise is completed) can be achieved using a single mobile device, offering a simpler and less costly alternative that also extends to additional balance exercises (e.g., when eyes are closed).

The effects of terminal visual feedback on balance training performance are not well understood. Extended balance training with concurrent visual feedback (i.e., feedback provided in real-time during the balance exercise) has been shown to result in greater balance improvements than training without feedback [97,98]. Similarly, a single session of balance

training with concurrent visual feedback has been shown to yield greater sway reductions than training without feedback under certain conditions, including reducing the root mean square (RMS) of the center of pressure for older adults on a compliant surface with feet displayed at a 30° angle [89]. However, it also requires that a properly placed screen be visible for the duration of each exercise. Because the timing of feedback can impact its efficacy [170–172], the effects of concurrent feedback during balance training may not translate to terminal feedback. For simple tasks, concurrent feedback may result in immediate balance improvement, but the user may also become reliant on the feedback, leading to poor retention of benefits. Terminal feedback, on the other hand, may result in smaller immediate balance improvements but superior retention [47,173]. However, because the "simplicity" of a task is difficult to assess as it relies upon both the task complexity and user skill level, it is difficult to predict the effect of terminal feedback on balance training in older adults [173].

Goodwin and Goggin compared the use of terminal visual feedback and a combination of concurrent and terminal visual feedback on older adults' dynamic balance and found that both types of feedback improved balance performance during a single training session [174]. Greater retention of balance performance was achieved following training with terminal feedback compared to a combination of concurrent and terminal feedback. However, to our knowledge no studies have directly examined terminal visual feedback or compared solely concurrent to solely terminal visual feedback.

We sought to extend the existing literature by performing a pilot study that directly compared the effects of training with concurrent or terminal visual feedback on older adults completing a common balance exercise. We evaluated the effects by quantifying the RMS and velocity of the postural sway angle. This preliminary study represents a necessary first step in a

series of studies that would be needed to develop a balance training technology that leverages a single mobile device to provide terminal visual feedback outside of clinical settings.

2.3 Methods

2.3.1 Participants

Nineteen older adult participants were recruited through the University of Michigan Health Research website (demographics shown in Table 2.1). All participants self-reported that they were in good general health (i.e., medically stable, no frequent back or lower extremity pain, no severe visual impairment, no history of fainting) and had no muscular or neurological disorders that would affect balance performance. Healthy older adults were included in this pilot study because they were readily accessible, could complete a large number of trials within a single session, and would potentially use a home-based balance training technology for preventative balance training. The study was approved by the University of Michigan Institutional Review Board (study HUM00015990), and all participants gave written informed consent in accordance with the Helsinki Declaration.

Table 2.1: Study participant demographics.

	Age	Sex	Height (m)	Mass (kg)
Group 1: Concurrent First (N = 10)	70.4 ($\pm$3.0)	7 Female	1.64 ($\pm$0.10)	72 ($\pm$16)
Group 2: Terminal First (N = 9)	70.0 ($\pm$4.0)	5 Female	1.66 ($\pm$0.06)	72 ($\pm$9)

2.3.2 Protocol

All participants partook in a single-day balance training session in which they stood on a foam pad (regular balance pad, $50 \times 41 \times 6$ cm, Airex AG, Sins, Switzerland) with their feet together. This balance exercise was selected because it was sufficiently challenging such that older adults could benefit from feedback, but was not so difficult that they would routinely step

out of position during a 30s trial [89]. The participants were barefoot and wore comfortable clothing, and they were instructed to stand quietly while maintaining the pose. They were told to place and move their arms however they liked, but to not touch the support in front of them unless they needed to do so to prevent a fall. No additional instructions were given regarding balance strategy.

For the duration of training, participants wore a single (six degree of freedom) IMU (MTx, XSens Inc., Eschende, The Netherlands) on an elastic belt approximately positioned over the approximate center of mass (vertebrae L3) level dorsal to the spine[175–177]. IMU data (acceleration and angular rate) were collected at 100 Hz using custom software and the trunk sway angles were extracted using XSens' proprietary sensor fusion algorithm. From among the options for measuring balance performance (e.g., center of pressure displacements, clinical measures such as the Berg Balance Score), IMUs were selected because they can be found in smartphones and are well-suited for accessible, at-home training systems.

Using custom software and livestreamed or recorded trunk sway data, visual feedback was displayed on a projector screen placed 10 feet in front of the participant with the center of the display approximately level with the participant's eyes. A pair of horizontal and vertical axes shown at all times represented the medial-lateral (ML) and anterior-posterior (AP) sway angles, respectively. Concurrent feedback was displayed as a single cursor on the screen denoting the current ML and AP angles of the participant, and terminal feedback was displayed before the trial as a stabilogram illustrating all ML and AP tilt angle pairs from the trial immediately preceding the current trial (see example feedback displays in Figure 2.1). Participants were shown examples of each type of feedback and told what the target represented. Then, prior to beginning training with each type of feedback, participants practiced with that feedback type

while standing with a shoulder width stance on a firm surface (a stance and surface different than the test conditions) for no more than one minute. Adopting a different exercise than the training exercise allowed the participants to acclimate to the feedback without beginning to learn the training balance exercise prior to the start of data collection. No additional instructions were given regarding how to interpret or apply the feedback.
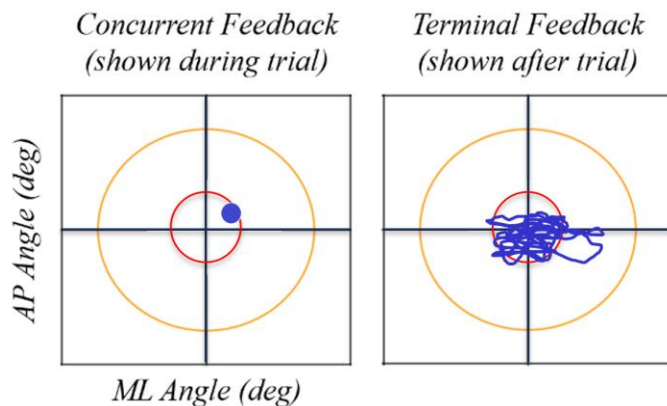
Figure 2.1: Example feedback displays for concurrent and terminal feedback.

Feedback was provided using a crossover design wherein participants completed a block of training with concurrent visual feedback and a block of training with terminal visual feedback, where order was randomly assigned by alternating between subsequent participants. Participants completed a total of 38 trials during the training session, performing 19 trials within the concurrent feedback block and 19 trials within the terminal feedback block (see Figure 2.2). So as to avoid the effects of fatigue, the total number of training trials was selected to yield a training duration less than the typical duration of a single-day balance therapy or at-home balance training session; the active training duration was 19 min compared to an optimal training duration of 31–45 min [82].

Each block consisted of four baseline trials with no feedback followed by five sets of three 30s training trials, with feedback provided during the first and second trials and no feedback provided during the third trial (i.e., feedback provided 2/3 or 67% of the time). While the optimal ratio of trials with feedback to trials without feedback is unknown, providing feedback on fewer than 100% of trials (i.e., including some trials without feedback) has been shown to encourage integration and motor learning [47,178–182]. Participants took a short break of approximately 5 min between blocks. Participants 1 through 7 did not complete the last (19th) trial in the terminal block and the last baseline (4th) trial in the concurrent block due to a change in experimental design to better balance the baseline trials. As a result, seven participants completed 36 trials and 12 participants completed 38 trials, and three of the total 708 trials were excluded from the analysis due to data loss.

2.3.3 Data analysis

The IMU data recorded using the custom software were also imported to MATLAB™ (Mathworks, Natick, MA, USA) where the angles were filtered using a second order Butterworth
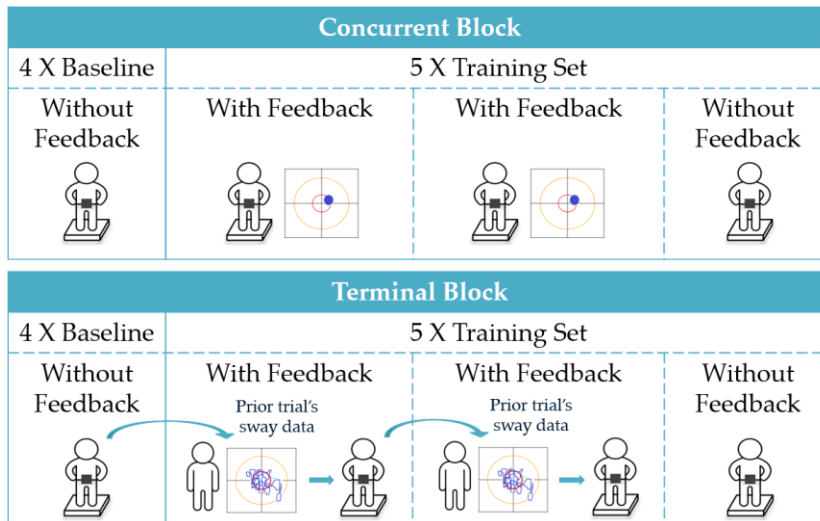
Figure 2.2: Trial structure for concurrent and terminal feedback blocks. Each block (terminal and concurrent) consisted of four baseline trials with no feedback followed by five sets of three 30s training trials, with feedback provided during the first and second trials and no feedback provided during the third trial.

31

filter with a 2 Hz cutoff frequency and then analyzed. The IMU axes were aligned with the body

axes via assumed alignment [63]. Performance features calculated from the IMU data included

the RMS of the sway angle from vertical (Phi RMS, degrees; $\text{Phi\_Angle}^2 = \text{AP\_Angle}^2 +$

ML_Angle^2), RMS in the AP direction (AP RMS, degrees), RMS in the ML direction (ML

RMS, degrees), mean sway velocity (MV, degrees/s), path length as computed by the sum of the

magnitude of the differences between sway data points (PL, degrees), and area of a 95th

percentile confidence interval elliptical fit to the sway data (i.e., elliptical area; EA, degrees^2)

[29,83]. These features were calculated as

$$\text{Phi RMS} = \sqrt{\frac{1}{J}\sum_{j=1}^{J}(AP[j] - \frac{1}{J}\sum AP[j])^2 + (ML[j] - \frac{1}{J}\sum ML[j])^2}$$

$$\text{AP RMS} = \sqrt{\frac{1}{J}\sum_{j=1}^{J}(AP[j] - \frac{1}{J}\sum AP[j])^2}$$

$$\text{ML RMS} = \sqrt{\frac{1}{J}\sum_{j=1}^{J}(ML[j] - \frac{1}{J}\sum ML[j])^2}$$

$$\text{MV} = \frac{\sum_{j=1}^{J-1}\sqrt{(AP[j+1] - AP[j])^2 + (ML[j+1] - ML[j])^2}}{T}$$

$$\text{PL} = \sum_{j=1}^{N-1}\sqrt{(AP[j+1] - AP[j])^2 + (ML[j+1] - ML[j])^2}$$

$$\text{EA} = \pi z_{0.95}^2 \lambda_1^{0.5}(\sigma_{AP\,ML}^2)\lambda_2^{0.5}(\sigma_{AP\,ML}^2)$$

where J refers to the number of data points, AP[j] refers to the jth AP data point, T is the total

time elapsed (i.e., the time at which data point J was collected minus the time at which the first

data point was collected), $z_{0.95}$ is the z-score for a 95% confidence level and $\lambda_1(\sigma_{AP\,ML}^2)$ and

$\lambda_2(\sigma_{AP\,ML}^2)$ are the 1st and 2nd eigenvalues of the covariance of the AP and ML data. Based on

results from previously published studies involving different modalities of feedback, smaller

RMS and EA values typically indicate better balance performance [165,166,168,183], while in

some studies MV has increased while participants use concurrent feedback following limited

training [166,183]. Note that while prior research has reported variable sway results for people

with balance impairments (e.g., sometimes increased sway, sometimes decreased sway) [184–

187], older adults have previously exhibited increased sway relative to younger adults when

completing standing balance on a foam surface, as done here [89].

A single linear mixed-effects regression (LME) was used to compare the changes in

performance as a function of training and feedback status. The dependent variable was the log of

one performance feature, and all tests were performed with $\alpha = 0.05$. The maximal model was

$$\text{ln Feature} \sim 1 + \text{Order} + \text{Block} + \text{TrialNumber}^{a} + \text{ConcurrentFeedbackRemoved} + \text{TerminalFeedbackRemoved} + \text{Block:TrialNumber}^{a} + \text{Block:Order} + \text{ConcurrentFeedbackRemoved:Order} + \text{TerminalFeedbackRemoved:Order} + \text{Age} + \text{Sex} + (1|\text{Participant}).$$

The fixed effects include the intercept ('1'), the order in which the feedback modes were

used (Order), a Boolean for being in the concurrent feedback block ('Block'), the exponentiated

number of trials completed after the first baseline ('TrialNumber ^{a}', considered $0 < a \leq 5$ in

increments of 0.1), a Boolean for concurrent/terminal feedback being removed

('ConcurrentFeedbackRemoved'/'TerminalFeedbackRemoved'), age and sex of the participant,

and the interaction terms listed. The random intercept is for participant ID ('1|Participant'), and

':' is used to denote an interaction. This maximal model was then reduced for each feature

independently by removing terms that yielded lower Akaike information criteria (AIC) scores

and that were not of direct interest (i.e., all terms except 'TrialNumber',

'ConcurrentFeedbackRemoved', and 'TerminalFeedbackRemoved'). The included terms are

shown in Table 2.2.

Table 2.2: Terms included in the final models for each feature and the significance of those terms. 'Yes *' denotes inclusion and significance as determined by $p < 0.05$, 'Yes' denotes inclusion without significance, and 'No' denotes exclusion.

Natural Log of Feature	Exponent on Trial Number (a)	Intercept (1)	Order	Block	Trial Number[a]	Concurrent Feedback	Natural Log of Feature
Phi RMS	0.4	Yes	No	Yes *	Yes *	Yes *	Yes
AP RMS	0.5	Yes *	No	Yes *	Yes *	Yes *	Yes
ML RMS	0.1	Yes *	No	No	Yes *	Yes *	Yes
MV	0.1	Yes	No	No	Yes *	Yes *	Yes
PL	0.1	Yes	No	No	Yes *	Yes *	Yes
EA	0.3	Yes *	No	Yes	Yes *	Yes *	Yes

Natural Log of Feature	Block: TrialNumber[a]	Block: Order	Concurrent Feedback Removed: Order	Terminal Feedback Removed: Order	Age	Sex	Participant
Phi RMS	No	No	No	No	No	Yes	Yes
AP RMS	No	No	No	No	No	Yes *	Yes
ML RMS	Yes *	Yes *	Yes	No	No	No	Yes
MV	Yes *	No	No	Yes	No	No	Yes
PL	Yes *	No	No	Yes	Yes	No	Yes
EA	No	No	No	No	No	Yes	Yes

2.4 Results

Figure 2.3 shows the measured data as well as the combined effect of all included model

terms for the Phi RMS of a representative exemplar participant.

Table 2.3 reports the significance and effect sizes of individual LME factors. As the

number of trials with concurrent feedback increased, sway angle (Phi RMS, AP RMS, ML RMS,

EA) decreased while mean velocity (MV) increased (see Table 2.3). Terminal feedback resulted

in the same reduction in sway angle (Phi RMS, AP RMS, EA) as concurrent feedback, but with a

decrease in MV.
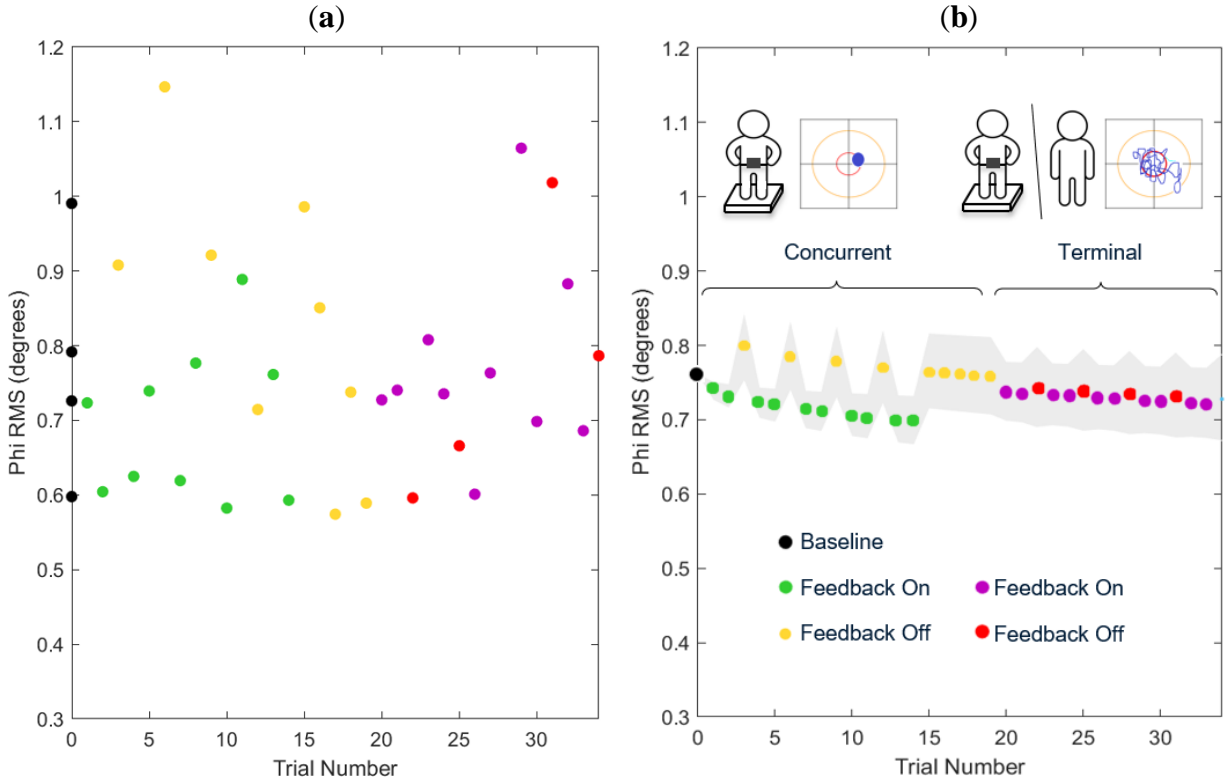
Figure 2.3: (a) Measured Phi RMS for an exemplar participant in Group 1; (b) Predicted Phi RMS values and 95% confidence intervals for the same exemplar participant calculated using an LME, where the 95% confidence band included only the effects of direct interest (i.e., 'TrialNumber a', 'ConcurrentFeedbackRemoved', and 'TerminalFeedbackRemoved'). Phi RMS decreased significantly and at the same log rate with both types of feedback. Phi RMS increased significantly with the removal of concurrent feedback, but not significantly with the removal of terminal feedback.

The effects of removing feedback were significantly smaller after training with terminal compared to concurrent feedback (see Table 2.3). After concurrent feedback was removed, all features exhibited a significant change in the opposite direction as the effects of training with feedback. In contrast, the differences observed following training with terminal feedback were largely maintained once terminal feedback was removed.

When comparing the predicted feature values at baseline and the end of the first block, terminal feedback resulted in significant decreases in Phi RMS, AP RMS, and EA while concurrent feedback resulted in no significant changes in the same features (see Table 2.4). Ultimately, repeated practice with either type of feedback resulted in significant decreases in MV

(with terminal yielding a greater decrease; $p = 0.037$, estimate -0.081, $[-0.1593, -0.003]$) and

PL, while only terminal feedback resulted in significant decreases in RMS and EA.

Table 2.3: Effects of trial number and removal of feedback on the log of each feature during the first training block. Features include Phi RMS (degrees), AP RMS (degrees), ML RMS (degrees), MV (degrees/s), PL (degrees), and EA (degrees2). * denotes significance (p < 0.05).

Natural Log of Feature	Exponent on Trial Number (a)	Effect of Training with Concurrent Feedback		Difference in the Effects of Training with Terminal vs. Concurrent Feedback	
		p-Value	Estimate [95% CI]	p-Value	Estimate [95% CI]
Phi RMS	0.4	<0.001 *	−0.030 [−0.046, −0.014]	0.975	−0.000 [−0.047, 0.046]
AP RMS	0.5	<0.001 *	−0.038 [−0.052, −0.023]	0.752	0.007 [−0.037, 0.052]
ML RMS	0.1	0.004 *	−0.095 [−0.159, −0.031]	<0.001 *	0.099 [0.049, 0.149]
MV	0.1	0.012 *	0.044 [0.010, 0.078]	<0.001 *	−0.116 [−0.142, −0.090]
PL	0.1	0.004	0.052 [0.016, 0.087]	<0.001 *	−0.127 [−0.154, −0.010]
EA	0.3	<0.001 *	−0.073 [−0.115, −0.030]	0.927	0.005 [−0.109, 0.120]
Natural Log of Feature	Exponent on Trial Number (a)	Effect of Training with Concurrent Feedback		Difference in the Effects of Training with Terminal vs. Concurrent Feedback	
		p-Value	Estimate [95% CI]	p-Value	Estimate [95% CI]
Phi RMS	0.4	<0.001 *	0.092 [0.038, 0.146]	0.711	0.011 [−0.045, 0.066]
AP RMS	0.5	<0.001 *	0.121 [0.051, 0.192]	0.526	0.024 [−0.049, 0.096]
ML RMS	0.1	0.003 *	0.106 [0.036, 0.175]	0.573	−0.016 [−0.072, 0.040]
MV	0.1	<0.001 *	−0.170 [−0.207, −0.132]	0.251	−0.027 [−0.074, 0.019]
PL	0.1	<0.001 *	−0.185 [−0.224, −0.146]	0.209	−0.031 [−0.080, 0.017]
EA	0.3	0.003	0.149 [0.050, 0.248]	0.944	0.004 [−0.098, 0.106]

Table 2.4: Difference between the predicted log feature value at baseline and at the end of the first block. * denotes significance (p < 0.05).

Natural Log of Feature	After Training with Concurrent Feedback		After Training with Terminal Feedback	
	p-Value	Estimate [95% CI]	p-Value	Estimate [95% CI]
Phi RMS	<0.001 *	−0.030 [−0.046, −0.014]	0.975	−0.000 [−0.047, 0.046]
AP RMS	<0.001 *	−0.038 [−0.052, −0.023]	0.752	0.007 [−0.037, 0.052]
ML RMS	0.004 *	−0.095 [−0.159, −0.031]	<0.001 *	0.099 [0.049, 0.149]
MV	0.012 *	0.044 [0.010, 0.078]	<0.001 *	−0.116 [−0.142, −0.090]
PL	0.004	0.052 [0.016, 0.087]	<0.001 *	−0.127 [−0.154, −0.010]
EA	<0.001 *	−0.073 [−0.115, −0.030]	0.927	0.005 [−0.109, 0.120]

2.5 Discussion

2.5.1 Effects of balance training with feedback while feedback was used

While receiving either type of feedback during a single session of balance training, older

adult participants in this study exhibited improved postural steadiness as characterized by RMS

and EA. However, participants exhibited decreased mean sway velocity only with terminal feedback.

An increased number of trials with either type of feedback resulted in decreased RMS and EA (Phi RMS $p < 0.001$, AP RMS $p < 0.001$, EA $p < 0.001$), indicating that participants could use concurrent visual feedback and terminal visual feedback to maintain a more stable posture. Although not the focus of this work, these findings are consistent with prior research that has shown decreases in RMS and EA when concurrent feedback was provided as a real-time balance aid [34,88,89,93]. In addition, sway velocity increased with concurrent feedback ($p = 0.012$) and decreased with terminal feedback ($p < 0.001$). Because sway velocity has been linked to increased postural control activity (i.e., amount of balancing activity needed to maintain a given level of postural stability [29,33,90]), we posit that increased postural control activity with concurrent feedback and decreased activity with terminal feedback accompanied the decrease in sway angles [34]. The measured change in sway velocity suggests that participants used concurrent feedback to make many rapid postural corrections while they used terminal feedback to make smaller, slower corrections. Therefore, while training with both types of feedback resulted in decreased sway, concurrent feedback may have elicited postural corrections each time the feedback showed a deviation from center (resulting in many rapid corrections) while terminal feedback may have elicited improvements to a participant's internal model relating intrinsic feedback to deviations from center [47,173]. These findings align with the guidance hypothesis which predicts that, for simple tasks, concurrent feedback accelerates training during the acquisition phase as knowledge of the outcome can be used from moment to moment to correct errors. In contrast, terminal feedback is predicted to produce less immediate improvement because the delayed feedback can only guide the next balance attempt [47,173]. These findings

may also reflect that the terminal feedback conveyed limited velocity information (i.e., characteristics of change in direction, but not speed) as compared to the concurrent feedback. While future studies may investigate the effects of providing additional velocity information via the terminal feedback display, we opted to keep the feedback presentation format as consistent as possible in this pilot study as it was the first in a series of studies needed on the topic.

Comparing these results to prior studies, the concurrent feedback findings align with those reported by Dos Anjos et al. [34] (i.e., decreased COP EA and MV among adults when receiving concurrent COP feedback while standing with feet together on a firm surface), Halická et al. (i.e., decreased COP RMS among older adults when receiving concurrent COP feedback while standing with heels together and feet displayed at an angle of 30° on a foam surface) [89], and Dault et al. (i.e., increased COP MV among older adults when receiving concurrent COP feedback while standing with feet apart on a firm surface) [188]. In contrast, Halická et al. reported no change in the RMS of the center of mass as measured using accelerometers on the lower back [89], and Dault et al. reported no reduction in COP sway amplitude [188]. However, these studies included fewer older adult participants and/or fewer trials than the current study, making it potentially difficult to detect the current study's small effect size.

Because our aim was to compare the effects of balance training with concurrent versus terminal feedback, we conducted a direct comparison of these two feedback types rather than comparing to a control group that trained without feedback. However, feedback has been shown to yield significantly less postural sway (30–50%) when used as a real-time aid compared to balancing without feedback [89–96,168]. Similarly, after an extended training program, training with concurrent visual feedback has yielded greater improvements in clinical balance test scores than training without feedback [97,98]. The changes observed here within a single block of

balance training with concurrent feedback were likely greater than the changes that would have occurred during training without feedback. Because terminal feedback yielded changes equal to or larger than balance training with concurrent feedback, terminal feedback likely also yielded greater changes than would have occurred without feedback.

2.5.2 Effects of balance training with feedback after feedback was removed

Once either type of feedback was removed after a single session of balance training, older adult participants in this study reduced their mean sway velocity. However, only after a session with terminal feedback did participants exhibit improved postural steadiness as characterized by RMS and EA.

After training with concurrent feedback, RMS and EA values were not significantly different than baseline values (Phi RMS $p = 0.910$, AP RMS $p = 0.557$, ML RMS $p = 0.732$, EA $p = 0.815$), suggesting that participants did not experience a significant change in motor response during the single session, a finding that agrees with Wiesmeier et al. [189]. In contrast, after training with terminal feedback, RMS and EA values were both lower than baseline values (Phi RMS $p = 0.022$, AP RMS $p = 0.005$, EA $p = 0.013$), indicating that a change in motor response occurred. These findings align with the guidance hypothesis' claim that concurrent feedback is detrimental to skill retention because participants grow dependent on artificial feedback and disregard natural feedback while terminal feedback is beneficial for balance skill retention as participants improve their internal balance mechanisms [47,173]. After training, the resulting decrease in MV values relative to baseline values was significantly greater with terminal feedback than concurrent feedback ($p = 0.037$), suggesting that participants achieved better postural control performance with less postural control activity after receiving terminal compared to concurrent feedback [29,33,90].

The findings from this study were consistent with some prior studies comparing concurrent and terminal visual feedback on simple or complex tasks, albeit with different tasks and training schedules than employed herein [189]. Ranganathan and Newell tested a single session of concurrent or terminal visual feedback in a force-production task and found that concurrent feedback facilitated the adoption of different strategies to achieve the goal, but that the improvement was not retained. Unlike the current findings, Ranganathan and Newell found that terminal feedback did not yield improvements; however, they also found that the strategies acquired during training were retained [170]. Further, in a complex rowing-type task, Sigrist et al. found that terminal feedback yielded greater retained improvements than concurrent feedback during multi-day training due to poor retention of benefits from concurrent training [171].

The findings from this study also differed from some results for other types of tasks. Yamamoto et al. found that concurrent visual feedback yielded retained improvements for low-skilled learners completing a single session of training on a load-control task, while terminal feedback did not result in improvements [172]. Chang et al. studied joint mobilization and found that both concurrent and terminal visual feedback resulted in retained improvements after a single session of training, and that there was no significant difference between the effects of the two feedback types [190]. Our findings add to a growing body of literature comparing the effects of concurrent and terminal feedback.

In an analysis of the effects of concurrent and terminal visual feedback on ankle co-contraction using electromyography (EMG) data from the same dataset used for this study, ankle stiffness increased when concurrent feedback was used but not when terminal feedback was used [27]. In combination with the results of this study, these findings imply that concurrent feedback was used to decrease sway and increase sway velocity while stiffening the ankles. In contrast,

terminal feedback yielded significant decreases in sway and sway velocity without changes in ankle stiffness. When concurrent feedback was removed, ankle stiffness significantly decreased while sway increased, and when terminal feedback was removed, neither ankle stiffness nor sway significantly changed. As stiffening the ankles is generally considered to be a maladaptive strategy, together these analyses suggest that terminal visual feedback may present a viable alternative to concurrent visual feedback during a single session of balance training as terminal feedback yields sway improvements and avoids maladaptive ankle stiffening. While further research is needed to fully examine the effects of such training, these findings suggest that terminal visual feedback should be further investigated as an alternative to concurrent visual feedback; the use of terminal feedback would also avoid the need for specialized equipment such as large, stationary displays. A balance training technology leveraging terminal visual feedback may require only a single, ubiquitous mobile device such as a smartphone, making such systems easily accessible to most. Prior studies have demonstrated that feedback-based balance training completed outside of clinical settings has the potential to yield balance improvements similar to those achieved during clinical training supervised by a physical therapist [191–194]. Consequently, the terminal visual feedback employed in this pilot study should be studied further as an accessible alternative to supervised clinical training.

Limitations of this study included: a small sample size, analysis of a single maximal model, performance of a single balance exercise, and a single session of balance training. Future work should evaluate the effects of training over multiple sessions, investigate retention over longer periods of time, and assess the effects of training on fall risk. Such a longitudinal study might also compare the effects of home-based training with concurrent or terminal visual feedback to in-clinic training with a physical therapist. Additionally, future work could explore

different terminal feedback displays beyond the stabilogram presented in this study (e.g., a stabilogram with color coding for velocity or various summary statistics). Finally, additional balance training exercises and participant populations should be evaluated in order to assess the generalizability of these results to other balance tasks and populations.

2.6 Conclusion

This pilot study compared the immediate effects of concurrent and terminal visual feedback for older adults completing a common balance exercise. Both types of feedback yielded sway reductions. However, only training with terminal visual feedback yielded small, short-term, single-task sway reductions following the completion of the training protocol, potentially due to an adaptive mechanism, while training with concurrent feedback may have increased participants' reliance on external information. These preliminary results suggest that terminal visual feedback may be a viable alternative to concurrent visual feedback for use in at-home balance training technologies. As balance training technologies employing terminal visual feedback may be achieved using only a single ubiquitous mobile device such as a smartphone without need for specialized equipment such as a large, stationary display, these preliminary findings offer promise for simple, affordable, and accessible balance training devices. Future research may further support that terminal visual feedback offers the potential for improved training retention in addition to practical advantages such as supporting a broader range of balance exercises.

Chapter 3 Differences Between Physical Therapist Ratings, Patient Self-Ratings, and Posturographic Measures when Assessing Static Balance Exercise Intensity

3.1 Abstract

In order for balance therapy to be successful, the training must occur at the appropriate dosage. However, physical therapist (PT) visual evaluation, the current standard of care for intensity assessment, is not always effective during telerehabilitation. Alternative balance exercise intensity assessment methods have not previously been compared to expert PT evaluations. The aim of this study was to assess the relationship between PT participant ratings of standing balance exercise intensity and balance participant self-ratings or quantitative posturographic measures. Ten balance participants with age or vestibular disorder-related balance concerns completed a total of 450 standing balance exercises (three trials each of 150 exercises) while wearing an inertial measurement unit on their lower back. They provided per-trial and per-exercise self-ratings of balance intensity on a scale from 1 (steady) to 5 (loss of balance). Eight PT participants reviewed video recordings and provided a total of 1,935 per-trial and 645 per-exercise balance intensity expert ratings. PT ratings were of good inter-rater reliability and significantly correlated with exercise difficulty, supporting the use of this intensity scale. Per-trial and per- exercise PT ratings were significantly correlated with both self-ratings (r =0.77– 0.79) and kinematic data (r =0.35–0.74). However, the self-ratings were significantly lower than the PT ratings (difference of 0.314–0.385). Resulting predictions from self-ratings or kinematic data agreed with PT ratings approximately 43.0–52.4% of the time, and agreement was highest for ratings of a 5. These preliminary findings suggested that self-ratings best

indicated two intensity levels (i.e., higher/lower) and sway kinematics were most reliable at intensity extremes.

3.2 Introduction

Balance ability deteriorates with age [162,195,196], leading to increased fall risk and fall prevalence in healthy older adults [157]. Balance can also be impaired by the presence of sensory or neurologic disorders such as peripheral sensory loss [70,71], vestibular disorder [71–73], multiple sclerosis [74–76], cerebrovascular accident [77], traumatic brain injury [78,79], and Parkinson's disease [80,81]. Low balance confidence and fear of falling are associated with increased fall risk [197,198], anxiety [158–160], depression [158,159], and institutionalization [160,161], and with decreased activity [159,162,163], social participation [163,164], and quality of life [159,163].

Balance training, which is traditionally performed in a clinical setting with the instruction of a physical therapist (PT), can improve balance ability when it occurs at the appropriate dosage such that the training is at or near the limits of an individual's ability [82,83,199]. Dosage has been described as the combination of frequency, intensity, time, and type (FITT) where frequency refers to the regularity of training sessions, intensity refers to "the degree of challenge to the balance control system relative to the capacity of the individual to maintain balance" [200], time refers to the duration of each exercise and of the session, and type refers to the exercise itself [201–203]. While frequency, time, and type are easily quantified [201,203], intensity depends on both the difficulty of the exercise and the balancing ability of the individual, reflecting how challenging an exercise is for a particular individual at a specific time; it is therefore more difficult to assess [201–203]. Unlike aerobic (e.g., percent of maximum heart rate) or resistance (e.g., percent of the 1-repetition maximum) exercise intensity [204], there is no standard assessment for balance exercise intensity. Most PTs visually observe the patient, employing their expert assessment to qualitatively adjust task intensity [120,121]. However,

visual expert assessment is more difficult during increasingly common telerehabilitation or home-based training during which a PT is not physically present.

Telerehabilitation has grown in popularity as a solution to both misdistribution of physical therapy services [205,206] and public health concerns such as those posed by COVID-19 [207–210]. Access to traditional physical therapy services is increasingly limited. It is predicted that by 2030, the United States alone will have a shortage of 140,000 PTs, resulting in the majority of patients having difficulty accessing necessary physical therapy services [84,85,211]. Moreover, PTs are less available in low-income countries [205,212,213], where the majority of people with disabilities live [205]. Availability of physical therapy is also lower in rural settings [205,206,212], where chronic conditions amenable to physical therapy are prevalent [206]. In other countries such as Singapore, PTs are concentrated in acute-care facilities, leading to lesser availability in post-acute care sites [212].

While telerehabilitation may improve access to care, only 29% of PTs in a 2022 vestibular rehabilitation study expressed that telerehabilitation was as effective as in-person care [207]; 94% of PTs in the same study reported concerns about the safety of testing balance without a caregiver present, and 92% of PTs reported that technology limitations affected their ability to view patients' bodies remotely. PTs have also reported that inappropriate lighting and patient positioning with respect to the camera can negatively affect clinical decision making [207,214]. Relatedly, patients have reported a lack of appropriate technology including computers with cameras [209], making visual assessment impossible in some cases.

In addition to telerehabilitation, home exercise programs may complement existing affordable physical therapy options available to patients, which have been limited in their duration. For example, until recently, public insurance for older adults in the United States (i.e.,

Medicare) covered only approximately 14-16 outpatient physical therapy visits [212]. In

Singapore, only select follow-up rehabilitation services can be paid for with compulsory medical

savings. And in Bangladesh, public funding for physical therapy is limited [212]. As

employment rates are lower for people with disabilities, extended physical therapy care is often

financially inaccessible [205,212]. However, training without a professional's guidance has been

shown to be less effective than supervised training [86,87].

In contexts where visual assessment of balance task intensity is difficult such as

telerehabilitation and home-based training, PTs may time exercises, employ quantitative

posturography, or ask for patient self-assessments [208]. Timing standing balance exercises may

reflect the intensity of a task, but additional performance aspects such as arm movements or

trunk sway may be of importance, and there may be a ceiling effect if task duration is limited

(e.g., 30 s) [119].

Quantitative posturography, which is possible with inertial measurement units (IMUs)

found in ubiquitous technology such as smart phones, can measure an individual's center of mass

during standing balance and may be indicative of task intensity [100,111,122–125]. Alsubaie et

al. compared kinematic measures to adults' self-ratings of intensity using 5 and 10-point scales,

finding correlations of >0.6 in healthy adults and older adults [111] and >0.5 in adults with

vestibular disorders [112] completing static standing balance exercises (i.e., exercises with the

feet in place and a goal of maintaining quiet posture) [215]. However, the relation between the

kinematic measures and self-ratings with PT (expert) assessments were not evaluated.

Self-report measures of intensity are analogous to the Borg Rating of Perceived Exertion

for aerobic exercise [216] or the OMNI Resistance Exertion Scale for resistance exercise

[217,218]. Espy et al. proposed a 10-point self-rating scale modeled after the Rate of Perceived

Exertion and found that self-ratings of intensity are independent of heart rate in adults playing Wii games, supporting that the scale measured intensity beyond solely aerobic exertion [203]. Shenoy et al. examined the same scale in people post-stroke and reported good test-retest reliability, good-to-excellent correlation with self-ratings of perceived challenge, and good-to-excellent correlation with clinical balance test scores [219]. Farlie et al. proposed both 13-element and 5-point self-rating scales [200], reporting strong correlation (r = 0.70) between the scales in older adults completing standing balance tasks. However, they also reported that the 5-point scale was of poor person reliability and unable to statistically detect differences in intensity [220]. While these studies suggest that self-assessments hold promise as measures of balance task intensity, it is important to understand the relationship between self-report measures and PT expert assessments as the current standard of care. Farlie et al. reported a strong correlation (r = 0.70) between self-rater and PT 5-point ratings of intensity, but they did not further comment on the differences [220]. The relationship between self-rater and PT assessments of intensity is still poorly understood.

While quantitative posturography and self-assessment have both shown promise as methods for remote assessment of balance task intensity, few comparisons have been made to conventional visual assessment by expert PTs. This study aimed to further assess the differences between PT expert assessments of balance intensity and self-assessments and kinematic measures.

3.3 Methods

In this study on balance exercise intensity assessment, PT participant intensity ratings (i.e., PT ratings) were compared to balance participant intensity self-ratings (i.e., self-ratings) and kinematic measures.

48

3.3.1 Participants

Two types of participants completed this study: balance participants with age or vestibular disorder-related balance concerns and PT participants. Balance participants completed standing balance exercises while wearing an IMU, and they provided self-ratings of balance intensity. PT participants reviewed video recordings of the balance participants and provided ratings of balance intensity. 450 balance exercise trials were completed by 10 adult balance participants. Six older adult balance participants (2 F, 4 M, 69.0 ± 3.6 years) self-reported to be generally healthy with no muscular or neurological disorders, and four balance participants (2 F, 2 M, 61.7 ± 25.6 years) self-reported vestibular dysfunction. In addition, 1935 intensity ratings were provided by eight PT participants who specialized in the treatment of balance disorders (16 ± 10 years of experience). The number of participants and resulting quantity of data are consistent with a number of related previously published studies [221–224]. The study was approved by a University of Michigan Review Board (HUM00086479), and all participants gave written informed consent in accordance with the Helsinki Declaration.

3.3.2 Intensity rating scales

Both PT and balance participants were provided a 5-point intensity rating scale (see Table 3.1; also reported by Bao et al., Bao et al., and Kamran et al. [100,122,123]). The scale was informed by a scale developed by Espy et al. [203]. Different descriptors were provided to PT and balance participants with the intent of capturing similar performance aspects while using familiar terminology.

Table 3.1: The 1-5 balance intensity scale provided to PT and balance participants

Rating	Descriptions for Balance Participants	Descriptions for PT Participants
1	I feel completely steady	Independent with no sway
2	I feel a little unsteady or off-balance	Supervision with minimal sway
3	I feel somewhat unsteady, or like I may lose my balance	Close supervision with moderate sway
4	I feel very unsteady, or like I definitely will lose my balance	Requires physical assistance or positive stepping strategy after 15 seconds
5	I lost my balance	Unable to maintain position with assist or step out in the first 15 seconds of the exercise

3.3.3 Procedures

3.3.3.1 Completion of balance exercises

Each balance participant completed 15 static standing balance exercises during which the participant was asked to maintain their feet in place and maintain a quiet posture. The exercises were selected from 54 possible options resulting from variations in surface (firm, foam), stance (feet apart, feet together, partial heel to toe, heel to toe, single leg stance), visual input (eyes open, eyes closed), and head movement (none, pitch, yaw) [215]. Six exercises were excluded due to excessive difficulty for the study population (e.g., combinations of a single leg stance, eyes closed, and yaw or pitch head movements; combinations of a single leg stance and a foam surface). The exercises were selected so that each participant performed exercises spanning the intensity scale (i.e., from 1 to 5). Three 30-second trials were completed for each exercise resulting in a total of 45 total trials per balance participant. Because the active exercise duration (15 exercises x 3 trials x 30 s = 22 min 30 s) was less than the optimal duration of a balance training session (31-45 min), fatigue was expected to be minimal [82].

For the duration of testing, the balance participant wore a single six-degree-of-freedom IMU (MTx, XSens Inc, Eschende, Netherlands) on an elastic belt approximately positioned at the center of mass (vertebrae L4/L5) level dorsal to the spine[225–227]. IMU data were collected at 100 Hz using custom software, and the trunk sway angles were extracted using XSens' proprietary sensor fusion algorithm. Balance participants also wore an overhead harness positioned to provide no support unless the balance participant experienced a loss of balance, and they were provided a handrail for additional safety. They were instructed to touch the handrail, step out of position, or rely on the harness only when needed, continuing the trial after use of these additional supports. After each trial, the balance participant provided a per-trial self-rating of intensity. Additionally, after each exercise (i.e., collection of three trials), the balance participant provided a per-exercise self-rating of the overall intensity of that exercise.

3.3.3.2 Evaluation by physical therapist participants

All trials were video recorded from three angles such that the coronal plane, the sagittal plane, and the plane midway between the coronal and sagittal plane were visible. PT participants viewed de-identified videos showing the balance participant from all three angles of each trial once (see Figure 3.1) and provided per-trial intensity ratings via an electronic PDF form. Additionally, after viewing the videos for all three trials, they rated the overall intensity for that specific exercise. A PT participant rated all 45 trials from each balance participant for whom they were a rater, and each balance participant's videos were rated by 3-5 randomly selected PT participants. Trial order was not randomized so that the assessments could more closely reflect clinical practice in which patients often repeat multiple repetitions of the same exercises one after the other.

51
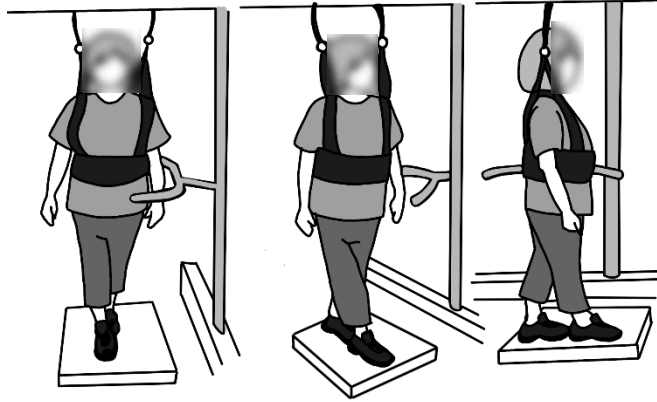
Figure 3.1: Layout of the video viewed by the PT participants. The video showed the coronal plane (left), sagittal plane (right), and the plane midway between the coronal and sagittal plane (center).

Twenty one per-trial PT ratings were excluded due to missing data. Consequently, 450 per-trial and 150 per-exercise self-ratings and 1935 per-trial and 645 per-exercise PT ratings were analyzed.

3.3.4 Data analysis

MATLAB (R2021b, Mathworks, Natick, MA) was used to process and analyze the data according to the plan summarized in Figure 3.2. The ordinal rating data were treated as continuous throughout without impact on the statistical results, as is supported by recent literature [228–232].

3.3.4.1 Evaluation of physical therapist participant intensity ratings

Because to our knowledge only one prior study examined PT ratings and reported limited separation [220], we first examined inter-rater reliability and the relationship between ratings and task difficulty. High inter-rater reliability was a prerequisite for further analysis due to its association with scale validity, study replicability, and the accuracy of alternative assessments.
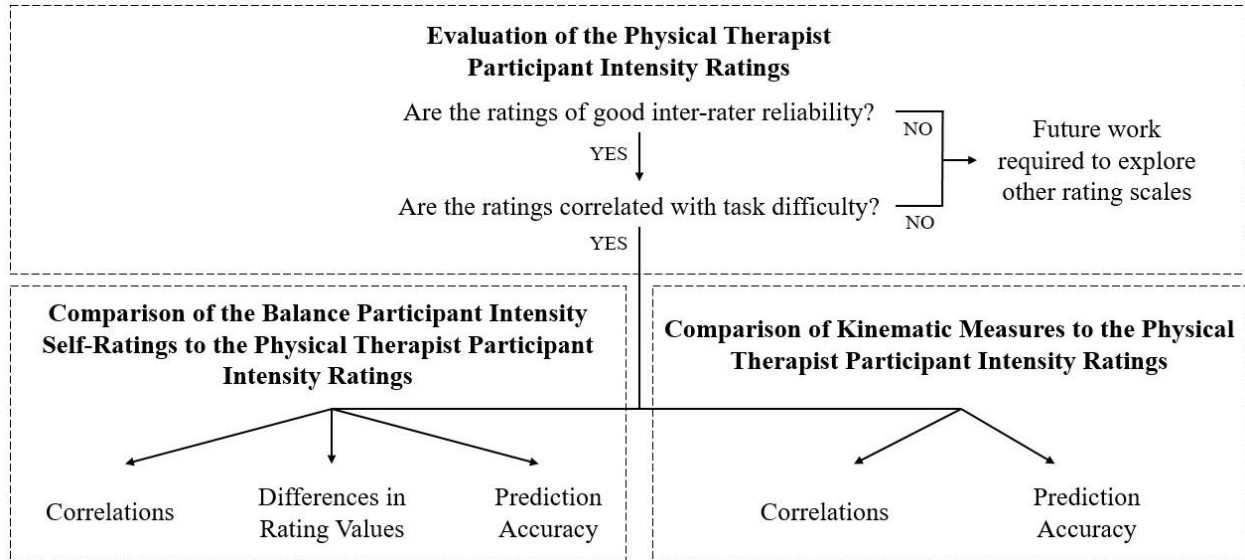
Figure 3.2: An overview of the analysis components. After assessing the PT ratings, these ratings were then compared to self-ratings or kinematic measures.

Reliability is an indicator of a scale's internal structure and as such, is a prerequisite to the scale's validity [233,234]. Low inter-rater reliability may also obfuscate true variation and negatively affect replicability [235–237]. Low inter-rater reliability would also impose a ceiling on the accuracy of alternative assessment methods (e.g., self-assessments or kinematic measures) because the alternative assessment could at best agree with only the majority PT rating. Similarly, weak correlation between the PT intensity ratings and task difficulty would suggest that the ratings scale may not be capturing intensity and may accidentally be capturing a different construct.

The effect of increasing exercise difficulty on PT ratings was evaluated by regressing the ratings against four dimensions of exercise difficulty: surface (coded 1: firm, 2: foam), stance (coded 1: feet apart, 2: feet together, 3: partial heel to toe, 4: heel to toe, 5: single leg), visual input (coded 1: eyes open, 2: eyes closed), and head movements (coded 1: no movements, 2: pitch or yaw movements). These dimensions and their relative difficulties were based on

information from Klatt et al. [215]. The regression was performed using a linear mixed model in which intensity rating was the outcome, one dimension of exercise difficulty was a fixed effect, and the specific balance participant and PT participant were random effects (rating = intercept + dimension of exercise difficulty + balance participant + PT participant + error) [111].

Additionally, the inter-rater reliability of the per-trial PT ratings was evaluated as ICC(2,1) via a linear mixed effects model that decomposed the variance. Fixed effects included the intercept and trial number (i.e., 1, 2, or 3), and random effects included all possible interactions between trial number, exercise, balance participant, and PT participant. The intraclass correlation coefficient (ICC) of the PT per-trial ratings was then calculated by dividing the variance of the subset of random effects that included the rater by the variance from all sources [238,239]. The inter-rater reliability of the PT per-exercise ratings was calculated using the same approach without the inclusion of random effects associated with trial number (since no trial number was associated with the exercise as a whole). ICCs less than 0.5 indicated poor reliability, ICCs between 0.5 to 0.75 indicated moderate reliability, ICCs between 0.75 to 0.9 indicated good reliability, and ICCs greater than 0.9 indicated excellent reliability [239].

3.3.4.2 Comparison of balance participant intensity self-ratings to physical therapist intensity ratings

The overall strength of the relationship between the per-exercise PT and self-ratings was quantified by the Spearman correlation coefficient. The systematic and random differences between the PT and self-ratings were then assessed by examining a contingency table of the two rating modes and quantified by the average and variance of the per-trial rating differences. The structure of these differences was further explored by using a paired t-test to compare the sample variances among the three PT ratings and the three per-trial self-ratings.

The overall effects of these differences were assessed by calculating how frequently a PT participant's rating could be accurately predicted given the self-ratings, i.e., the accuracy when using self-ratings to predict per-trial and per-exercise PT ratings. The predictions were made using a linear model of the per-trial or per-exercise self-ratings.

3.3.4.3 Comparison of kinematic measures to physical therapist intensity ratings

Correlations between trunk kinematics and PT ratings were assessed by first calculating kinematic features and then conducting correlation tests.

Prior to feature calculation, the IMU angular position data were aligned with the body axes via assumed alignment [63] and filtered using a second order Butterworth filter with a 3 Hz cutoff frequency [111]. Kinematic features were then calculated including: root mean square (RMS) of the angular position (Phi RMS, degrees; $Phi\_Angle^2 = AP\_Angle^2 + ML\_Angle^2 = Pitch^2 + Roll^2$), RMS in the anterior-posterior (AP) direction (AP RMS, degrees; i.e., Pitch), RMS in the medial-lateral (ML) direction (ML RMS, degrees; i.e., Roll), mean sway velocity (MV, degrees/s), path length as computed by the sum of the magnitude of the differences between roll and pitch sway data points (degrees), and area of a 95th percentile confidence interval elliptical fit to the roll and pitch sway data (i.e., elliptical area; EA; $degrees^2$) [29,83]. Smaller RMS and EA values have been associated with better balance performance [165,166,168,183], while reports of the relationship between MV and balance performance are mixed [166,183,240]. As suggested by Alsubaie et al. and Schieppati et al., the logarithm of each of these kinematic features were also considered [111,241].

The strength of the relationship between each kinematic feature and the PT ratings was then evaluated using correlation as calculated using a linear model with rating as the outcome variable, kinematic feature as a fixed effect, and balance participant as a random effect (rating =

intercept + feature + balance participant + error) [111]. The marginal correlation was calculated as[242]:

$$R^2 = \frac{\sigma_f^2}{\sigma_f^2 + \sigma_\alpha^2 + \sigma_\varepsilon^2}$$

$$\sigma_f^2 = var(\beta x)$$

where σ_f^2 is the marginal variance calculated from the multiplication of the feature coefficient β and the feature x, σ_α^2 is the variance of the balance participant random effect, and σ_ε^2 is the error variance.

The overall effects of these various correlations were assessed by calculating how frequently a PT participant's rating could be accurately predicted given the sway kinematics. Per-trial and per-exercise PT ratings were predicted using a linear model that included all kinematic features from the trial or all three trials, respectively. The predictions were then rounded to yield integer kinematics-predicted intensity ratings.

Finally, the overall strength of the relationship between sway kinematic measures and intensity ratings was assessed using the Spearman correlation between the kinematics-predicted and per-trial or per-exercise PT ratings.

3.4 Results

3.4.1 Evaluation of physical therapist participant intensity ratings

The per-trial and per-exercise PT ratings were both of good inter rater reliability (per-trial: ICC = 0.868, per-exercise: ICC = 0.860). Additionally, increases in exercise difficulty were significantly correlated with increases in per-trial and per-exercise PT ratings (see Table 2.1).

Table 3.2: Linear relationship between per-trial and per-exercise PT ratings and aspects of exercise difficulty. * denotes significance (p < 0.05).

Exercise Aspect	Per-Trial Intensity Ratings		Per-Exercise Intensity Ratings	
	Estimate [95% CI]	p-Value	Estimate [95% CI]	p-Value
Surface	0.366 [0.241, 0.492]	≤ 0.001 *	0.354 [0.137, 0.571]	≤ 0.001 *
Stance	0.607 [0.561, 0.653]	≤ 0.001 *	0.606 [0.526, 0.686]	≤ 0.001 *
Visual Input	0.584 [0.455, 0.713]	≤ 0.001 *	0.631 [0.409, 0.853]	≤ 0.001 *
Head Movements	-0.337 [-0.465, -0.210]	≤ 0.001 *	-0.300 [-0.520, -0.081]	0.007 *

3.4.2 Comparison of balance participant intensity self-ratings to physical therapist intensity ratings

The per-exercise self-ratings were significantly correlated with the PT ratings (r = 0.769, 95% CI = [0.735, 0.799], p ≤ 0.001).

As shown in Figure 3.3, self-ratings agreed with PT ratings most often for ratings of a 5 (per-trial and per-exercise self-ratings of a 5 agreed with PT ratings 74.8% and 77.5% of the time, respectively). Self-ratings of a 4 also most often corresponded to a PT rating of a 5 (per-trial: 63.0%, per-exercise: 47.5% for self-ratings of a 4) while self-ratings of a 3 corresponded to various PT ratings, and self-ratings of a 2 or 1 most often corresponded to PT ratings between 1 and 3.

The per-trial and per-exercise self-ratings were lower than the PT ratings (absolute per-trial rating difference: 0.385, per-exercise: 0.314, 95% CI = [0.048, 0.581], p = 0.021). Additionally, the standard deviations of the difference in per-trial or per-exercise ratings were 0.920 and 0.961 [0.910, 1.015], respectively. Self-ratings exhibited a smaller variance between trials of the same exercise than the PT ratings did (0.102, 95% CI = [0.049, 0.154], p < 0.001).

As a result, when using self-ratings to linearly predict per-trial or per-exercise PT ratings, the accuracies were 46.6% and 45.9%, respectively.
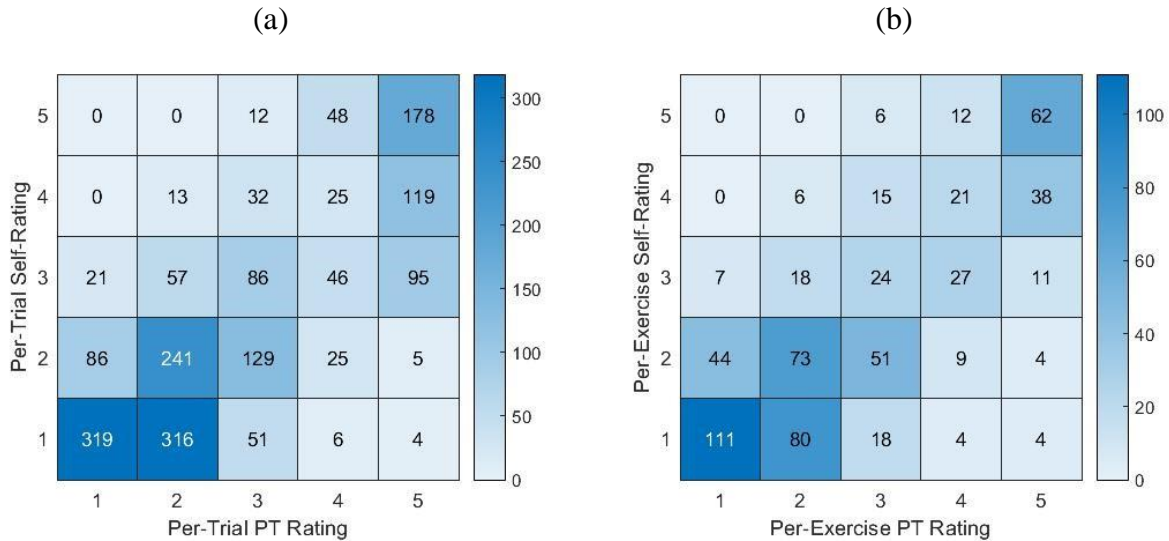
Figure 3.3: Contingency tables for the counts of PT ratings and (a) per-trial or (b) per-exercise self-ratings.

3.4.3 Comparison of kinematic measures to physical therapist intensity ratings

The kinematic features were significantly correlated with PT ratings (see Table 3.3). When using all kinematic features together to predict PT ratings, the resulting predictions were significantly correlated with per-trial or per-exercise PT ratings (per-trial: $r = 0.698$, 95% CI = [0.675, 0.721], $p \leq 0.001$; per-exercise: $r = 0.826$, 95% CI = [0.799, 0.850], $p \leq 0.001$) and agreed with the PT ratings 43.0% and 52.4% of the time, respectively. As shown in Figure 3.4, kinematics-predicted per-exercise ratings agreed with PT ratings most often for ratings of a 5 (kinematics-predicted ratings of a 5 agreed with PT ratings 92.7% of the time). Kinematics-predicted per-exercise ratings of a 4 also most often corresponded to a PT rating of a 5 (42.0% for kinematics-predicted ratings of a 4) but also often corresponded to a 4 (39.1% for kinematics-predicted ratings of a 4). Kinematics-predicted ratings of a 3 corresponded to various PT ratings, and self-ratings of a 2 or 1 most often corresponded to PT ratings of a 2 or 1.

58

(a)   (b)
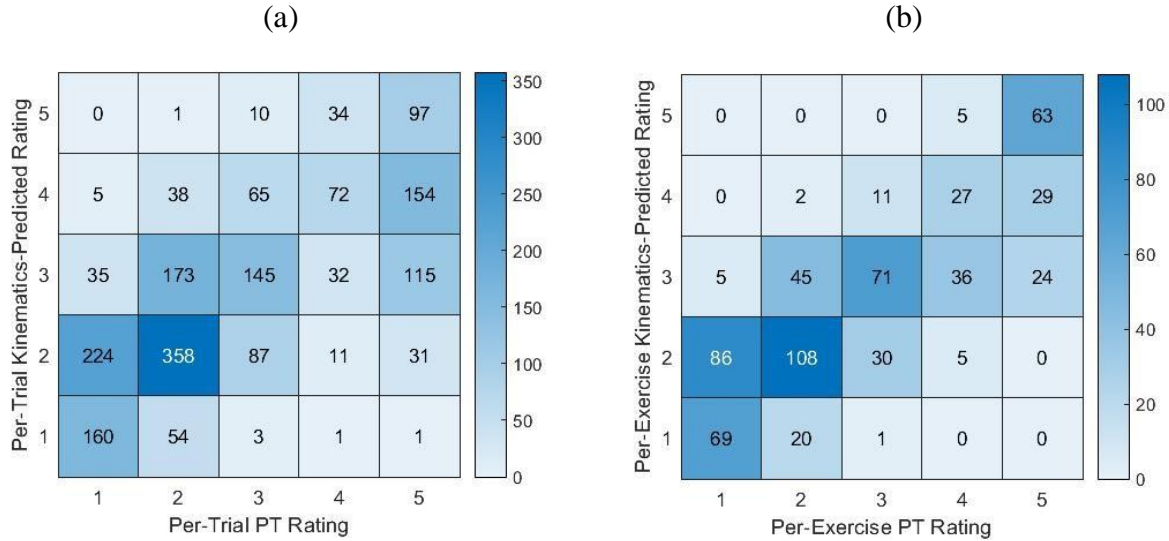
Figure 3.4: Contingency tables for the counts of PT ratings and (a) per-trial or (b) per-exercise kinematics-predicted ratings.

Table 3.3: Correlation coefficients between kinematic features and per-trial PT ratings. RMS denotes root mean square, and MV denotes mean velocity. * denotes significance (p < 0.05).

Kinematic Feature	No Transform		Log Transform	
	R	p-Value	R	p-Value
Phi RMS	0.588	≤ 0.001 *	0.724	≤ 0.001 *
AP RMS	0.482	≤ 0.001 *	0.622	≤ 0.001 *
ML RMS	0.657	≤ 0.001 *	0.735	≤ 0.001 *
Phi MV	0.609	≤ 0.001 *	0.728	≤ 0.001 *
AP MV	0.548	≤ 0.001 *	0.664	≤ 0.001 *
ML MV	0.618	≤ 0.001 *	0.739	≤ 0.001 *
Path Length	0.651	≤ 0.001 *	0.731	≤ 0.001 *
Elliptical Area	0.349	≤ 0.001 *	0.736	≤ 0.001 *

3.5 Discussion

3.5.1 Evaluation of physical therapist participant intensity ratings

The per-trial and per-exercise PT ratings were of good inter-rater reliability, supporting that the study results may be replicable and that it would be possible for the alternative assessments to accurately predict PT ratings. Higher ratings were also associated with higher exercise difficulty along three out of four dimensions [215] when accounting for differing individual balance participant ability, suggesting that the ratings do reflect task intensity. While

higher ratings were not associated with more difficult head movement conditions, this could be due to the majority of balance participants having no vestibular dysfunction and consequently being less affected by head movement. Similarly, Alsubaie et al. and Anson et al. reported significant associations between balance exercise difficulty and self-ratings of exercise intensity or postural stability [70,111].

It is important to note that while the descriptors for PT ratings of 1, 2, and 3 referenced amount of sway, prior research has reported variable sway results for people with balance impairments (e.g., sometimes increased sway, sometimes decreased sway) [184–187]. Increased sway may be interpreted as poorer control over the body's position while decreased sway may reflect an adaptive strategy in which people stiffen in order to simplify the balance task by reducing the degrees of freedom of movement [243]. As a result, future work may investigate alternative scale descriptors.

3.5.2 Comparison of balance participant intensity self-ratings to physical therapist intensity ratings

While the self-ratings were strongly correlated with the PT ratings, the self-ratings were an imperfect approximation of PT ratings. As has been described by the Dunning-Kruger effect and reported in other contexts [244–246], balance participants overestimated the quality of their performance, self-rating the exercise as less intense than the ratings provided by the PT participants. Accounting for this offset may therefore improve the agreement between PT and self-ratings. However, the significant standard deviation in the rating difference suggests that a simple adjustment is inadequate when using self-ratings as a support to PT assessment. The standard deviation in rating difference may be partially driven by the lower variation in self-ratings between the three trials of an exercise compared to the PT's ratings. This may reflect

60

differences in rating strategy such as the balance participants more heavily considering their performance of prior trials when rating the current trial. The variation in rating difference may also be due to differences in participants' determinations of what constituted a loss of balance, imperfect observations of the performance (e.g., a PT participant not seeing or a balancer participant not noticing movement of the feet), imperfect recollection of the performance when providing the rating, or accidental misuse of the scale (e.g., selection of a 1 when intending to select a 5). These factors likely played some role as is reflected in imperfect agreement for ratings of 4 or 5 and occasional confusion between ratings of 1 and 5 (see Figure 3). Confusion about the directionality of the scale (i.e., whether 5 is most or lease intense) is further evidenced by trials where the self-rating and multiple PT ratings all agree (e.g., 1) while a single PT rating disagrees (e.g., 5).

As a result of these differences, predicted PT ratings based on self-ratings exhibited moderately low accuracy. The common confusion between ratings of a 4 or a 5 as well as between ratings of a 1 or a 2 and the overall ambiguity for ratings of a 3 might suggest that balance participants are better able to distinguish between two levels of balance intensity (e.g., higher-lower). The confusion between ratings of 1, 2, or 3 may also reflect the aforementioned scale limitation in which the PT's descriptors reference sway, which may indicate either good or poor balance. As a result of these issues, if using self-ratings to support intensity assessment during telehealth or other contexts in which traditional PT assessment might be difficult, self-ratings might be used to suggest higher or lower intensity but may not suggest more granular levels of intensity.

3.5.3 Comparison of kinematic measures to physical therapist intensity ratings

The kinematics-predicted intensity ratings were also imperfect yet informative approximations of PT ratings, as reflected by strong correlations, but moderately low prediction accuracies. The correlations between kinematic features and per-trial PT ratings were higher in the ML direction than in either AP or Phi directions, suggesting that, on average, PT participants based their evaluation of balance intensity more heavily upon movement in the ML direction. Similar correlation values as well as higher correlations in the ML direction were also reported by Alsubaie et al. in two investigations of intensity self-ratings (R between 0.56 and 0.88) [111,112]. The correlation coefficients were slightly higher when using the logarithm of the kinematic feature compared to the untransformed values, especially so for EA. Higher correlation between ratings and the logarithm of the kinematic feature than with the original measure were also reported by Alsubaie et al. regarding intensity self-ratings and by Scieppati et al. and Anson et al. regarding postural stability self-ratings [70,111,241].

Agreement between kinematics-predicted intensity ratings and PT ratings was higher than for self-ratings. The prediction accuracies were likely similarly affected by accidental misuse of the scale or imperfect recollection at the time of rating by PTs. Additionally, as observed in one trial, kinematic measures may inaccurately reflect balance ability if the balance participant accidentally stops the exercise early. Kinematic measures summarizing the time series without consideration of the temporal order may also inaccurately reflect balance ability during trials with distinct periods of behavior (e.g., weight shifted during the trial). Agreement was highest for kinematics-predicted ratings of a 5. If using kinematics to support PT assessments during telehealth or other applications, kinematics may be more heavily considered during high-intensity exercises with ratings near a 5 or for low-intensity exercises with ratings of a 1 or 2.

In this first and necessary study on the differences between alternative modes of balance intensity assessment, both self-ratings and sway kinematics were shown to have the potential to support PT assessment of balance exercise intensity when expert visual assessment is difficult or limited, with sway kinematics being more accurate than self-ratings. Intensity assessments might be used in conjunction with frameworks for exercise progression such as the one proposed by Klatt et al. so that balance training can be remotely assessed and progressed over time [247]. However, the results from this study suggest that self-ratings and conventional trunk kinematic measures cannot fully replicate or substitute for PT assessments. Based on our findings, PTs might employ self-ratings and/or sway kinematic measures to supplement their partial visual assessments during telerehabilitation or home-based training. If doing so, our preliminary results suggest that the PT should consider self-ratings as indications of high versus low intensity rather than five levels, and kinematic measurements should be more heavily considered during exercises at intensity extremes (e.g., very high or very low). These extreme ratings may assist in avoiding unsafe exercises or those that are considerably too easy; however, the lack of reliability at moderate intensities limits the use of these alternative rating methods. Combining self-ratings of intensity with kinematic measures as well as employing more complex techniques may lead to more accurate predictions, as reported by Bao et al. and Kamran et al. [122,123]. Further exploration of related machine learning architectures and expanded datasets might further improve the prediction accuracy.

Limitations of this study included the performance of a subset of balance exercises (i.e., static standing) and a subset of balance participants that would benefit from balance training (i.e., older adults and adults with vestibular disorders). The kinematics-predicted ratings were also estimated via a single linear model of the selected kinematic features, which limited the

63

interpretation of model coefficients and which may have limited the prediction accuracy. Future work could include the exploration of alternate scale descriptors without reference to amount of sway, evaluation of additional balance-related pathologies and balance exercises, evaluation of the effects of PT experience level, analysis of full-body kinematics and use of identifiable videos (i.e., without blurred faces), and the use of data science methodologies such as machine learning approaches to capture additional trends in the kinematic data.

3.6 Conclusion

This study examined the relationship between PT intensity ratings, self-assessments, and kinematic measures. Both self-ratings and trunk kinematic features correlated significantly with PT ratings of intensity. Based on the findings from this study, self-ratings may better distinguish between two levels of intensity (i.e., higher-lower) than five levels of intensity. Furthermore, kinematics-predicted intensity ratings at either extreme (i.e., 1: steady or 5: loss of balance) may be more reliable indicators of intensity than the other ratings in the evaluated scale. These findings suggest that self-assessments and kinematic measurements may support PT intensity assessments during contexts in which visual assessment is difficult (e.g., during telerehabilitation).

Part II:

Advancing Inertial Sensors for Use During Real-World Running

Chapter 4 Error-State Kalman Filter for Lower-Limb Kinematic Estimation: Validation for Running

4.1 Abstract

Inertial measurement units (IMUs) provide the opportunity to study running gait outside of traditional laboratory environments. Previous work has demonstrated the efficacy of an error state Kalman filter (ErKF) in estimating 3D lower-limb kinematics during walking gait; however, such methods have not previously been applied to running gait. The purpose of this study was to extend and evaluate an ErKF algorithm for 3D lower-limb kinematic estimation during running on a level treadmill. To our knowledge, this is the first study to evaluate a filter-based algorithm for three-dimensional lower limb joint angles during running. After making necessary modifications to accommodate salient differences in running versus walking inertial data, the ErKF joint angle estimates and extracted key gait features were compared to marker-based optical motion capture (OPTIC) estimates as well as a previously published running dataset. The sagittal plane joint angle estimates were similarly accurate to those from OPTIC as well as previously published IMU-based methods employing machine learning algorithms (RMSD < 8 deg). Frontal and transverse plane estimates, while comparable to those reported

previously, may require additional study before use. Many of the resulting key features of gait were comparable to OPTIC estimates and published data. These results suggest that ErKF algorithms may yield 3D lower-body kinematic estimates during running which are comparable in accuracy to existing machine learning methods while offering additional benefits such as adaptation to an experimental design (e.g., speed, running surface, etc.). ErKF algorithms should be further developed for kinematic assessments during "real-world" running using wearable inertial sensors.

4.2 Introduction

Running gait analysis has traditionally been restricted to laboratory environments in which treadmill or short overground runs are analyzed using "gold-standard" biomechanical data obtained using multi-camera marker-based optical motion capture (i.e., stereo-photogrammetric) systems [38,126]. However, these methods can be obtrusive and necessarily limit analyses to pre-defined and artificial running environments [18]. Running kinematics may differ between running environments[132]; for example, sagittal plane kinematics differ at footstrike between treadmill and overground running [132], tibial shock increases over the course of exhaustive runs in controlled laboratory settings but not real-world marathon races [134–136], and both surface and surface regularity can impact numerous biomechanical measures [248]. In addition, traditional marker-based motion capture systems are relatively expensive, require time-consuming setup, and need highly trained staff to operate [127,128]. While marker-less motion capture systems may alleviate some of these technical challenges [249], analyses are restricted to limited capture volumes [249–251].

Body-worn inertial measurement units (IMUs) provide an alternative technology that may address these limitations, offering the opportunity to unobtrusively capture overground running mechanics in a variety of training and racing environments [18]. IMUs are also relatively accessible and easy to wear on a day-to-day basis. However, because IMUs directly measure proper acceleration and angular velocity, the derivation of many of the biomechanical features traditionally used in analyses of running gait, like joint angles, presents a challenge.

As a natural result of IMUs directly measuring proper acceleration and angular velocity, the majority of common IMU-based running gait metrics derive from these measurands [31,146]. These metrics can have significance for performance or injury outcomes; for example, tibial

acceleration is often monitored as a metric of running workload [252]. However, position-domain measures such as stride length, foot inclination angle, or center of mass vertical excursion are also informative and have traditionally been evaluated [146,253,254]. Position-domain measures may also be more easily understood by and communicated to coaches and athletes, a central need for devices providing biomechanical feedback [253]. Robust algorithms for the estimation of position-domain kinematic measures from IMU measurands (proper linear acceleration and angular velocity) may increase the set of kinematic measures that may be studied and employed in "real-world" running contexts.

When estimating position information from IMUs, the primary challenge is the accumulation of drift error and other errors arising from several sources including measurement noise, soft tissue artifacts, sensor-to-body segment misalignment, and finite sampling rates. For example, drift errors due to fixed biases compound linearly when the gyroscope signal is integrated once to obtain angular position (i.e., orientation) and quadratically when the accelerometer signal is integrated twice to obtain linear position. Sensor fusion methods such as extended Kalman filters or complementary filters can be used to process accelerometer and gyroscope data in estimating position information [23,255]. These algorithms often leverage task-specific information to correct for drift. For example, the zero-velocity update (ZUPT) method uses the assumption that the foot has zero velocity during each stance phase to correct for drift in the foot's estimated linear velocity. More recently, various machine learning methods have been applied to the estimation of lower limb joint angles [256].

Much like in walking gait [253,257–260], many of the algorithms estimating joint angles from IMU data during running have focused on the sagittal plane [261–267]. Sagittal plane joint angles have been estimated with varying success, yielding correlations between IMU-based and

68

marker-based motion capture based estimates between 0.82 [268] and 0.99 [261–263,266] and root mean square difference (RMSD) between 3.7 [269] and 13.0 [261] deg. Frontal and transverse plane joint angles have been estimated in fewer studies and less accurately than sagittal plane estimates, with correlations between 0.72 [266] and 0.99 [266] (see Table 4.9 and 4.10 in section 4.5.2 for more detail). In all planes, the majority and the most accurate of algorithms have employed machine learning rather than the aforementioned sensor fusion approaches. To date, no studies have sought to validate the accuracy of sensor fusion algorithms in estimating more than a single sagittal plane joint angle and a single frontal or transverse plane joint angle during running. It is possible that filter-based algorithms such as Kalman filters, which have shown success in walking gait [149,150], may produce three-dimensional joint angle estimates of similar accuracy to those resulting from marker-based motion capture, marker-less motion capture, and existing commercial or machine learning based inertial motion capture algorithms. However, compared to existing inertial motion capture algorithms, filter-based methods such as the ErKF considered herein may offer benefits such as requiring smaller datasets for algorithm development [151] and allowing for intentional adaptation between experiments with varying sensor noise characteristics or placement, running surfaces and inclines, etc.

Potter et al. recently developed an error-state Kalman filter (ErKF) algorithm that estimated 3-dimensional lower limb kinematics using data from seven IMUs. The algorithm leveraged several known biomechanical constraints to improve estimates through ZUPT, gravitational, joint center, and joint axis-based corrections [149,270]. Importantly, these methods make minimal assumptions about task conditions, as opposed to prior algorithms which have assumed level ground [150] or straight [271] walking. As a first step in validating this algorithm,

Potter et al. considered a 3-body mechanical model (a "walker" with a pelvis and two legs). When evaluating the algorithm on both simulated and experimental data, the RMS differences for the three estimated hip joint angles were ≤ 0.2 deg compared to simulation and ≤ 1.4 deg compared to experimental marker-based motion capture. The RMS differences for stride length and step width were $\leq 1\%$ and 4%, respectively compared to simulation and 7% and 5%, respectively compared to experimental motion capture [149]. Potter et al. then considered a full 7-body model and evaluated it on human subject data and for both fast and slow walking. They report RMSD relative to marker-based motion data that is generally ≤ 5 deg for all three estimated ankle joint angles and flexion/extension and abduction/adduction of the hip and knee joint angles. Additionally, the RMSD of stride length and step width estimates were both ≤ 0.05 m for the fastest walking gait (> 0.8 m/s) [270]. However, this ErKF algorithm has not yet been validated for running gait, and it is possible that the differences between running and walking gait (e.g., shorter contact times, higher signal to noise ratios) may impact the efficacy of the algorithm [272].

In this study, we aimed to extend and evaluate this ErKF algorithm for lower-limb kinematic estimation during level treadmill running (where simultaneous optical, marker-based motion capture is possible). To our knowledge, this was the first study to evaluate a filter-based algorithm for three-dimensional lower limb joint angles during running. This study presents a first and necessary step towards the estimation of lower-limb kinematics from body-worn IMUs using algorithms which can be intelligently adjusted in order to accommodate various "real-world" running contexts.

4.3 Methods

In this study, participants ran indoors on a treadmill with kinematic data recorded simultaneously via IMU and optical, marker-based motion capture (OPTIC). The three-dimensional limb positions and joint angles estimated via IMU and an ErKF algorithm were compared to OPTIC estimates resulting from common methods. Due to limitations of the marker set as discussed in section 4.4.1, joint ranges of motion were also compared to those from a previously published dataset [273]. This dataset was selected due to its increased number of markers including non-collinear marker clusters as well as the similarity of task and participants (i.e., treadmill running at a speed of 12.6 km/h, 28 participants with weekly mileage greater than 20 km, age 34.8 ± 6.7 years, height 1.76 ± 0.07 m, mass 69.6 ± 7.7 kg).

4.3.1 Participants

Six recreational runners (6 male, 36.8 ± 10.6 years, 1.72 ± 0.05 m, 70.4 ± 5.2 kg; running history shown in Table 4.1) participated in a single day of running. Inclusion criteria included being between 18 and 50 years of age, being a recreational runner as defined by Hoitz et al. [274], having a rearfoot strike pattern, and being able to run without fatigue for at least 55 minutes. The study was approved by the University of Rome Foro Italico Review Board (CAR 82/2021) and all participants gave written informed consent in accordance with the Helsinki Declaration.

Table 4.1: Participant self-reported running history.

Participant	Years of Regular Running	Typical Pace (min:s/km)	5 km Race Time (min:s)
1	>15	4:40	17:00
2	5	4:45	20:22
3	3	5:15	20:30
4	6	4:30	23:00
5	10	4:00	N/A
6	5	4:50 to 5:10	22:45

4.3.2 Equipment

Kinematic data was collected simultaneously via OPTIC and IMUs. Seven nine-axis IMUs (Opal, APDM Wearable Technologies Inc., Portland, OR) were worn on the feet over the shoe laces, the medial distal tibial shafts, the lateral proximal thighs, and the lumbar spine. All IMUs were secured with elastic bands. OPTIC data was collected using a 7 camera Vicon system (Vicon Industries, Inc., Hauppauge, NY) and a conventional gait model (CGM) in which participants wore 45 markers: 38 in standard Plug-In-Gait (PiG) full body placements [275] and one on each IMU face. OPTIC and IMU data were synchronized and sampled at 200 Hz [276,277].

4.3.3 Procedures

After a warmup and familiarization period, the participants completed two six-minute running trials on a treadmill (T170DE, COSMED, Rome, Italy) at 14 km/hr and 0% incline. At the beginning of the session, anatomical measurements benefitting motion capture analysis were recorded (bilateral leg length, knee width, ankle width, shoulder offset, elbow width, wrist width, and hand thickness). Prior to each trial, the participant completed a static standing calibration.

4.3.4 Data Analysis

Nexus 2 (Vicon Motion Systems Inc., Oxford, UK) and MATLAB (R2022b, Mathworks, Natick, MA) were used to process and analyze the data. Due to errors in the collection of OPTIC data, two trials were excluded. A resulting total of over 1500 strides were analyzed.

4.3.4.1 Optical Motion Capture Data Processing

Prior to gap filling, marker labels were manually cleaned, including the removal of labels during periods in which inordinately large changes in marker location were observed, indicating

high noise levels. Gaps were then filled using Nexus' automated pipelines with parameters similar to those previously reported [278–283]. Woltring spline fill was applied to gaps of up to 10 frames (or 5% of the sampling rate), rigid body fill was applied to gaps of up to 20 frames in the pelvis markers, and pattern fill was applied to gaps of up to 20 frames using automated donor trajectories. Finally, unlabeled trajectories were deleted and data was exported to MATLAB where the marker locations were filtered with a fourth order low pass Butterworth filter with cutoff frequency 10 Hz [273,284,285].

Three-dimensional lower limb joint angles were estimated using a combination of standing calibration data and running data. As shown in Figure 4.1, the rigid transformations between segment frames and ISB-recommended anatomical frames [286] were estimated during static standing. Then, during running, the segment frames were estimated and subsequently transformed to the anatomical frames. The segment frame definitions were selected to maximize the non-collinearity of the makers used in defining the rigid body [287], and collinearity was assessed by calculating the planar angles $\Theta_{1\text{-}3}$ as shown in Figure 4.1.

In order to define the anatomical frames during static standing, the hip joint centers were estimated following Hara et al. via the LASI, LPSI, RASI, and RPSI markers and the leg length [288]. The knee and ankle joint centers were estimated using average joint axes as measured in a previously published study [273]. From this published dataset, average knee and ankle joint axes were defined in the knee and ankle axis, respectively (as defined in Figure 4.2). The knee and ankle centers for participants in this study were then calculated by traveling from the lateral joint marker half of the joint width along the estimated joint axis. In order to assess the effect of inaccuracies in the joint center estimates on the resulting joint angle estimates, the joint center estimates were perturbed, and the effect on the joint angle estimates was observed. Six

perturbations were performed for each joint: ± the inter-person standard deviation from the

published dataset along each of the primary body axes.
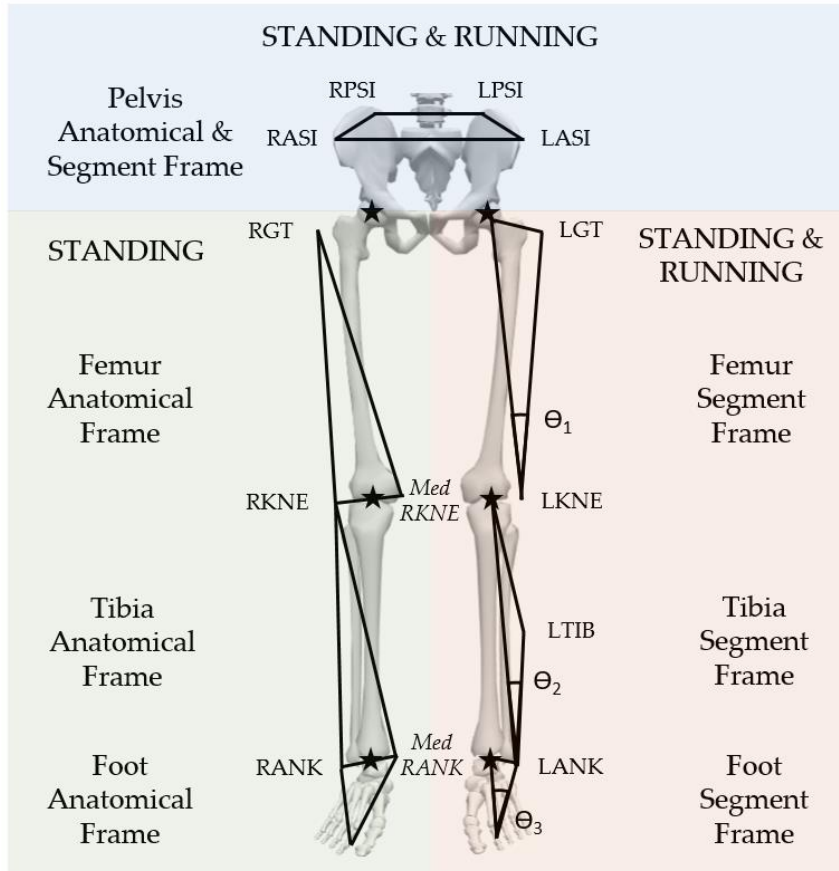
Figure 4.1: Locations used to define the lower-body anatomical and segment frames. The segment frames can be defined during both static standing and running while the anatomical frames are defined and related to the segment frames during only static standing. In order to reduce the effect of marker near-collinearity between markers placed on each segment (e.g., GT, KNE, THI), the joint center estimated using the proximal, "upstream", body segment is used in estimating the orientation of the distal, "downstream", body segment. R and L denote right and left, PSI and ASI denote posterior and anterior superior iliac, GT denotes greater trochanter, THI denotes thigh, KNE denotes the lateral femoral epicondyle, *Med KNE* denotes the estimated medial femoral epicondyle, TIB denotes tibia, ANK denotes lateral ankle, *Med ANK* denotes the estimated medial knee, and Θ_1, Θ_2, Θ_3 are the planar angles of the thigh and shank.

4.3.4.2 IMU Data Processing

The original ErKF algorithm was developed by Potter, et al. for estimating three-

dimensional, three degree of freedom lower limb joint angles during walking gait given IMU

data from the feet, shanks, thighs, and lower back [149,270]. First, a high-level summary of the

ErKF algorithm for walking is provided for context while a detailed description is available

74

[149,270]. Second, the modifications to this previously published algorithm which are needed to extend it to running are detailed below.
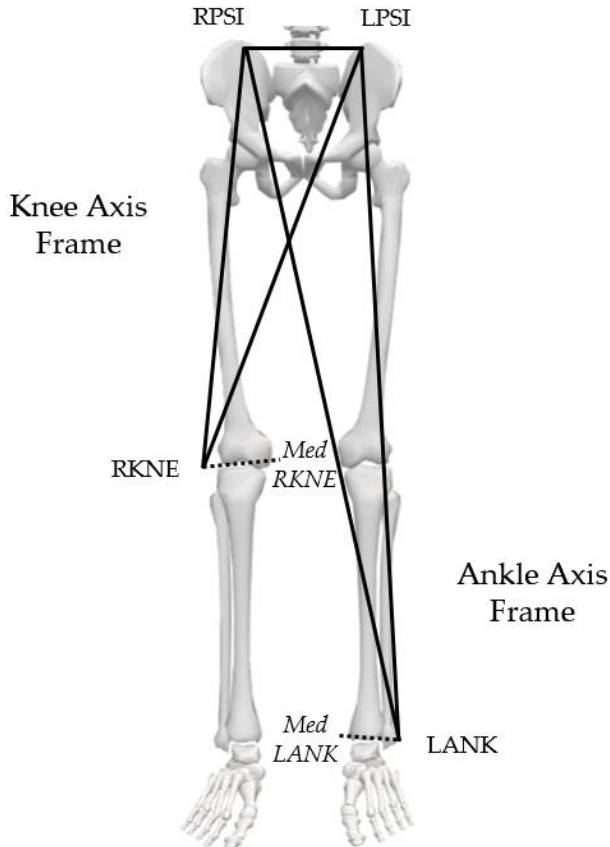
Figure 4.2: Locations used to define the knee and ankle axis frames used to translate the knee and ankle joint axis estimates from a previously published dataset to the current dataset during static standing. R and L denote right and left, PSI denotes posterior superior iliac, KNE denotes lateral knee, *Med KNE* denotes the estimated medial knee, ANK denotes lateral ankle, and *Med ANK* denotes the estimated medial knee.

Summary of the ErKF Algorithm for Walking

The ErKF algorithm functions in two principal steps as shown in Figure 4.3. First, the state is projected forward one time step via the "predict" step during which acceleration and angular velocity measurements are pulled and integrated to estimate the state. The error covariance is also updated using the estimated process noise variance.

Next, the state is updated using known kinematic states and constraints. These constraints are incorporated probabilistically using the general measurement model

$$z = h(x) + c$$

where z is the observed measurement, h(x) is the expected measurement represented as a function of the state x, and c is Gaussian noise of covariance C. This model is applied to four constraints as shown in Figure 4.4. The ZUPT correction applies a zero-slip assumption such that the velocity of the feet is approximately zero during the stance phase of walking as identified by low dynamics (i.e., acceleration magnitude close to gravity, angular rate close to zero, and angular acceleration close to zero). The gravitational tilt correction assumes that the acceleration during still periods (as defined by low dynamics) is due only to gravity and therefore the orientation of the acceleration vector is approximately aligned with the global vertical. The joint axis correction assumes that the hip and knee joints act as approximate hinges in which the joint axis is constant and shared between proximal and distal segments. Note that because the motion of the ankle joint is complex, the ankle is not assumed to be an approximate hinge. Finally, the joint center correction assumes that there are constant hip, knee, and ankle joint centers which are approximately shared by proximal and distal segments. By applying these constraints probabilistically, they can be more or less strictly enforced; for example, the knee can be modified to be more or less "hinge-like".

The initial state, rotation matrices describing the IMU sense frames in the global frame (i.e., $R_{IMU/Global}$), and joint center locations in the IMU sense frame were estimated using the marker-based motion capture data, a limitation noted by Potter et al. [64]. Further derivation of these equations including additional formulas for the Jacobian of the process model ($F_{xj,k}$), the

76

Jacobian of the error-state reset operation with respect to the error state (G_k), and the process noise variance (Q_j) are available [149,270].
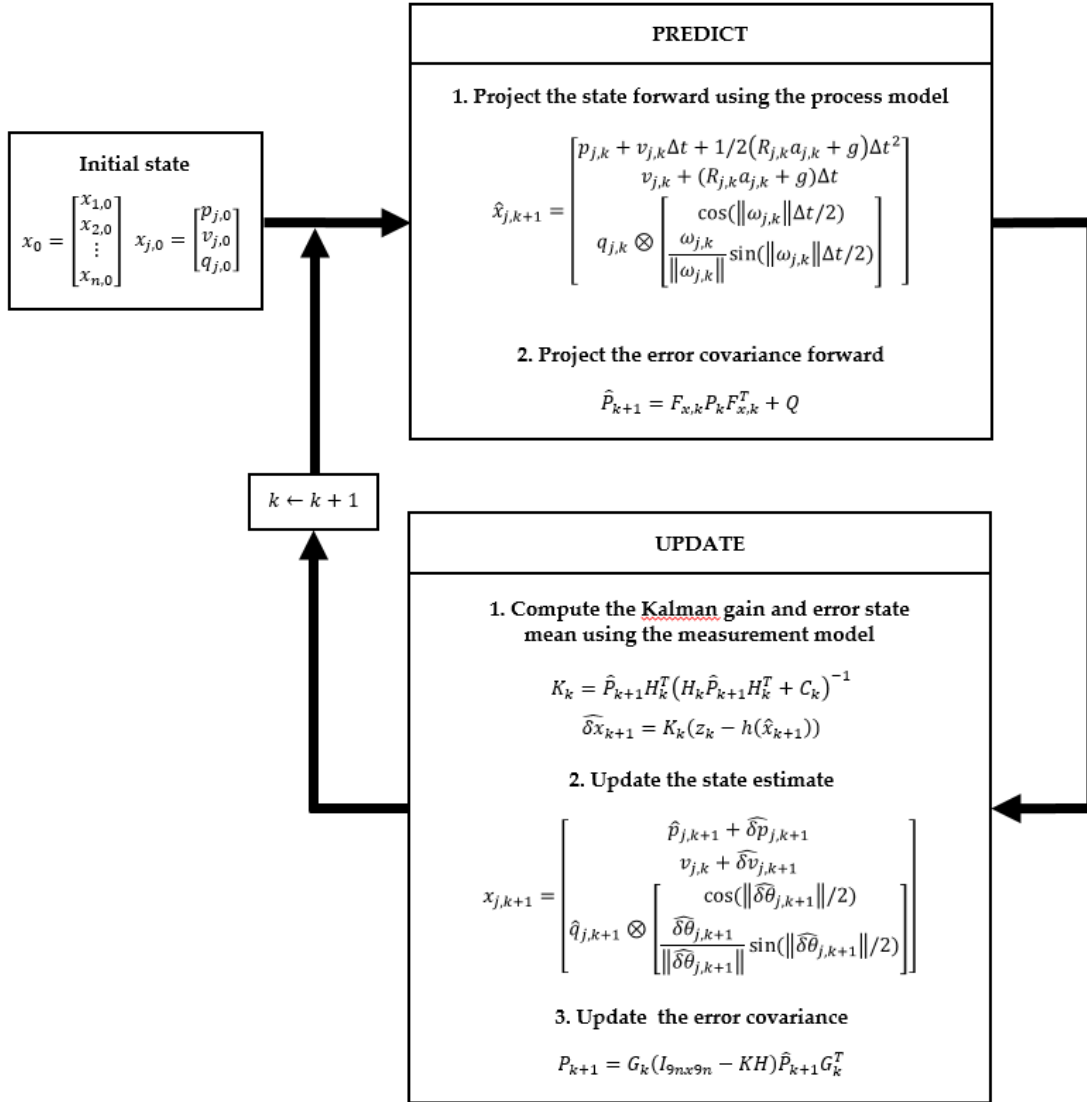
Figure 4.3: The ErKF algorithm used in estimating lower limb kinematics from IMU data. x_j is the (10x1) state (i.e., position, velocity, and quaternion orientation) of the jth IMU where j = [1,n], p_j is the (3x1) position vector of the IMU in the global lab-fixed frame, v_j is the (3x1) velocity vector of the IMU in the global frame, q_j is the (4x1) quaternion rotation vector describing the IMU sense frame in the global frame, k is the time-step, Δt is the sample time, $a_{j,k}$ and $w_{j,k}$ are the measured acceleration and angular velocity of the jth IMU at time-step k, $R_{j,k}$ is the rotation matrix corresponding to $q_{j,k}$, P_k is the error covariance at time-step k, $F_{xj,k}$ is the Jacobian of the process model for the jth IMU at time-step k, I_{mxm} is an mxm identity matrix, T denotes the transpose of a matrix, Q_j is the process noise variance for the jth IMU, z_k is the observed measurement at time step k, $h_k(x_k)$ is the expected measurement represented as a function of the state x at time step k, C_k is the Gaussian noise covariance at time step k, H_k is the Jacobian of the measurement (i.e., update) model at time step k, K is the Kalman gain, $\widehat{\delta x}$ is the error state mean, and G_k is the Jacobian of the error-state reset operation with respect to the error state at time-step k. Full details available[149,270].

Joint Axis Correction

$$h_{JA}(x) = R_1 e_1 - R_2 e_2$$

$$z_{JA} = \begin{bmatrix} 0 \\ 0 \\ 0 \end{bmatrix} \quad C = \sigma_{JA}$$

Gravitational Tilt Correction

$$h_{tilt}(x) = R^T \begin{bmatrix} 0 \\ 0 \\ 1 \end{bmatrix} \quad z_{tilt} = \frac{a}{\|a\|}$$

$$C = \sigma_{tilt}$$

ZUPT Correction

$$h_{ZUPT}(x) = v_{IMU}$$

$$z_{ZUPT} = \begin{bmatrix} 0 \\ 0 \\ 0 \end{bmatrix} \quad C = \sigma_{ZV}$$

Joint Center Correction

$$h_{JC}(x) = (p_1 + R_1 r_1) - (p_2 + R_2 r_2)$$

$$z_{JC} = \begin{bmatrix} 0 \\ 0 \\ 0 \end{bmatrix} \quad C = \sigma_{JC}$$
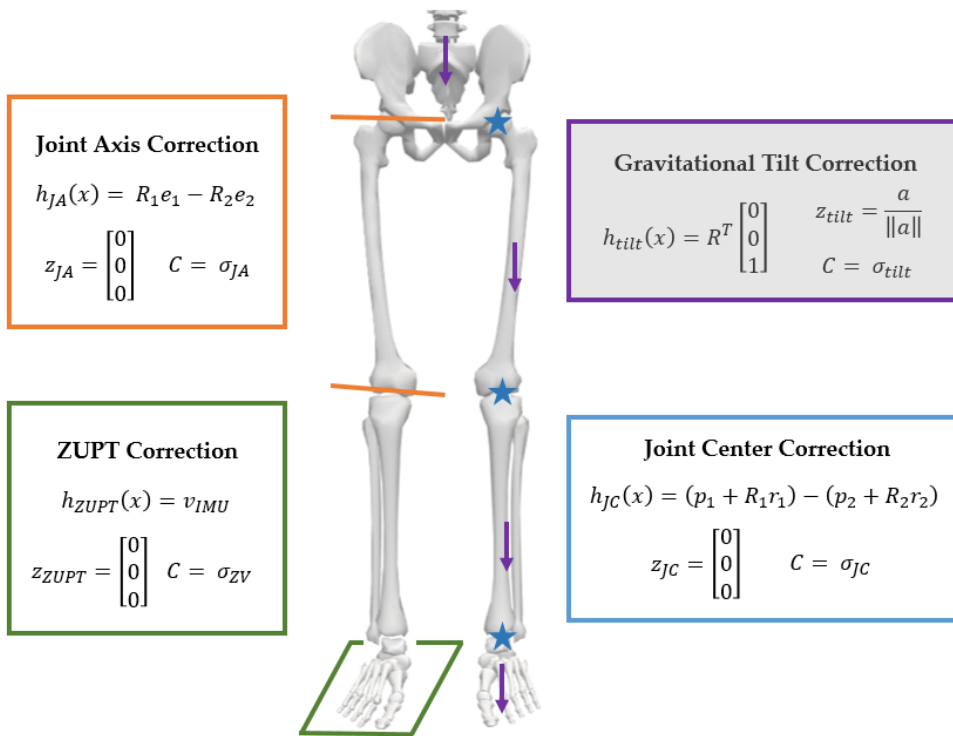
Figure 4.4: Summary of the known kinematic states and constraints included in the ErKF algorithm. Gray shading denotes use for only walking and not running gait. z is the observed measurement, $h(x)$ is the expected measurement represented as a function of the state x, C is the Gaussian noise covariance, *JA* is the hip or knee joint axis correction, σ is the noise covariance parameter, the subscript i indexes the two adjacent body segments, R is the rotation matrix describing the IMU sense frame in the global lab-fixed frame, e is the unit joint axis for segment i expressed in the frame of IMU_i, *ZUPT* is the zero velocity update correction, v_{imu} is the (3x1) velocity vector of a foot mounted IMU in the global frame, *tilt* is the gravitational tilt correction, T denotes the transpose of a matrix, a is the tridimensional measured acceleration, $\|a\|$ is the norm of the measured acceleration, *JC* is the joint center correction, r_i is the position of the joint center in the frame of IMU_i, and p_i is the position of IMU_i in the global frame.

Modification of the ErKF Algorithm for Running

Four principal modifications to the ErKF algorithm were made to accommodate salient differences in walking versus running inertial data.

First, the gravitational correction used for walking was not employed for running as there were no periods of adequately low movement as defined by acceleration, angular velocity, and angular acceleration data thresholds.

Second, while the ZUPT corrections for walking were applied to stance periods identified by acceleration, angular velocity, and angular acceleration thresholds, the ZUPT corrections for

running were applied during midstance as detected by low gyroscopic energy of the feet

[289,290] calculated as

$$E_\omega(t) = \sum_t^{t+\Delta T} \|\omega_t\|^2$$

where ω is the triaxial angular velocity of the foot, t is the time at which to evaluate energy, and ΔT is the duration over which to evaluate energy (0.02s in this study).

Because gyroscopic energy is influenced by sensor noise as well as foot contact type, a unique energy threshold was automatically selected on a per-trial and per-foot basis so as to minimize the threshold while maintaining an average of at least 5 data points per stride below the threshold. An example of the resulting midstance periods detected is shown in Figure 4.5.
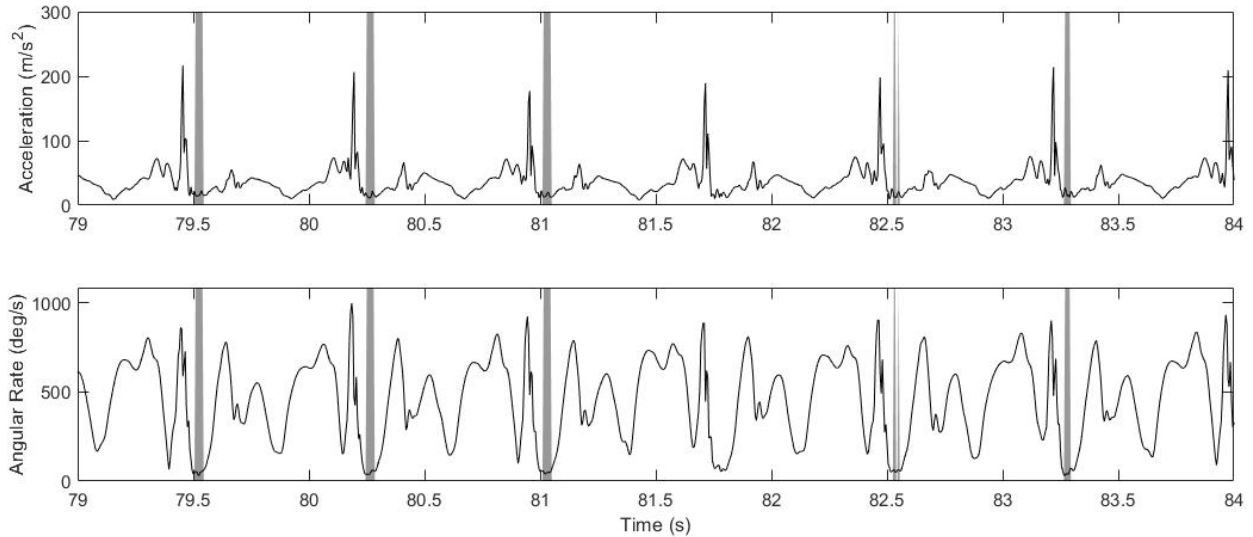
Figure 4.5: Example midstance periods as detected by low gyroscopic energy of the foot (displayed as shaded bands).

Third, a new method for sensor-to-segment alignment was employed due to differences in the OPTIC marker set. While Potter et al. [149] employed an augmented data method in which marker clusters on each IMU and each body segment were used for alignment, the alignment in this study combined functional and augmented data methods [63]. As shown in Figure 4.6, each sensor-to-segment rotation (i.e., the rotation matrix describing the IMU sense frame in the

anatomical frame, $R_{IMU/Anatomical}$) was defined using the relationship between global, anatomical, and IMU sense frames, or

$$R_{IMU/Global} = R_{Anatomical/Global}R_{IMU/Anatomical}$$

where $R_{IMU/Global}$ is the rotation matrix describing the IMU sense frame in the global frame, and $R_{Anatomical/Global}$ is the rotation matrix describing the anatomical frame in the global lab-fixed frame. For each body segment, $R_{Anatomical/Global}$ was defined using the OPTIC data as previously described. For each IMU, $R_{IMU/Global}$ was defined using the gravity vector during static standing and, for all IMUs with the exception of the lumbar IMU, the principal angular velocity during running. It was assumed that the lumbar IMU horizontal axis was aligned with the medial-lateral pelvis.
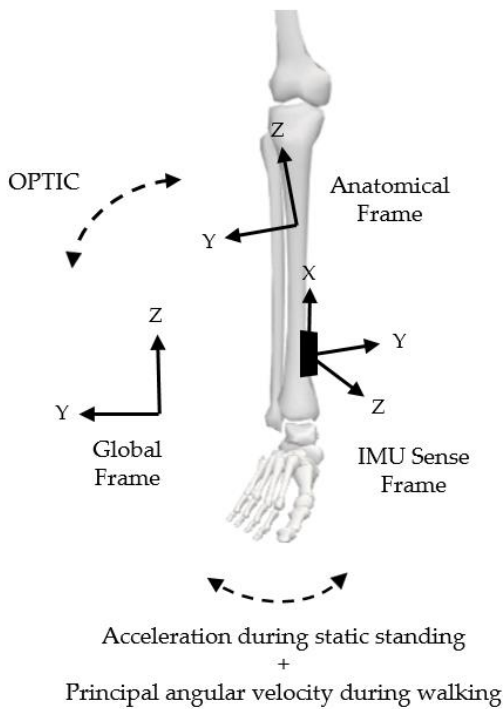
Figure 4.6: Relation between anatomical, global lab-fixed, and IMU sense frames. The rotation between anatomical and global frames were defined using OPTIC data, while the relationship between anatomical and IMU sense frames were defined using two functional movements.

Finally, the joint center locations in the IMU sense frames were identified by the mean of the OPTIC-estimated joint centers during running as defined in the IMU sense frame.

Fourth, new noise parameters governing the probabilistic application of corrections in the ErKF algorithm were selected in order to optimize range of motion and angle waveform accuracies (see Table 4.2). The differences between noise parameters selected for running gait and the parameters selected for various walking gaits demonstrate intelligent modification of the algorithm using task-specific knowledge. For example, approximate zero velocity periods during running often exhibit higher velocities than zero velocity periods during walking, as is reflected in the noise of the ZUPT correction. Similarly, the hip is much more "hinge-like" during forward running than lateral walking, as is reflected in the noise of the hip joint axis correction. Note that the high uncertainty of the knee joint axis correction may be due to inaccuracy of the joint axis estimates rather than the knee being less "hinge-like".

Table 4.2: Noise parameters governing the ErKF algorithm for running with comparison values selected for various walking gaits (e.g., fast, slow, backward, lateral) by Potter et al.[64]. Accelerometer noise is σ_a, gyroscope noise is σ_w, noise for the zero-velocity update is σ_{ZV}, noise for the ankle, knee, and hip joint center updates are $\sigma_{JC,Ankle}$, $\sigma_{JC,Knee}$, and $\sigma_{JC,Hip}$, and noise for the knee, and hip joint axis updates are $\sigma_{JA,Knee}$ and $\sigma_{JA,Hip}$.

Noise Parameter	σ_a (m/s²)	σ_w (deg/s)	σ_{ZV} (m/s)	$\sigma_{JC,Ankle}$ (m)	$\sigma_{JC,Knee}$ (m)	$\sigma_{JC,Hip}$ (m)	$\sigma_{JA,Knee}$ (deg)	$\sigma_{JA,Hip}$ (deg)
Value for Running	0.179	2.46	0.11	0.01	0.04	0.01	45.84	0.75
Value for Walking[64]	0.013	2.83	0.01	0.01	0.01	0.01	1.15	57.30

4.3.4.3 Comparison of optical motion capture and ErKF kinematic estimates

The OPTIC and ErKF estimates were compared by first segmenting the strides and then comparing both the time series and other key kinematic features. Strides were segmented using the initial contact times as identified by the primary peaks in the resultant acceleration of the feet as shown in Figure 4.5 [54].

The time series joint angles were compared via four complementary metrics: coefficient

of determination (R^2), mean absolute different (MAD), root mean squared difference (RMSD),

and normalized root mean squared difference (NRMSD). The NRMSD was calculated by

dividing the RMSD by the average range of motion (ROM) exhibited within a stride. Because in

some cases there was an offset between OPTIC and ErKF estimates, RMSD and NRMSD were

also calculated after removing the offset by subtracting the average of each time series. Note that

similar offsets have previously been reported when comparing various motion capture methods

[64,249,291–293] and attributed to errors in joint center estimates [64,294,295], sensor-to-

segment alignment [64,292], or other calibration methods [292]. Additionally, recall that

gravitational corrections, which may be used to correct offsets, were not applicable to running.

Various features of gait were compared via RMSD and relative RMSD (rRMSD;

calculated as RMSD / average feature value). ROM estimates for each joint angle were evaluated

due to the associations between ROM and speed [296], injury rates [297,298], and foot strike

type [299]. Comparisons were made between OPTIC and ErKF estimates for the current study as

well as OPTIC estimates calculated using a publicly available dataset collected using an

expanded marker set without marker near-collinearity [273]. Stride length was calculated as the

distance between consecutive ipsilateral footfalls, and stride width was calculated as the

horizontal distance between each footfall and the line connecting ipsilateral footfalls of the other

foot as defined by Potter et al. [64]. Peak hip flexion and extension (associated with

compensatory pelvic tilt [300] and hip dysplasia and other disabilities [301,302]), peak knee

flexion during stance (associated with shock attenuation [135,303]), peak ankle dorsiflexion and

plantar-flexion (associated with fatigue [134]), and ankle dorsiflexion/plantarflexion at initial

contact (indicative of foot strike pattern [299,304] and fatigue [134]) were also evaluated (see

Figure 4.7).
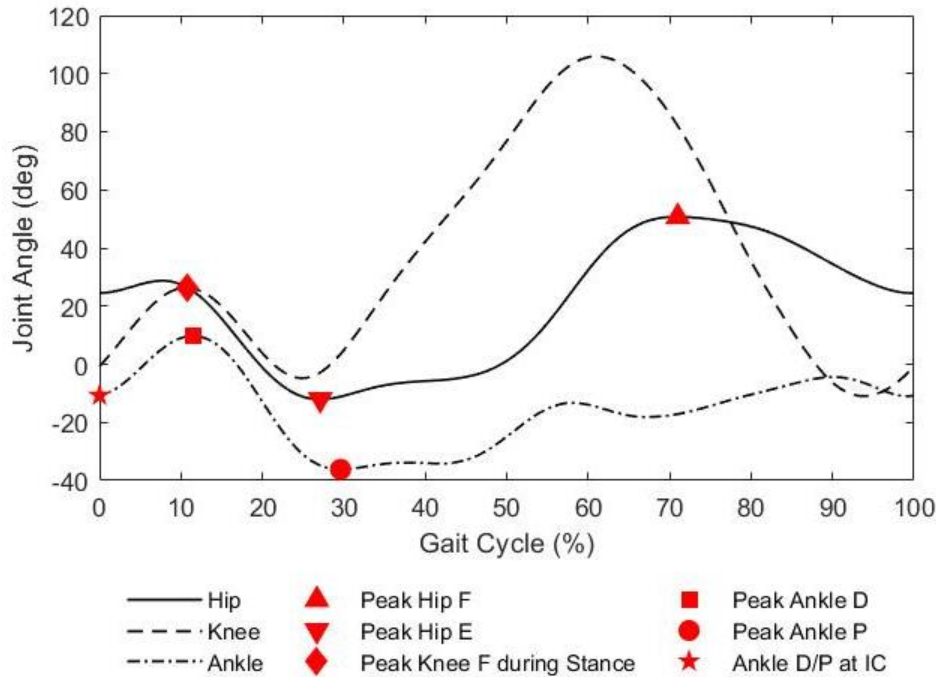
Figure 4.7: Features of gait demonstrated on representative average joint angle estimates over the gait cycle. Joint angles are flexion/extension (F/E) and dorsiflexion/plantarflexion (D/P). IC denotes initial contact.

4.4 Results

4.4.1 Assessing limitations of the optical motion capture results

While optical, marker-based motion capture is widely considered to be the "gold-standard" for measuring joint kinematics, numerous limitations have been documented. Primary among these limitations is that OPTIC methods track anatomical bodies rather than the underlying bones, resulting in soft-tissue artifacts (STAs) that produce errors in joint abd/adduction and internal/external rotation estimates that are comparable in magnitude to ranges of motion during running gait [305–308]. Nevertheless, studies frequently use OPTIC to

study running gait, and understanding the relationship between OPTIC and ErKF joint angle estimates will aid researchers in using and interpreting ErKF estimates.

While OPTIC estimates will unavoidably be influenced by STAs, the degree of impact on resulting joint angle estimates is influenced by the marker set employed. Optimally, each marker cluster includes four or more non-collinear markers [309] on locations with minimal soft-tissue presence (i.e., bony landmarks) such that STAs are minimized and have minimal contribution to the calculated joint angles. CGM marker sets are the most commonly used due to their minimal number of markers [310], and consequently a CGM marker set was employed in this study. However, the marker clusters include fewer than four markers, and the markers exhibit near collinearity. These limitations contribute to documented low reliability of coronal and transverse plane joint angle estimates [310–313]. In order to assess the effects of these limitations on the current study, the following results evaluate (1) the degree of collinearity of the marker trios in the standard CGM PiG marker set, and (2) the effects of potential errors in assumed joint centers. The degree of collinearity of a marker trio can be quantified via the planar angle. The marker trios used in defining the segment frames as shown in Figure 4.1 resulted in average thigh, shank, and foot planar angles [314] of $\theta_1 = 13.5$, $\theta_2 = 11.6$, and $\theta_3 = 11.3$ deg, respectively where $\theta = 0$ would mean collinearity of the three markers. Soft tissue movement during running resulted in marker cluster deformation characterized by average within-trial plantar angle standard deviations of $sd(\theta_1) = 0.6$, $sd(\theta_2) = 0.76$, and $sd(\theta_3) = 0.33$ deg.

The OPTIC joint angle estimates rely on first establishing the joint centers. The following results demonstrate how potential errors in the joint center estimates translate to errors in the joint angles by considering reasonable "perturbations" of the joint center estimates. Recall that the joint center estimates result from first calculating the average joint axes within a published

dataset [273] and then assuming that all participants in the current study exhibited the same joint axes such that the joint centers lie a distance of half the joint thicknesses along these average joint axes. As shown in Figure 4.8, hip and knee center perturbations resulted in substantial vertical shifts (i.e., offsets) in the knee Abd/Add, knee Int/Ext, ankle In/Ev, and ankle Int/Ext estimates as well as substantial trajectory (i.e., shape) changes in the knee Int/Ext, ankle In/Ev, and ankle Int/Ext estimates.

4.4.2 Representative ErKF results from a single trial

The initial success of the ErKF algorithm in estimating the lower limb joint angles was qualitatively assessed by examining the joint angle time series for drift, evaluating the initial convergence of the algorithm, and finally evaluating the joint angles over the course of the gait cycle.

The algorithm was effective at arresting drift, as can be observed by comparing the time series of the joint angle error estimates resulting from the ErKF algorithm to those resulting from simple offset removal and integration (see Figure 4.9). Additionally, errors in the initial state estimation were quickly overpowered by the algorithm's error models resulting in convergence within approximately 10 strides in all cases (see Figure 4.10). The first 10 strides were removed in all subsequent analyses.

The resulting joint angle estimates across the gait cycle for a representative trial are shown in Figure 4.11. Note that the OPTIC estimates of hip In/Ext, knee In/Ext, ankle In/Ext, and ankle In/Ev are poor due to the aforementioned limitations of OPTIC and a CGM [287,314–316] . For example, knee Int/Ext rotation as measured by OPTIC has previously exhibited a ROM between approximately 20 and 30 deg [273] and not < 5 deg (see Figure 4.12).

85
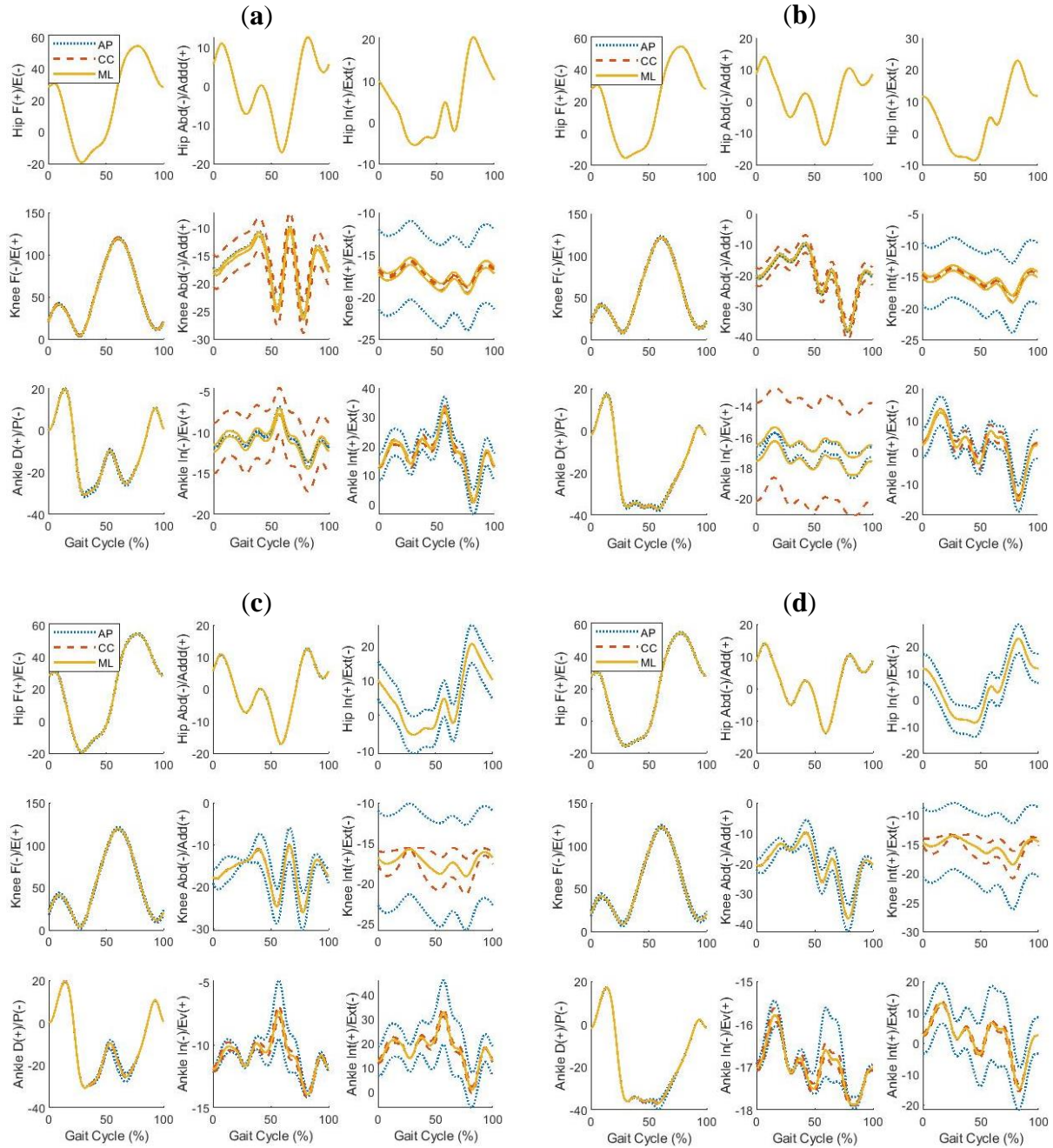
Figure 4.8: Representative joint angle OPTIC estimates when joint axis and consequently joint center estimates are perturbed by ± the inter-person standard deviation from a published dataset[273]. Blue, red, and yellow indicate perturbations in the anterior-posterior (AP), cranial-caudal (CC), and medial-lateral (ML) directions, respectively. Effects of knee center perturbations on the (**a**) left and (**b**) right sides of the body; Effects of ankle center perturbations on the (**c**) left and (**d**) right sides of the body. Joint angles are flexion/extension (F/E), dorsiflexion/plantarflexion (D/P), abduction/adduction (Abd/Add), inversion/eversion (In/Ev), and internal/external rotation (Int/Ext). All angles in degrees.
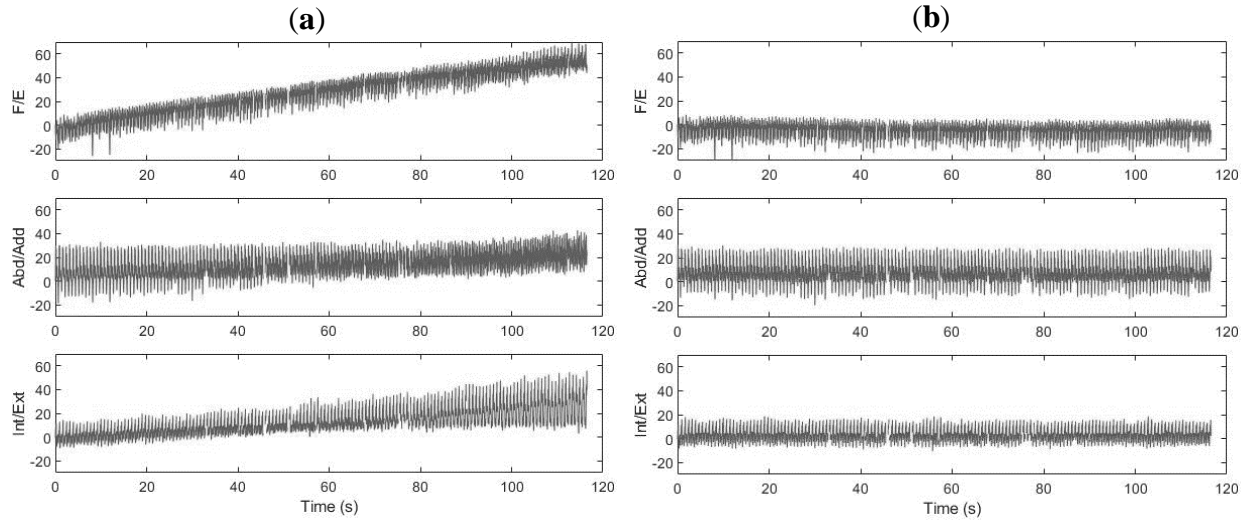
Figure 4.9: Representative joint angle differences (IMU - OPTIC) as estimated by raw integration (after removing gyroscope bias) and the ErKF algorithm. LAnkle angles estimated by (**a**) raw integration; (**b**) ErKF. Joint angles are flexion/extension (F/E), abduction/adduction (Abd/Add), and internal/external rotation (Int/Ext).
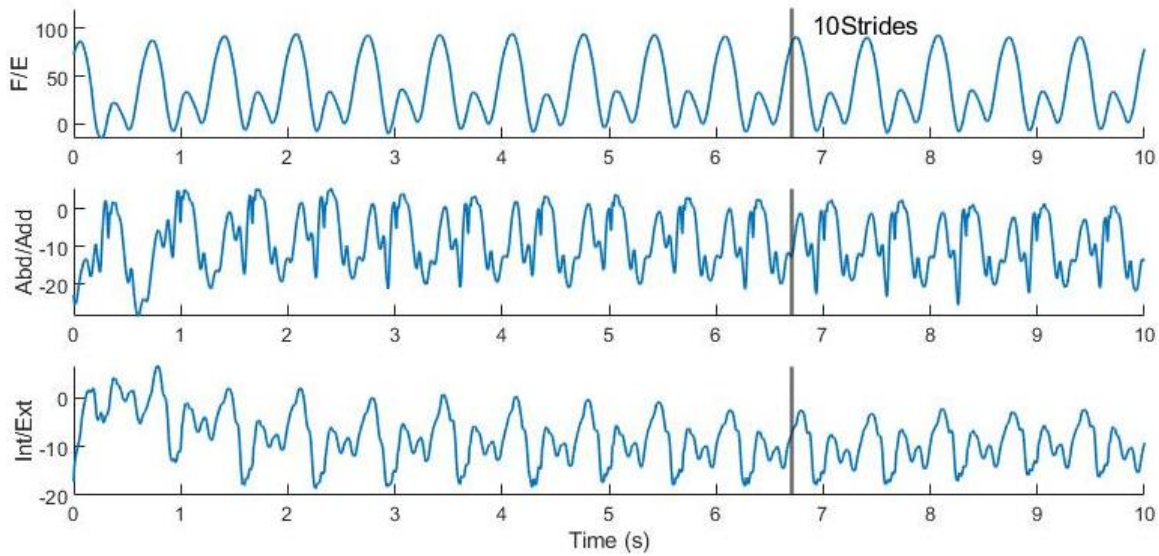
Figure 4.10: Representative convergence of the ErKF knee angle estimates at the start of a trial. Joint angles are flexion/extension (F/E), abduction/adduction (Abd/Add), and internal/external rotation (Int/Ext). All angles are in degrees.

87
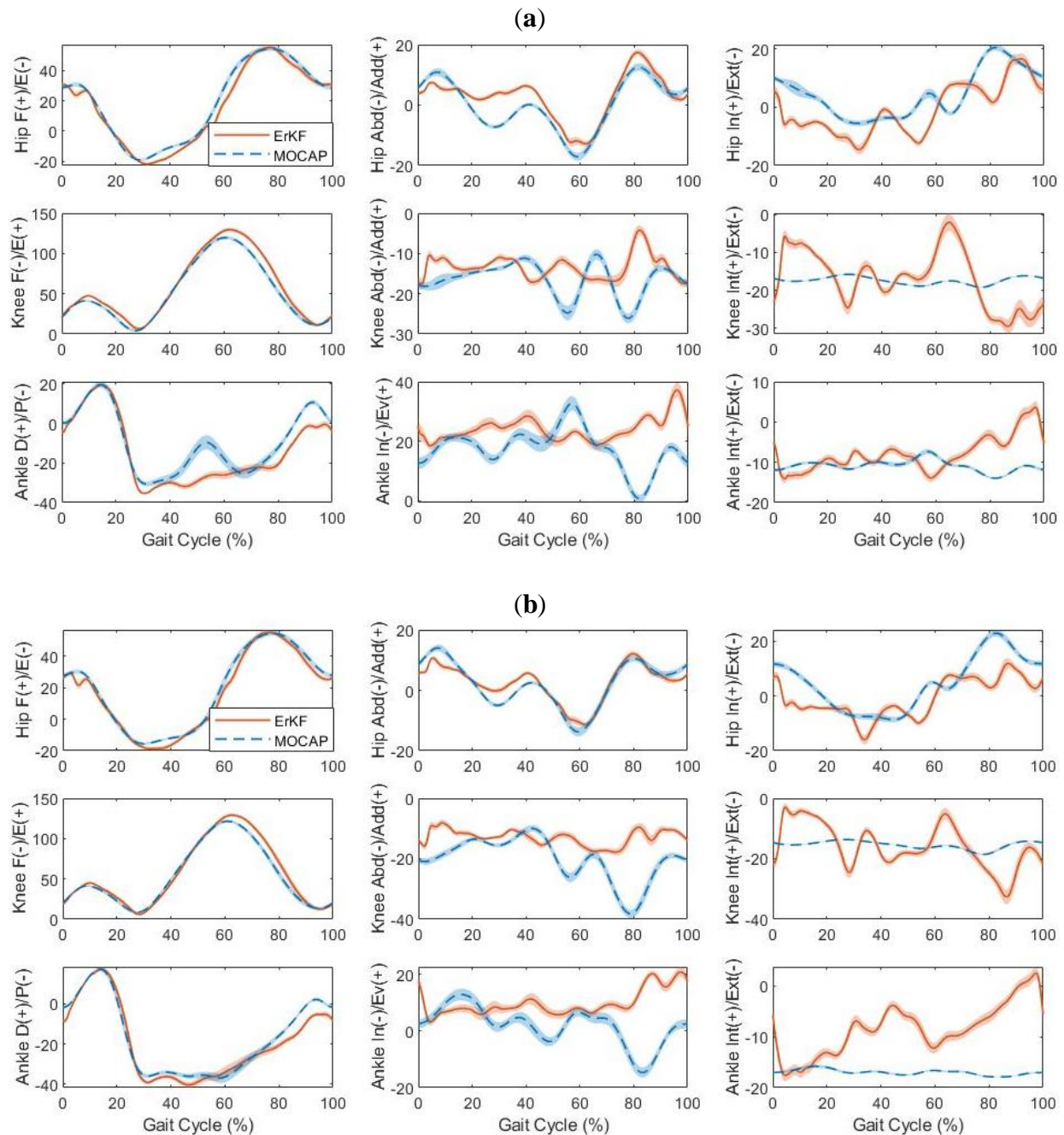
Figure 4.11: Representative ErKF and OPTIC joint angle estimates over the course of the gait cycle for a single trial: (**a**) Left; (**b**) Right. The curves signify the average over all 144 gait cycles while the shaded regions signify ± one standard deviation. Joint angles are flexion/extension (F/E), dorsiflexion/plantarflexion (D/P), abduction/adduction (Abd/Add), inversion/eversion (In/Ev), and internal/external rotation (Int/Ext). All angles in degrees.

4.4.3 ErKF results across all trials

Next, OPTIC and ErKF estimates are compared across all trials recorded in this study by considering first the similarity of the time series and then the resulting differences for other key features of gait.

The comparison between OPTIC and ErKF estimate time series across all ten trials considered in this study and for all joint axes with reliable OPTIC estimates are reported in Table 4.3. Recall that, due to the limitations of OPTIC and a CGM, the OPTIC estimates for knee and ankle Int/Ext and ankle In/Ev are not trustworthy (see section 4.4.1) [287,314–316] and so no meaningful comparisons can be made.

Table 4.3: Mean (standard deviation) of R^2, MAD, RMSD and NRMSD without the removal of constant offsets, and RMSD and NRMSD after the removal of constant offsets between OPTIC and ErKF joint angle estimates. Joint angles are flexion/extension (F/E), dorsiflexion/plantarflexion (D/P), abduction/adduction (Abd/Add), and internal/external rotation (Int/Ext). Green shading denotes ≤ 5 deg or 5%, yellow shading denotes ≤ 10 deg or 10%, and red shading denotes > 10 deg or 10%.

		R^2	MAD (°)	Without Offset Removal		With Offset Removal	
				RMSD (°)	NRMSD (%)	RMSD (°)	NRMSD (%)
Hip F/E	Right	0.98 (0.02)	3.3 (2.5)	5.7 (2.3)	9.1 (4.0)	1.1 (0.3)	1.7 (0.5)
	Left	0.98 (0.02)	3.4 (3.1)	6.2 (2.6)	9.8 (4.9)	1.2 (0.3)	1.8 (0.5)
Knee F/E	Right	0.99 (0.00)	4.3 (2.0)	6.9 (1.6)	6.7 (1.6)	1.0 (0.2)	0.9 (0.2)
	Left	0.99 (0.00)	5.7 (2.0)	7.7 (1.3)	7.4 (1.6)	1.0 (0.4)	1.0 (0.3)
Ankle D/P	Right	0.96 (0.03)	1.7 (0.9)	4.3 (1.1)	9.6 (2.2)	1.5 (1.5)	3.2 (3.0)
	Left	0.95 (0.02)	1.5 (1.7)	4.8 (1.3)	11.0 (2.6)	1.4 (1.1)	3.2 (2.5)
Hip Abd/Add	Right	0.89 (0.04)	0.8 (0.6)	3.1 (0.9)	14.6 (3.8)	0.9 (0.3)	4.3 (2.3)
	Left	0.47 (0.30)	1.8 (1.3)	4.2 (1.5)	18.1 (4.9)	0.9 (0.2)	4.4 (1.8)
Knee Abd/Add	Right	0.11 (0.38)	5.2 (1.7)	8.1 (1.3)	44.2 (7.1)	1.2 (0.2)	7.0 (2.1)
	Left	0.00 (0.43)	3.1 (1.4)	6.9 (1.4)	38.3 (5.5)	1.5 (0.8)	8.3 (4.2)
Hip Int/Ext	Right	0.49 (0.29)	4.7 (1.6)	8.4 (1.4)	35.0 (9.2)	1.5 (0.4)	6.3 (2.7)
	Left	0.43 (0.29)	8.4 (2.6)	11.3 (2.9)	45.0 (10.8)	2.1 (1.6)	8.4 (6.7)

Next, the agreement between OPTIC and ErKF estimates of other key features of gait are reported in Figure 4.12 and Table 4.4 - 4.7. ROMs from published reference data [273] are also

reported to aid in the interpretation of estimates in the hip In/Ext, knee In/Ext, ankle In/Ext, and

ankle In/Ev directions where the OPTIC results from this study are less reliable.
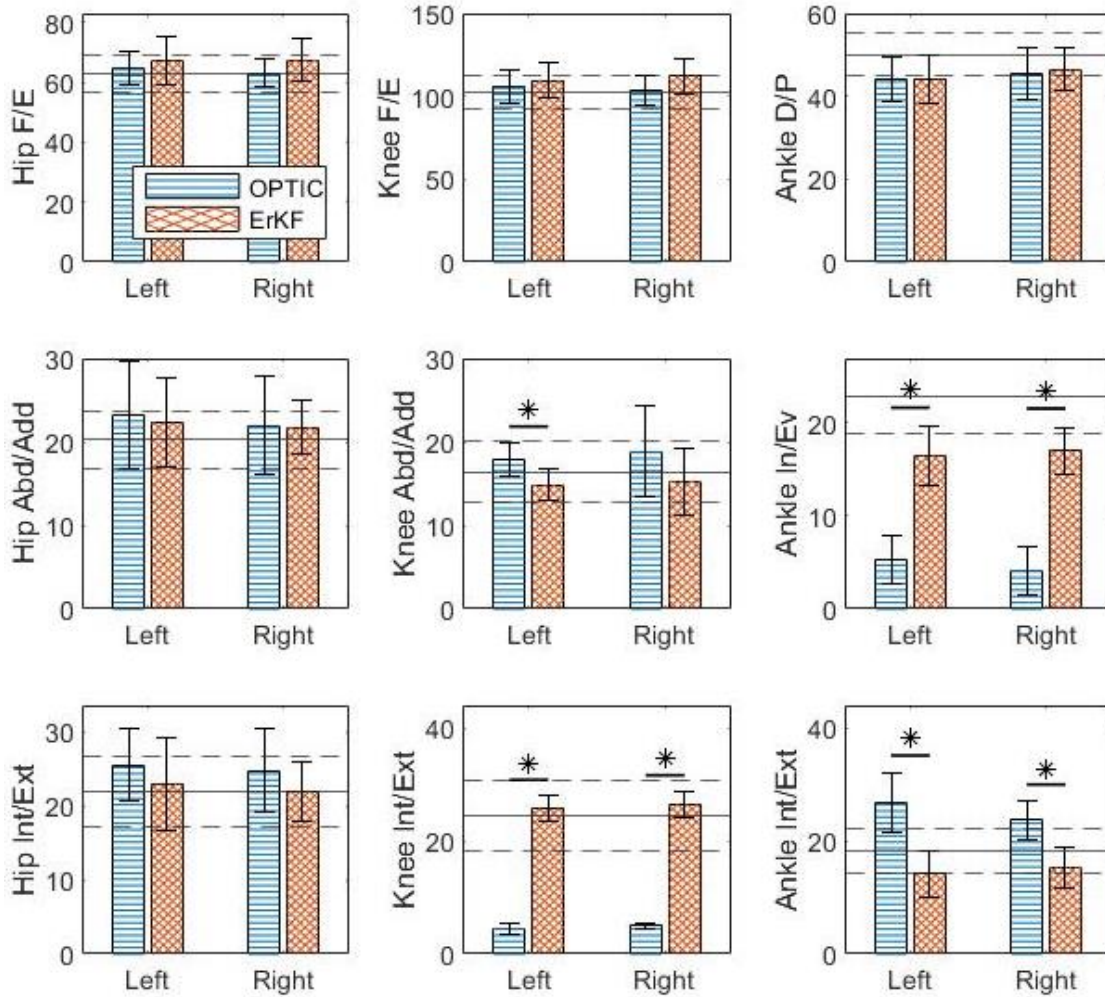
Figure 4.12: Comparison of ROM estimates from the ErKF versus OPTIC. Error bars denote ± one standard deviation between trials, and * denotes significance differences between ErKF and OPTIC estimates ($p < 0.05$). Horizontal lines denote the average ± one standard deviation of ROM estimates from published reference data[273]. Note that six out of the seven joint angles exhibiting significant differences are joint angles for which the OPTIC estimates are shown to be inaccurate. All angles in degrees.

Table 4.4: Mean (standard deviation) of ROM estimates from OPTIC and ErKF methods as well as a previously published dataset employing an expanded marker set[273]. Joint angles are flexion/extension (F/E), dorsiflexion/plantarflexion (D/P), abduction/adduction (Abd/Add), inversion/eversion (In/Ev), and internal/external rotation (Int/Ext). Gray shading indicates poor OPTIC estimates due to near marker collinearity and * denotes significance ($p < 0.05$). All angles in degrees.

		Published Comparison	OPTIC	ErKF
Hip F/E	Right	60.7 (6.9)	63.0 (4.8)	67.3 (8.9)
	Left	60.9 (6.0)	64.6 (5.6)	67.1 (9.9)
Knee F/E	Right	101.0 (10.9)	103.4 (8.9)	112.4 (10.3)
	Left	97.6 (9.7)	105.7 (9.9)	109.7 (11.1)
Ankle D/P	Right	47.0 (5.0)	45.5 (6.3)	46.4 (5.2)
	Left	47.3 (5.6)	44.1 (5.4)	44.1 (5.7)
Hip Abd/Add	Right	16.3 (3.0)	21.9 (5.9)	21.7 (4.4)
	Left	17.8 (2.9)	23.2 (6.4)	22.3 (7.3)
Knee Abd/Add	Right	12.5 (3.0)	18.9 (5.4)	15.3 (4.9)
	Left	13.5 (3.2)	17.9 (2.0)	14.9 (3.5)
Ankle In/Ev	Right	15.3 (3.2)	4.2 (2.6)	17.0 (4.1)
	Left	15.9 (3.2)	5.3 (2.5)	16.5 (5.8)
Hip Int/Ext	Right	17.8 (4.0)	24.8 (5.7)	22.0 (4.5)
	Left	18.5 (5.0)	25.5 (4.8)	23.0 (7.2)
Knee Int/Ext	Right	19.1 (5.2)	4.9 (0.6)	26.4 (5.6)
	Left	20.4 (5.1)	4.5 (0.1)	25.8 (6.5)
Ankle Int/Ext	Right	15.0 (3.1)	23.7 (3.4)	15.4 (7.7)
	Left	15.9 (3.6)	26.8 (5.2)	14.2 (10.8)

Table 4.5: RMSD and rRMSD of ErKF ROM estimates relative to OPTIC estimates. Joint angles are flexion/extension (F/E), dorsiflexion/plantarflexion (D/P), abduction/adduction (Abd/Add), inversion/eversion (In/Ev), and internal/external rotation (Int/Ext). Green shading denotes ≤ 5 deg or 5%, yellow shading denotes ≤ 10 deg or 10%, and red shading denotes > 10 deg or 10%.

		ROM RMSD (deg)	ROM rRMSD (%)
Hip F/E	Right	4.4 (2.8)	6.7 (4.3)
	Left	4.2 (2.2)	6.5 (3.1)
Knee F/E	Right	7.7 (3.7)	7.3 (3.4)
	Left	4.1 (2.4)	3.8 (2.2)
Ankle D/P	Right	2.9 (1.3)	6.2 (2.8)
	Left	4.8 (2.7)	10.6 (6.1)
Hip Abd/Add	Right	3.2 (1.5)	14.3 (5.7)
	Left	3.3 (3.6)	14.3 (12.4)
Knee Abd/Add	Right	6.2 (6.4)	28.0 (21.2)
	Left	4.4 (2.1)	23.5 (10.0)
Hip Int/Ext	Right	5.8 (2.5)	22.8 (9.4)
	Left	5.5 (4.7)	21.3 (17.3)

Table 4.6: Joint angle estimates at discrete gait events as estimated by OPTIC and the ErKF as well as resulting RMSD and rRMSD. NR indicates rRMSD values not reported due to small estimates (≤ 2 deg) appearing in the denominator of the rRMSD calculations. All angles in degrees. Green shading denotes ≤ 5 deg or 5%, yellow shading denotes ≤ 10 deg or 10%, and red shading denotes > 10 deg or 10%.

			OPTIC (deg)	ErKF (deg)	RMSD (deg)	rRMSD (%)
Hip	Peak Flexion	Right	53.8 (4.9)	55.3 (6.7)	3.0 (1.6)	5.6 (3.0)
		Left	52.2 (5.4)	52.6 (6.2)	2.8 (1.6)	5.4 (3.2)
	Peak Extension	Right	10.3 (5.1)	12.0 (5.8)	3.2 (1.7)	49.8 (55.8)
		Left	12.9 (4.9)	14.6 (4.7)	3.8 (2.8)	42.4 (46.1)
Knee	Peak Flexion During Stance	Right	6.9 (6.1)	7.3 (6.7)	1.6 (1.0)	22.5 (11.2)
		Left	3.4 (6.6)	6.9 (5.5)	4.1 (2.5)	104.7 (114.7)
Ankle	Peak Dorsiflexion	Right	30.0 (7.0)	32.3 (5.6)	2.9 (1.5)	11.0 (7.6)
		Left	28.8 (5.7)	29.1 (5.5)	2.3 (1.2)	7.9 (3.7)
	Peak Plantar-flexion	Right	15.9 (3.4)	14.1 (4.0)	2.9 (1.1)	19.2 (8.6)
		Left	15.7 (3.8)	14.9 (4.7)	3.2 (2.4)	21.5 (14.3)
	DP at Initial Contact	Right	-0.5 (4.3)	-6.5 (6.1)	6.0 (2.2)	NR
		Left	-0.7 (5.3)	-5.0 (6.1)	4.4 (1.8)	NR

Table 4.7: Comparisons of ErKF stride length and stride width estimates relative to OPTIC estimates. Mean (standard deviation across trials) of OPTIC estimates and ErKF estimates as well as MD, RMSD, and rRMSD of OPTIC and ErKF joint angle estimates. NR indicates rRMSD values not reported due to small estimates appearing in the denominator of the rRMSD calculations. RMSD denotes root mean square difference, rRMSD denotes relative root mean square difference, and MD denotes mean difference.

		OPTIC (m)	ErKF (m)	MD (m)	RMSD (m)	rRMSD (%)
Stride Length	Right	2.71 (0.11)	2.50 (0.12)	0.21 (0.03))	0.23 (0.03)	8.5 (1.1)
	Left	2.71 (0.12)	2.50 (0.13)	0.21 (0.03)	0.23 (0.03)	8.5 (1.1)
Stride Width	Right	0.04 (0.04)	0.07 (0.04)	0.03 (0.05)	0.07 (0.02)	NR
	Left	0.04 (0.04)	0.08 (0.04)	0.03 (0.05)	0.07 (0.02)	NR

4.5 Discussion

In this study, we extended an ErKF algorithm for lower-limb kinematic estimation during level treadmill running and compared the estimates to those from OPTIC data. The results demonstrate that many of the ErKF estimates are comparable to estimates made via OPTIC. The results also suggest that transverse and frontal plane joint angles estimated using OPTIC with a CGM marker set are unreliable, suggesting that IMU-based estimates with moderate errors may still be of comparable accuracy compared to current methods.

4.5.1 Assessing limitations of the optical motion capture results

The trustworthiness of the OPTIC results was assessed by evaluating (1) the degree of marker collinearity and (2) the effects of potential errors in assumed joint centers.

The degree of marker collinearity in this study as quantified by planar angles were comparable to those reported by Leboeuf et al. [314] who observed thigh and shank planar angles of $\theta_1 = 10$ - 30 and $\theta_2 = 7 - 21$ deg during standing. Leboeuf et al. examined the resulting effects of (1) marker misplacement by 1cm anterior-posterior and (2) soft tissue artifacts on the mean absolute difference (MAD) of estimated hip and knee angles relative to angles calculated by reverse kinematics with low weight applied to the lateral thigh and tibia markers. During walking, they reported similar MAD due to marker misplacement and soft tissue artifacts, with soft tissue artifacts resulting in average (standard deviation) MAD in hip Int/Ext of 7.6 (3.2) deg, knee Abd/Add 3.7 (1.5) deg, and knee Int/Ext 6.2 (2.6) deg [314]. The nearly-collinear markers used in the CGM for this study may therefore yield significant offsets between ErKF and OPTIC based hip Int/Ext, knee Abd/Add, and knee Int/Ext estimates.

In addition to the offsets arising from marker near-collinearity, the accuracy of the OPTIC joint angle estimates may be affected by errors in the joint center estimates. As shown in Figure 4.8, potential errors in the joint center estimates resulted in vertical shifts (i.e., offsets) but minimal changes in trajectory of the hip Int/Ext and knee Abd/Add joint angles. They also resulted in both vertical shifts and notable changes in trajectory in the knee Int/Ext, ankle In/Ev, and ankle Int/Ext joint angles.

As a result, subsequent comparisons between ErKF and OPTIC estimates are treated per Table 4.8, where joint angles expected to be accurate without marked offsets are compared using absolute measures such as RMSD without offset removal, joint angles expected to be accurate

but with offsets are compared using relative measures such as RMSD with offset removal, and joint angles expected to be markedly inaccurate are not compared. In addition, ErKF estimates are compared to published data whenever possible.

Table 4.8: Joint angles for which the OPTIC estimates are expected to be accurate without the presence of an offset, accurate with the presence of an offset, and inaccurate.

Accurate without Expected Offset	Accurate with Expected Offset	Inaccurate
Hip F/E	Hip Int/Ext	Knee Int/Ext
Hip Abd/Add	Knee Abd/Add	Ankle In/Ev
Knee F/E		Ankle Int/Ext
Ankle D/P		

4.5.2 ErKF estimates of joint angle time series

4.5.2.1 Sagittal plane joint angles

Having successfully arrested drift in the joint angle estimates over time, the accuracy of the resulting sagittal plan joint angle estimates are comparable to those achieved via IMU-based methods using machine learning algorithms, commercially available IMU-based systems, marker-less motion capture systems, and marker-based motion capture systems.

The high R^2 values (≥ 0.95 for all three joints; see Table 4.3) are comparable to those achieved via IMU-based methods using machine learning algorithms ($R^2 \geq 0.78$; see Table 4.9) or commercially available IMU-based systems [317] as well as the reliability of marker-based motion capture due to within-session repeatability [315], differing marker sets ($R^2 \geq 0.92$) [316], or differing kinematic estimation algorithms ($R^2 \geq 0.92$) [317]. They are also higher than those reported in comparisons of marker-less and marker-based motion capture; Song et al. reported $R^2 \geq 0.88$ when using Theia 3D [318], and Molina-Molina et al. reported $R^2 \geq 0.94$ for hip and knee angles and $R^2 = 0.38$ for ankle angles when using Simi Shape [319].

Table 4.9: A comparison of state-of-the art algorithms for estimating lower limb sagittal plane joint angles during running using IMU data. Differences are reported as the mean (standard deviation) relative to OPTIC. When multiple running speeds were examined, the results for the speed closest to 14 km/hr were reported, as that is the speed examined in this study. Joint angles are flexion/extension (F/E) and dorsiflexion/plantarflexion (D/P). M denotes male, F denotes female, ND denotes not described, Conv1D denotes one dimensional convolution, LSTM denotes long short term memory network, CNN denotes convolutional neural network, DeepConvLSTM denotes deep convolutional LSTM, ANN denotes artificial neural network, R denotes Pearson correlation, R^2 denotes coefficient of determination, RMSD denotes root mean square difference, rRMSD denotes relative root mean square difference, MAD denotes mean absolute difference, and MD denotes mean difference.

Testing Scheme	Ref.	Participants	Trial Duration	Algorithm	Metric			Hip F/E	Knee F/E	Ankle D/P
N/A	[268]	10 M	ND	ND	R	-		-	-	0.821
	[267]	5 M, 2 F	5 min	Kalman Filter	RMSD	deg		-	3.4 (1.1)	-
Inter-Subject	[261]	8 M	ND	ANN	RMSD	deg	Right	-	11.2 (7.3)	-
					R	-		-	0.91 (0.10)	-
					RMSD	deg	Left	-	13.0 (6.6)	-
					R	-		-	0.88 (0.13)	-
	[151]	292 M, 288 F	1 min	Conv1D, LSTM	RMSD	deg		0.79 (0.32)	1.3 (0.4)	0.9 (0.3)
	[265]	10 M	1 min	CNN	R^2	-		0.84 (0.10)	0.93 (0.04)	0.78 (0.10)
					RMSD	deg		5.6 (2.2)	6.5 (2.1)	4.7 (1.6)
					rRMSD	%		9.9 (2.2)	6.5 (1.8)	11.1 (3.1)
	[269]	10 M	ND	CNN	R	-		0.97 (0.01)	0.99 (0.00)	0.97 (0.02)
					RMSD	deg		5.2 (3.1)	5.0 (2.1)	3.7 (0.7)
	[266]	27	2 min	DeepConvLSTM	R	-		0.99 (0.01)	0.99 (0.01)	0.97 (0.02)
					MAD	deg	Right	4.1 (1.5)	3.6 (1.2)	5.9 (3.5)
					MD	deg		-0.3 (4.0)	-0.4 (1.8)	-0.1 (6.6)
					R	-		0.99 (0.01)	0.99 (0.01)	0.97 (0.02)
					MAD	deg	Left	4.2 (1.8)	3.7 (1.2)	5.2 (2.7)
					MD	deg		-0.2 (4.1)	0.3 (2.2)	0.1 (5.5)
Intra-Subject	[261]	8 M	3 min	ANN	R	-	Right	-	0.99 (0.0)	-
					RMSD	deg		-	3.1 (0.7)	-
					R	-	Left	-	0.99 (0.0)	-
					RMSD	deg		-	2.9 (0.9)	-
	[262]	10 M	ND	Musculoskeletal Model	R	-		0.98	0.99	0.98
					RMSD	deg		8.7 (3.2)	5.3 (3.0)	4.6 (1.7)
					rRMSD	%		16.5 (5.5)	6.1 (3.8)	8.4 (3.8)
	[263]	1	1 min	ANN	R	-		< 0.99	0.99	0.98
					RMSD	deg		8.4 (5.9)	7.1 (5.4)	7.2 (6.1)
	[264]	1		ANN	R	-		-	0.97	-
					RMSD	deg		-	3.8	-

The corresponding low RMSDs (≤ 7.7 deg; see Table 4.3) are comparable to those achieved via IMU-based methods using machine learning algorithms including those reported by Gholami et al. and Dorschky et al. (RMSD ≤ 6.5 deg; see Table 4.9) as well as commercially available IMU-based systems (RMSE generally < 10 deg) [317]. They were higher than those reported by Rapp et al.[151], who achieved excellent results when training a machine learning

model on a large simulated dataset (n = 280). However, Rapp et al. did not report introducing biases to the simulated acceleration and angular velocity data, nor did they report introducing simulated soft tissue artefacts, both of which may contribute significantly to errors in resulting joint angle estimates. The observed RMSDs are also comparable to or lower than those reported in comparisons of commercially available inertial or marker-less motion capture and marker-based motion capture; Van Hooren et al. reported RMSD ≤ 10.8 deg when using OpenPose and RMSD ≤ 9.8 deg when using DeepLabCut[320], Kanko et al. and Song et al. reported RMSD ≤ 5.2 deg and ≤ 5.1 deg, respectively when using Theia3D [318,321], Coll reported RMSD < 6 deg in a thesis on loaded running using Theia3D [322], and Wouda et al. reported RMSD generally < 10 deg when using XSens MVN Analyze [317]. After removing offsets between the OPTIC and ErKF joint angle estimates, the RMSDs decrease to ≤ 1.5 deg with corresponding NRMSD of ≤ 3.2% (see Table 4.3).

These results cumulatively suggest that the ErKF sagittal plane joint angle estimates may be similarly accurate to those made by other IMU-based algorithms, marker-less motion capture, and marker-based motion capture.

4.5.2.2 Transverse and frontal plane joint angles

The transverse and frontal plane ErKF joint angle estimates (without offset removal for hip Abd/Add estimates and with offset removal for knee Abd/Add and hip Int/Ext estimates per Table 4.8) exhibited smaller RMSD but lower R^2 than the sagittal plane estimates (see Table 4.3). However, the lowered R^2 values are expected due to the smaller ROMs [149].

Hip Abd/Add estimates exhibited only marginally higher RMSDs (right: 3.1 deg, left: 4.2 deg; see Table 4.3) compared to those reported by Rapp et al. (1.9 deg), who used a large simulated data set (with the significant limitations previously discussed in section 4.5.2.1) [151].

96

Similarly, the observed RMSDs are comparable to those reported in comparisons of commercially available inertial or marker-less motion capture and marker-based motion capture; Kanko et al. and Song et al. reported RMSDs of 2.7 and 4.5 deg, respectively, when using Theia3D [318,321], and Wouda et al. reported RMSDs generally less than 5 deg when using XSens MVN Analyze [317]. After removing offsets between the ErKF and OPTIC estimates, the RMSDs decreased to a comparable 0.9 deg (see Table 4.3). However, the small RMSD values nevertheless constitute a larger NRMSD due to a relatively small range of motion, as is reflected in R^2 values that are lower than those observed in the sagittal plane (right: 0.89, left: 0.47; see Table 4.3). These R^2 values are notably lower than those reported by Hernandez et al. (right: 0.98, left: 0.83) as the result of a machine learning algorithm trained on a modestly sized dataset (n=27) [266]. However, because the OPTIC marker set and calibration methods used by Hernandez et al. were not described, it is difficult to provide a well-informed comparison of their results and the results of this study. The observed R^2 values were also comparable to or higher than those resulting from differing kinematic estimation algorithms (R generally > 0.4 [317]) and those reported in comparisons of commercial IMU-based or marker-less motion capture and marker-based motion capture. Song et al. reported an R^2 of 0.74 when using Theia, Molina-Molina et al. reported an R^2 of 0.09 when using Simi Shape, and Wouda et al. reported R^2 generally > 0.20 when using XSens MVN Analyze [317–319]. Recall that low R^2 values may in part be due to small ROM.

Knee Abd/Add estimates exhibited similar RMSDs (right: 1.2 deg, left: 1.2 deg; see Table 4.3) compared to those reported by Rapp et al. (2.5 deg) when using a large simulated data set (with the limitations previously discussed) [151], although the RMSD reported by Rapp et al. may decrease if any offset between OPTIC and IMU-based estimates was removed. The

observed RMSDs were lower than those reported by Kanko et al. when comparing marker-less and marker-based motion capture (RMSD = 7.2 deg), Wouda et al. when comparing XSens MVN Analyze and marker-based motion capture (RMSD generally < 10 deg) [317,321], and Wouda et al. when comparing kinematic estimation algorithms (RMSD generally < 12 deg) [317]. However, the corresponding R^2 values were exceedingly low (right: 0.11, left: 0.00; see Table 4.3), again potentially due to the small ROM.

Hip Int/Ext estimates exhibited small RMSD after offset removal (right: 1.5 deg, left: 2.1 deg) but only moderate corresponding R^2 values (right: 0.49, left: 0.43; see Table 4.3). These results again may be due in part to the relatively small ROM. Moreover, they are largely comparable to those reported by Rapp et al. without offset removal (RMSD = 1.3 deg; limitations discussed previously) [151] as well as Hernandez et al. (right: R^2 = 0.52, left: 0.67; limitations discussed previously) [266]. The observed R^2 are also comparable to or improvements upon those reported in comparisons of commercial IMU-based or marker-less motion capture and marker-based motion capture; Kanko et al. reported an RMSD of 9.8 deg and Song et al. reported an RMSD of 12.8 deg and R^2 of 0.00 when using Theia3D [318,321], Molina-Molina et al. reported an R^2 of 0.58 when using Simi Shape [319], and Wouda et al. reported RMSD generally < 20 deg and R^2 generally > 0.01 [317].

These results together suggest that ErKF joint angle time series estimates in the sagittal plane may be comparable to those from marker-based motion capture, marker-less motion capture, and other IMU-based algorithms. Those transverse and frontal plane joint angle estimates which could be assessed (i.e., hip Abd/Add, hip Int/Ext, and knee Abd/Add) may be similarly accurate to those from other IMU-based algorithms or marker-less motion capture but nevertheless should be used with caution. While the remaining transverse and frontal plane joint

angle time series were not evaluated due to limitations in the common CGM marker set used, if

accurate, these ErKF estimates may provide additional information not achievable with OPTIC

and a CGM marker set.

Table 4.10: A comparison of state-of-the art algorithms for estimating lower limb frontal and transverse plane joint angles during running using IMU data. Differences are reported as the mean (standard deviation) relative to OPTIC. When multiple running speeds were examined, the results for the speed closest to 14 km/hr were reported, as that is the speed examined in this study. Joint angles are abduction/adduction (Abd/Add), inversion/eversion (In/Ev), and internal/external rotation (Int/Ext). M denotes male, F denotes female, ND denotes not described, Conv1D denotes one dimensional convolution, LSTM denotes long short term memory network, CNN denotes convolutional neural network, DeepConvLSTM denotes deep convolutional LSTM, ANN denotes artificial neural network, R denotes Pearson correlation, RMSD denotes root mean square difference, MAD denotes mean absolute difference, and MD denotes mean difference.

Testing Scheme	Ref.	Participants	Trial Duration	Algorithm	Angle		Metric		Value
N/A	[268]	10 M	ND	ND	Ankle In/Ev		R	-	0.835
Inter-Subject	[151]	292 M, 288 F	1 min	Conv1D, LSTM	Hip Abd/Add		RMSD	deg	1.9 (0.9)
					Hip Int/Ext		RMSD	deg	1.3 (0.8)
					Knee Abd/Add		RMSD	deg	2.5 (1.0)
					Knee Int/Ext		RMSD	deg	3.3 (1.0)
					Ankle In/Ev		RMSD	deg	1.6 (0.7)
					Ankle Int/Ext		RMSD	deg	1.8 (1.1)
	[266]	27	2 min	DeepConvLSTM	Hip Abd/Add		R	-	0.99 (0.01)
						Right	MAD	deg	2.3 (0.9)
							MD	deg	0.14 (1.9)
							R	-	0.91 (0.05)
						Left	MAD	deg	2.5 (1.0)
							MD	deg	-0.3 (2.3)
					Hip Int/Ext		R	-	0.72 (0.23)
						Right	MAD	deg	3.0 (1.2)
							MD	deg	-0.6 (2.3)
							R	-	0.82 (0.13)
						Left	MAD	deg	3.3 (1.6)
							MD	deg	-0.0 (3.1)
					Ankle Inv/Ev		R	-	0.87 (0.06)
						Right	MAD	deg	4.7 (2.7)
							MD	deg	0.7 (4.9)
							R	-	0.9 (0.06)
						Left	MAD	deg	4.5 (2.0)
							MD	deg	-0.4 (4.4)
Intra-Subject	[263]	1	1 min	ANN	Hip Abd/Add		R	-	0.96
							RMSD	deg	3.4 (3.2)
					Hip Int/Ext		R	-	0.78
							RMSD	deg	4.1 (3.8)

4.5.3 ErKF estimates of key features of gait

The ErKF estimates for many key features of running gait (e.g., ROM) were similar to estimates from traditional OPTIC methods. For those joint angles where OPTIC ROM estimates were reliable, the ErKF ROM estimates were generally not significantly different from the OPTIC estimates (with the exception of the left knee Abd/Add). The resulting RMSDs were $\leq$ 7.7 deg, with RMSD and rRMSD generally < 5 deg and 8% in the sagittal plane (see Table 4.5). Frontal and transverse plane ROMs exhibited similar RMSD but larger rRMSD due to smaller ROMs ($\leq$ 28.0%; see Table 4.5). Hip Abd/Add ROM estimates exhibited lower RMSD and rRMSD (approximately 3.3 deg ad 14.3%; see Table 4.5) than either knee Abd/Add or hip Int/Ext. Note that because ROM estimates are dependent on the range and not absolute value of joint angle estimates, offsets between ErKF and OPTIC estimates are inconsequential here.

Additionally, the ErKF ROM estimates were similar to those exhibited in a published dataset [273] (see Figure 4.12). Importantly, the ErKF estimates of knee Int/Ext, ankle Int/Ext, and ankle In/Ev were more similar to published values than were the OPTIC estimates arising from the limited CGM marker set. These results suggest that IMU-based transverse and frontal plane ROM estimates, while imperfect, may outperform estimates using CGM marker sets. Peak hip flexion and extension, peak knee flexion during stance, peak ankle dorsiflexion and plantar-flexion, and ankle D/P at initial contact were estimated with RMSD generally < 4.5 deg (see Table 4.6). These results are comparable to those reported by Gholami et al. (MAD generally < 6 deg).

Stride length estimates exhibited considerably higher RMSD (0.23 m) than previously achieved via alternate algorithms [54,290]. However, the high RMSD is in large part due to an MAD of 0.21 m. This offset may be the result of errors in the initial velocity estimate (see Table

4.7), and it is possible that introducing global position data (GPS) could remove this offset. The stride width estimates were poor (RMSD = 0.07 m relative to stride widths of 0.04 m; see Table 4.7), likely due to dependence on the combined frontal plane joint angles. Because much of the RMSD seemed to be due to systematic differences, estimates of stride-to-stride variation in stride length and stride width may be more accurate and could be investigated in future studies.

Together these results demonstrate that the ErKF algorithm was able to estimate many but not all key features of running gait similarly to traditional OPTIC methods. In addition, the ErKF algorithm estimated some transverse and frontal plane ROMs with greater accuracy than OPTIC using a common CGM marker set.

4.5.4 Limitations

Limitations of this study include the examination of a single running speed, limited number of participants, and inclusion of only healthy male participants. Additionally, use of a CGM marker set allowed for comparison to a common method for optical motion capture but also limited the validation of joint angles for which CGM is shown to be unreliable. Future work should also develop methods for estimating model inputs (i.e., the initial state, sensor to segment alignment, and joint axis estimates) from solely inertial data and not from optical motion capture data as done in this study.

4.6 Conclusion

Inertial motion capture offers the opportunity to unobtrusively capture overground running mechanics in a variety of training and racing environments [18]. The purpose of this study was to extend and evaluate an ErKF algorithm for 3D lower-limb kinematic estimation during level treadmill running (where simultaneous marker-based motion capture is possible). To

101

our knowledge, this was the first study to evaluate a filter-based algorithm for three-dimensional lower limb joint angles during running. The ErKF time series and key gait feature estimates were compared to optical motion capture with a common CGM marker set, and range of motion estimates were additionally compared to a previously published dataset [273]. The time series sagittal plane joint angle estimates were similarly accurate to those from marker-based or marker-less motion capture as well as other IMU-based methods. The frontal and transverse plane joint angle estimates (i.e., hip Abd/Add, hip Int/Ext, and knee Abd/Add) exhibited low RMSD but also demonstrated low R^2, and thus, further work is needed before these estimates are confidently used in place of OPTIC estimates. Many of the resulting key features of gait were comparable to OPTIC estimates and those from previously published data [273]. However, the poor accuracy of some estimates (e.g., stride width) highlights that comparable joint angle time series can still result in substantial differences in position-based gait features.

In this first evaluation for level treadmill running, the ErKF algorithm performed comparably to marker-based motion capture, marker-less motion capture, and existing commercial or machine learning based inertial motion capture algorithms. However, compared to existing inertial motion capture algorithms, filter-based methods such as the ErKF considered herein may offer benefits such as requiring smaller datasets for algorithm development[151] and allowing for intelligent adjustment of parameters designed to accommodate differences in experimental design such as gait speed or running surface. Thus, future work should further validate the ErKF algorithm, evaluate it for varying running conditions (e.g., speeds, surfaces), and develop IMU-based methods for the estimation of algorithm inputs including sensor-to-segment alignment matrices, joint axes, and joint centers.

Chapter 5 Positive Distance Running Experiences are Associated with Running Kinematics

5.1 Abstract

This study examined the relationships between positive running experiences and running biomechanics during long, outdoor training runs. Experienced runners (n = 12) completed a total of 23 30-minute runs while wearing inertial and heart rate sensors. They reported affective valence throughout the run and completed the Physical Activity Enjoyment Scale and Flow Short Scale upon the run's conclusion. Results revealed significant inter-run associations between psychological and biomechanical metrics that differed between measures of positive experience. Higher affective valence was moderately correlated with reduced peak tibial acceleration (R = -0.50, p = 0.016) and increased lower-body attenuation (R = 0.65, p < 0.001). Within aerial runs, higher affective valence was also moderately correlated with slower running speeds (R = -0.50, p = 0.036) with associated reductions in joint range of motion, less upper-body attenuation (R = -0.55, p = 0.029), and increased stability (vertical ratio of pelvis acceleration RMS: R = 0.48, p = 0.042). Increased physical activity enjoyment was moderately correlated with increased lower-body attenuation (R = 0.56, p = 0.008). An increased level of flow was moderately correlated with decreased head and ankle stabilization and increasing intensity of arm movement (head peak acceleration: R = 0.50, p = 0.016; peak foot roll rate: R = 0.48, p = 0.020; arm vertical acceleration RMS: R = 0.47, p = 0.050) and, in aerial runs, an increased degree of aerial running (duty factor: R = -0.48, p = 0.046; flight time: R = 0.49, p = 0.037). Intra-run associations between psychological and biomechanical metrics were frequently significant but differed

between runs and were strongly confounded with time. The inter-run associations may be explored as a means to support positive "real-world" running experiences, and future work may examine intra-run associations in running conditions that may induce a wider range of psychology and biomechanics.

5.2 Introduction

Running performance is influenced not only by physical (i.e., physiological and biomechanical) factors such as maximal oxygen uptake, lactate threshold, and running technique [152,153] but also by runner psychology. Psychological skills such as mindfulness as well as other factors such as mental fatigue and verbal encouragement have all been suggested to influence endurance performance [154]. However, the mechanisms through which these myriad factors contribute to endurance performance is less clear. The psychobiological model, based in motivational intensity theory, is currently the sole model for how psychological factors affect endurance performance. It attributes the influence of physical and psychological factors on endurance performance to their shared modulation of perceived effort [154,323].

Numerous psychological factors and mental training exercises have been shown to influence perceived effort and sports performance. For example, motivational self-talk has been associated with decreases in perceived effort and improvements in performance in running, cycling, swimming, volleyball, dressage, and more [324–330]. Similarly, while findings are equivocal, some studies have reported that associative attentional focus is associated with improved performance and increased perceived effort [331].

Many physical factors have been associated with perceived effort or performance. For example, maximum oxygen uptake has been associated with improved performance in elite runners [332,333]. Additionally, improved running economy has been associated with stride lengths within the preferred range, smaller vertical oscillation, greater leg stiffness, less leg extension at toe-off, larger stride angles, low activation of lower limb muscles during propulsion, and more [334,335].

The relationships between psychological and physical factors are less clear, with the majority of related studies reporting both physical and psychological responses to an intervention but not evaluating their interaction [336–341]. For example, studies have reported on the psychological and physical effects of facial expression during endurance exercise. The results are mixed, with reports that facial expression impacted both perceived effort and affective valence (i.e., good-to-bad feeling) during cycling [342], economy but not affective valence during endurance running [343], and neither time to exhaustion nor affective valence during cycling [344]. However, the identification of causal relationships between the physical and psychological responses to running could support an improved understanding of running interventions and may enable intentional improvement of the running experience through gait modification.

To this end, initial studies have identified relationships between affective valence and running biomechanics. Lussiana and Gindre examined the lower-body running biomechanics of well-trained runners during a 15 minute run on a track at a self-selected speed. They grouped runners by global running pattern, where aerial runners exhibited longer flight times and greater center of mass displacements and terrestrial runners exhibited long contact times and smaller center of mass displacements [345,346]. Positive affective valence at the conclusion of the run was correlated with increasingly aerial-type biomechanics (i.e., decreased contact time and increased leg stiffness) in aerial runners and increasingly terrestrial-type biomechanics (i.e., decreased flight time) in terrestrial runners [155]. Van der Bie and Kröse examined arm biomechanics during an 8 minute run on a treadmill at a self-selected speed. Positive affective valence throughout the run was negatively correlated with normalized anterior-posterior and medial-lateral arm acceleration variance [156].

These initial studies suggest that biomechanics may be related to pleasure during running. However, both studies were conducted in an environment that differed from the average training run for most distance runners, which may affect both runner psychology and biomechanics. In a recent review of 33 studies comparing biomechanical measures during motorized treadmill and overground running, Van Hooren et al. found that seven biomechanical measures including contact time, vertical center of mass displacement, and peak propulsive force differed between treadmill and overground running conditions [132]. Similarly, in a review and meta-analysis of 34 studies comparing physiological, perceptual, and performance measures during treadmill and overground running, Miller et al. found that similar oxygen uptake but differing blood lactate concentration, heart rate, and rate of perceived exertion occurred during submaximal treadmill compared to overground running [133]. Various perceptual and psychological differences between the acute effects of indoor and outdoor exercise have also been reported including differing perceived exertion, anxiety, affect, and attentional focus [138–144]. In addition, continuous observation by the researcher may influence perceived exertion, hormone levels, and anxiety [145]. If provided, verbal encouragement may also affect numerous biomechanical and physiological measures [145]. As a result, the initial treadmill and track-based literature investigating the relationship between affective valence and running biomechanics may or may not translate to typical outdoor training runs.

The objective of this study was to investigate the relationships between positive running experiences and running biomechanics during long outdoor training runs. Three measures of positive experience (i.e., affective valence, enjoyment, and flow) were considered. This study represents the first and necessary step in establishing relationships between biomechanics and

positive running experiences which, with additional study, may support improved running experiences and performance outcomes.

5.3 Methods

In this study, well-trained runners completed a 30 minute "out-and-back" run on a popular, paved, outdoor running path without the continual presence of research staff. Throughout the run, the participants wore inertial sensors and heart rate monitors, and intermittently reported their affective valence. As is common for examinations of enjoyment and flow[347,348], the participants reported their physical activity enjoyment level and level of flow at the end of the run.

5.3.1 Participants

Twelve recreational to elite runners (8 female, 4 male, 29 ± 9 years, 170 ± 9 cm, 65.4 ± 8.3 kg; details shown in Table 5.1) participated in this study. Each participant completed between 1 and 5 runs (1.9 ± 1.0 runs, 20.6 ± 4.9 °C, no rain) resulting in a total of 23 runs. Participants were recruited via flyers, electronic postings, and word of mouth. They self-reported to have run at least 20 miles per week for the last 4 weeks [274], have run for at least 30 minutes at a time at least 2 times/week for the past 4 weeks, have run at least 6 months / year and at least 20 miles / week for the previous 2 years, and have no current injuries or illnesses that prevent running, alter the running gait, and/or alter the running experience. These requirements were designed to ensure that the testing procedure did not lead to significant fatigue, which would affect the running biomechanics, and so that there was an increased likelihood of positive running experiences.

The study was approved by the University of Michigan Review Board (HUM00202634), and all participants gave written informed consent in accordance with the Helsinki Declaration.

Table 5.1: Participant demographics.

Participant	Sex	Age	Height (cm)	Weight (kg)	Highest Level of Performance	Current Level of Performance
1	F	21	152	52.6	High School	Recreationally Competitive
2	F	22	173	64.4	College	College
3	F	22	173	61.3	College	College
4	F	23	165	66.9	High School	Recreationally Competitive
5	F	25	175	61.9	High School	Recreationally Competitive
6	F	29	160	57.3	Recreationally Competitive	Recreationally Competitive
7	F	29	170	63.2	Professional	Recreational
8	F	41	170	57.1	Recreationally Competitive	Recreationally Competitive
9	M	19	174	72.9	High School	Recreationally Competitive
10	M	31	165	71.2	High School	Recreationally Competitive
11	M	33	185	80.2	College	Recreationally Competitive
12	M	48	180	76.3	Recreationally Competitive	Recreationally Competitive

5.3.2 Equipment

During each run, the participant wore their native, preferred running shoes which all exhibited tall stack heights (approximately 30 – 40mm) and therefore a high degree of cushioning. They additionally wore inertial sensors, heart rate monitors, earbuds, smart phones, and a watch. A total of 13 six-degree-of-freedom inertial measurement units (IMUs; Opal, APDM Wearable Technologies Inc., Portland, OR) were worn to measure the kinematics of

major body segments. They were worn on the feet over the shoe laces, the medial distal tibial shafts, the lateral proximal thighs, the lumbar spine, the thoracic spine at the level of the sternum, the upper arms, the wrists, and the head (see Figure 5.1). The lumbar and leg IMUs were secured with tape (Sher-Light Adhesive Tape, Covidien, Mansfield, MA), and the thoracic and upper body IMUs were secured with elastic straps (APDM Wearable Technologies Inc., Portland, OR). All were sampled synchronously at 500 Hz [276,349].

Two chest strap heart rate monitors (H10, Polar Electro Inc., Kempele, Finland), two earbuds (Vista 2, Jaybird Sport, Salt Lake City, UT), and two smart phones (Galaxy A13, Samsung Electronics, Yongin-si, South Korea) were all worn with duplicates used to reduce data loss. Electrocardiogram (ECG) waveforms were collected using the heart rate monitors and a smart phone application (ECGLogger, Matti Mononen) at the maximum available sampling frequency of 130 Hz. Audio data were recorded via the earbuds and smart phones.
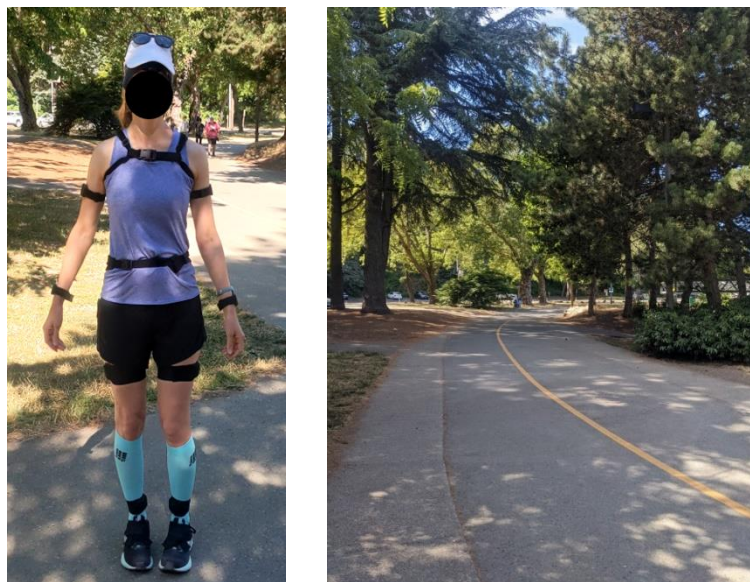
Figure 5.1: An exemplar participant equipped with all sensors (left) and an exemplar portion of the running path (right).

5.3.3 Procedures

Prior to starting a run, each participant completed defined calibration movements (quiet standing and walking) which were used in processing the inertial data [350,351]. During these calibration movements, they practiced reporting their affective valence on a single item 11-point scale ranging from -5: Very Bad to +5: Very Good (i.e., the Feeling Scale; FS; see Appendix Figure 5.10) [155,156,352–355].

Each participant then ran for 30 minutes on an approximately flat, continuous paved path by a lake (no stoplights or other crossings; see Figure 5.1) and turned around after 15 minutes. They were asked to run at their self-selected moderate, training speed resulting in average heart rates between minutes 10 and 30 that ranged from 129 to 179 beats per minute (first quartile: 152, median: 160, third quartile: 165).

Each participant self-reported positive experiences using three measures: affective valence, enjoyment, and flow. Affective valence ranges from pleasant to unpleasant and is one of two dimensions composing affect (valence and arousal) [356,357], while enjoyment is a positively valenced emotion about a particular behavior and is linked to intrinsic motivation [358–360]. Finally, flow is a hallmark of optimal experiences characterized by complete absorption in the task at hand. Flow has been proposed to be the outcome of appropriate challenge-skill balance, clear goals, and unambiguous feedback and is characterized by complete concentration on the task at hand, merging of action and awareness, loss of self-consciousness, a sense of control over the outcome, the transformation of time, and intrinsic reward [347,361].

Each participant verbally reported their affective valence throughout the run at their discretion using the FS. Frequency and timing of FS reports were not constrained in order to minimally disrupt the running experience. Immediately after the run, each participant reported

their level of flow using the Flow Short Scale (FSS; see Appendix Figure 5.11) [362–365] and their level of enjoyment on the Physical Activity Enjoyment Scale (PACES; see Appendix Figure 5.12) [348,353,358].

5.3.4 Data Analysis

After calculating interpretable kinematic metrics from the inertial data, the inter- and intra-run relationships between each kinematic metric and measure of positive experience were evaluated.

5.3.4.1 Calculation of kinematic metrics from inertial data

Established methods were used for sensor-to-segment alignment, stride segmentation, and the calculation of kinematic metrics. All data processing was conducted in MATLAB (R2022b, Mathworks, Natick, MA).

The IMU data were first segmented to isolate each calibration movement as well as the 30 minute run. During the run, any portions uncharacteristic of steady-state running (e.g., the turn at the approximate 15 minute mark) were removed (see Figure 5.2). Additionally, the first 10 minutes of the run were excluded from analysis due to physiological and biomechanical changes associated with warming up (see Figure 5.2) [366]. The IMU data were then rotated so that the sense axes approximately aligned with the body segment's anatomical axes. This sensor-to-segment alignment was done using a functional method [63] using both the quiet standing and walking calibration movements. During quiet standing, it was assumed that the global vertical (i.e., the gravitational acceleration vector) was aligned with the anatomical vertical axis. Similarly, during walking, it was assumed that the principal angular velocity was aligned with the anatomical medial-lateral axis. Subsequently, the accelerometer and gyroscope data were

112

filtered using fourth order low-pass Butterworth filters with cutoff frequencies of 60 Hz and 50

Hz, respectively [252,276].
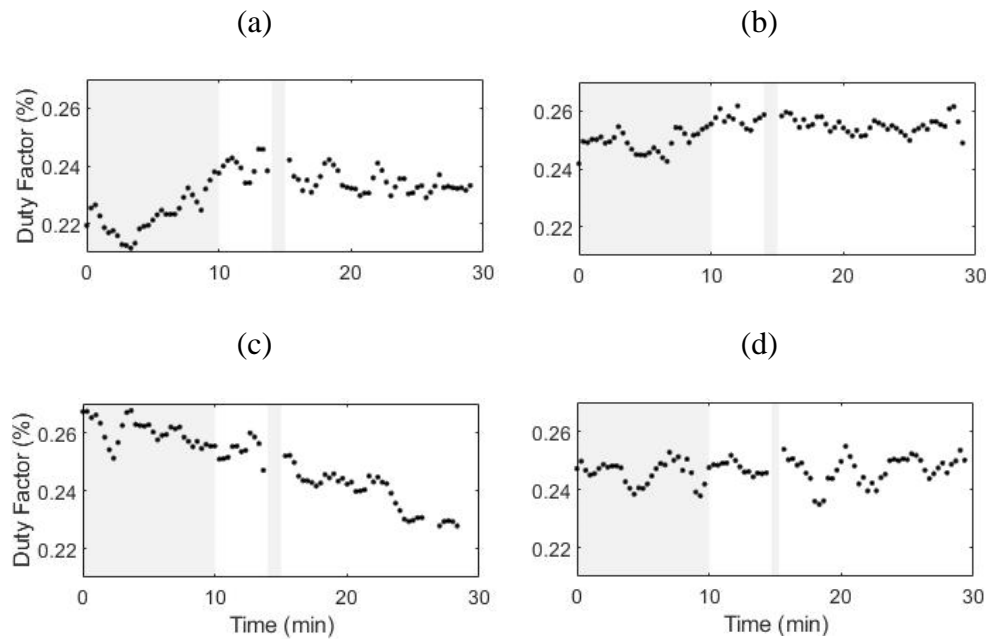
Figure 5.2: Duty factor (i.e., portion of the time spent in contact with the ground, contact time / stride time) over the duration of a 30 minute run for four exemplar runs. The gray bands indicate where data were excluded due to transient changes attributable to warming up and turning around. Many runs, including (a) and (b), exhibited biomechanical changes during the initial 10 minute warm-up period. However, as demonstrated in (c) and (d), some runs exhibited biomechanical changes after the end of the warm-up period, and some runs exhibited no notable biomechanical changed during or after the warm-up period.

Windowing of the temporal data

When assessing inter-run relationships between a kinematic measure and positive

experience (i.e., affective valence, enjoyment, or flow), the kinematic data were aggregated over

the entire run from minute 10 to minute 30. Affective valence was also aggregated over the run

using the average.

When assessing intra-run relationships between a kinematic measure and positive

affective valence, the kinematic data were aggregated using a sliding window 60 s in duration

which was translated by 20 s at a time (see Figure 5). Doing so allowed possible dynamic trends

within a run to be studied. The window duration (60 s) was selected so that each window would include at least three times the number of strides required for stable estimation of running kinematic during treadmill running[367]. The number of strides was increased in an effort to reduce the effects of increased noise resulting from the variability of over ground running (e.g., slight turns, the navigation of passersby, and unevenness of the path). The window translation (20 s) was selected to capture even the most frequent observed changes in affective valence. The window translation was also shorter than the time between queries in prior research[368–372]. For each window, the associated affective valence was the FS rating most recently given by the participant. In the case that an FS rating was updated during a window, the newly given FS rating was associated with that window only if the FS rating was updated in the first half of the window (i.e., it was the majority rating for the window).
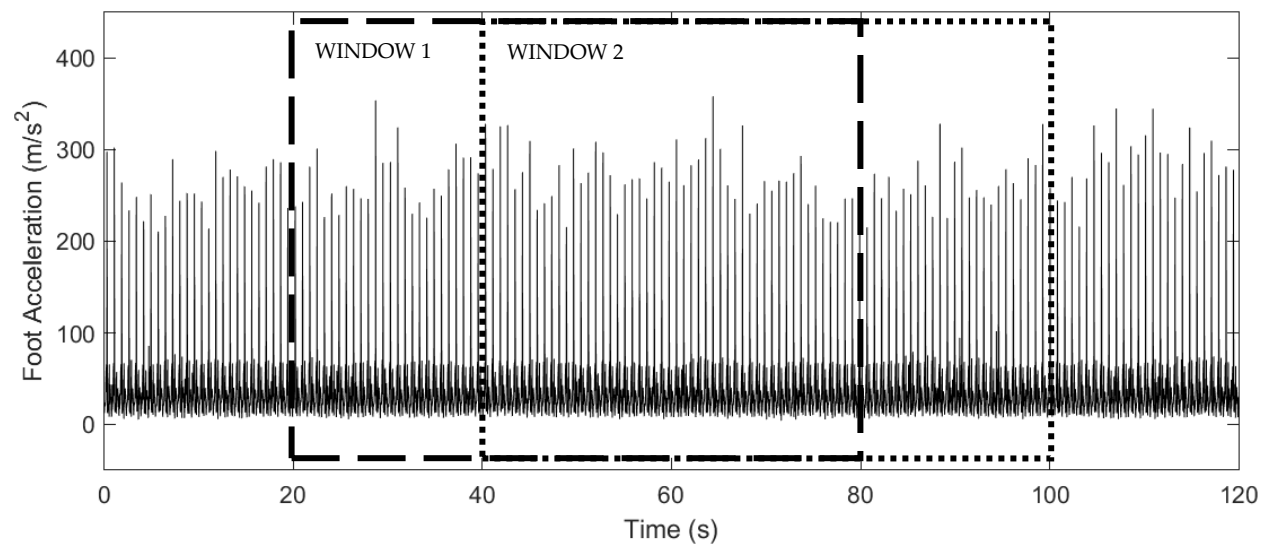
Figure 5.3: Sliding window used to aggregate the time series data and generate discrete data points. The window is of duration 60 s and is translated by 20 s.

Following these data cleaning and windowing steps, a variety of interpretable kinematic measures were calculated including spatiotemporal measures, peak accelerations and their attenuation, stability, joint ranges of motion (ROMs), and coordination variability.

Spatiotemporal measures

Foot position (subsequently used in calculating stride length) was estimated via the zero-velocity update method using a gyroscopic energy threshold [65]. The kinematic data were then segmented into strides by each initial contact (IC). ICs were identified by first estimating the step frequency as the dominant frequency of the resultant sacral acceleration [373]. The time at which the right or left foot resultant acceleration reached its peak between each of the sacral acceleration peaks was taken as the foot contact estimate [39,374]. Toe-off events for a given foot were identified by the minimum of the foot resultant angular velocity [374].
The common spatiotemporal running gait measures shown in Table 5.2 were calculated and averaged between the left and right sides of the body.

Table 5.2: Spatiotemporal running gait measures and their definitions [39,375,376].

Stride Time	Time between initial contacts of the same side
Contact Time	Time between initial contact and toe-off of the same side
Flight Time	Time between toe-off and initial contact of opposite sides
Duty Factor	Contact Time / Stride Time
Stride Length	Distance between initial contacts of the same side
Speed	Stride Length / Stride Time

Peak accelerations and attenuation

The average peak vertical accelerations of the tibia (peak tibial acceleration; PTA), pelvis (peak pelvic acceleration; PPA), and head (peak head acceleration; PHA) were calculated and assessed on an absolute scale as well as per kilogram of body weight (per BW).

Additionally, the time-domain attenuation of the peak acceleration between distal and proximal segment pairs including the shank, pelvis, or head were calculated as [31,146]:

$$Attuenuation = 1 - \frac{Proximal\ Peak\ Vertical\ Acceleration}{Distal\ Peak\ Vertical\ Acceleration}$$

such that attenuation $= 0$ indicates that the peak acceleration of the proximal segment is the same as that of the distal segment, while attenuation $= 1$ indicates that the proximal segment experienced 0 acceleration.

Stability

Stability was assessed via the proportion of pelvic movement in the medial-lateral (ML), anterior-posterior (AP), and vertical directions as defined as [137,377,378]:

$$AP\ ratio\ of\ pelvis\ acceleration\ RMS = \frac{RMS(pelvis\ AP\ acceleration)}{RMS(pelvis\ resultant\ acceleration)}$$

where RMS is the root mean square.

Joint ranges of motion

Hip and knee ROMs were calculated by first integrating the ML angular rate data and then linearly de-trending using the assumption that the motion was periodic (i.e., the joint angle was the same at each initial contact). Additionally, the average peak roll rate of the foot was calculated due to its strong positive correlation with angle frontal plane ROM [379].

Coordination variability

Coordination variabilities between the foot, shank, thigh, and pelvis body segments were calculated via vector coding methods [380–382]. Because coordination patterns differ at different points in the running gait cycle, coordination variability was evaluated during four periods: each third of stance (early, mid, and late stance) and the last third of swing (terminal swing) [381].

Intensity of arm movement

The intensity of the arm movement was assessed via the RMS of the vertical, AP, and ML components of the arm acceleration.

Data exclusions

Heart rate data for two runs were excluded due to data loss. Inertial data from the head-mounted IMU (used in calculating the PHA, shank-to-head attenuation, and pelvis-to-head attenuation) were excluded for one run due to data loss and for another run due to poor sensor attachment. Affective valence data were excluded for the last 5 minutes of one run due to data loss.

5.3.4.2 Statistical analysis

Both inter- and intra-run associations between running kinematics and positive psychology were assessed using Pearson correlation coefficients, linear regression, and parametric bootstraps conducted in R [383] with dplyr [384]. The ordinal psychological ratings were treated as continuous variables without impact on the statistical results [228–232]. Significance was determined using a critical p-value of 0.05. Corrections for multiple comparisons were not used because all tests were reported and discussed, and because this was a preliminary and exploratory study intended to identify areas of promise for future study. For this reason, reducing the risk of type II errors (i.e., false negatives) was prioritized with the recognition that the risk of type I errors (i.e., false positives) [385,386] increased.

Because each run should be reasonably independent, inter-run associations between each kinematic measure and FS, PACES, and FSS ratings were tested for Pearson correlation. Correlation coefficients of less than 0.4 were considered weak, coefficients between 0.4 and 0.7 were considered moderate, and coefficients of 0.7 and greater were considered strong [387]. The associated regression coefficients (i.e., *βs)* were assessed using a linear model. In order to simplify interpretation, the kinematic feature was first scaled to have a standard deviation of one

so that a regression coefficient (β) of one signified that a difference of one in the psychological rating was associated with a difference of one standard deviation in the given kinematic measure. Intra-run associations between each kinematic measure and the FS ratings were assessed by calculating the Pearson correlation for each run individually. Because the data within a run are not independent, confidence intervals for the correlation coefficients were calculated using a linear model (rating ~ 1 + kinematic measure + time) and parametric bootstrap. Runs exhibiting constant FS ratings were necessarily excluded from the analysis of intra-run correlations.

In addition to considering the group of all 23 runs, sub-group analyses were performed for each global running pattern (i.e., aerial, terrestrial). Aerial runs are characterized by shorter contact times, longer flight times, and greater leg stiffness than terrestrial runs and reflect different approaches to optimizing running economy [155,345,346]. Because running kinematics differ between these two groups, the inter-run correlations may be affected by grouping all runs. It is also possible that the intra-run correlations would differ due to differing approaches to efficiency optimization. A run was classified as aerial if the average duty factor was < 0.276 and terrestrial if > 0.288 [346]. Rather than classifying each runner as either aerial or terrestrial, each run was individually classified as some participants exhibited both run types.

5.4 Results

5.4.1 Distribution of psychological states

Participants provided between 2 and 14 ratings per run (average: 8), reporting affective valence between 0: neutral and 5: very good. The number, range, and variability of affective valence ratings all differed between participants and runs (see Figure 5.4), although affective valence between repeated runs by the same participant often exhibited more similarity than between runs by different participants. The aggregated distributions of affective valence,
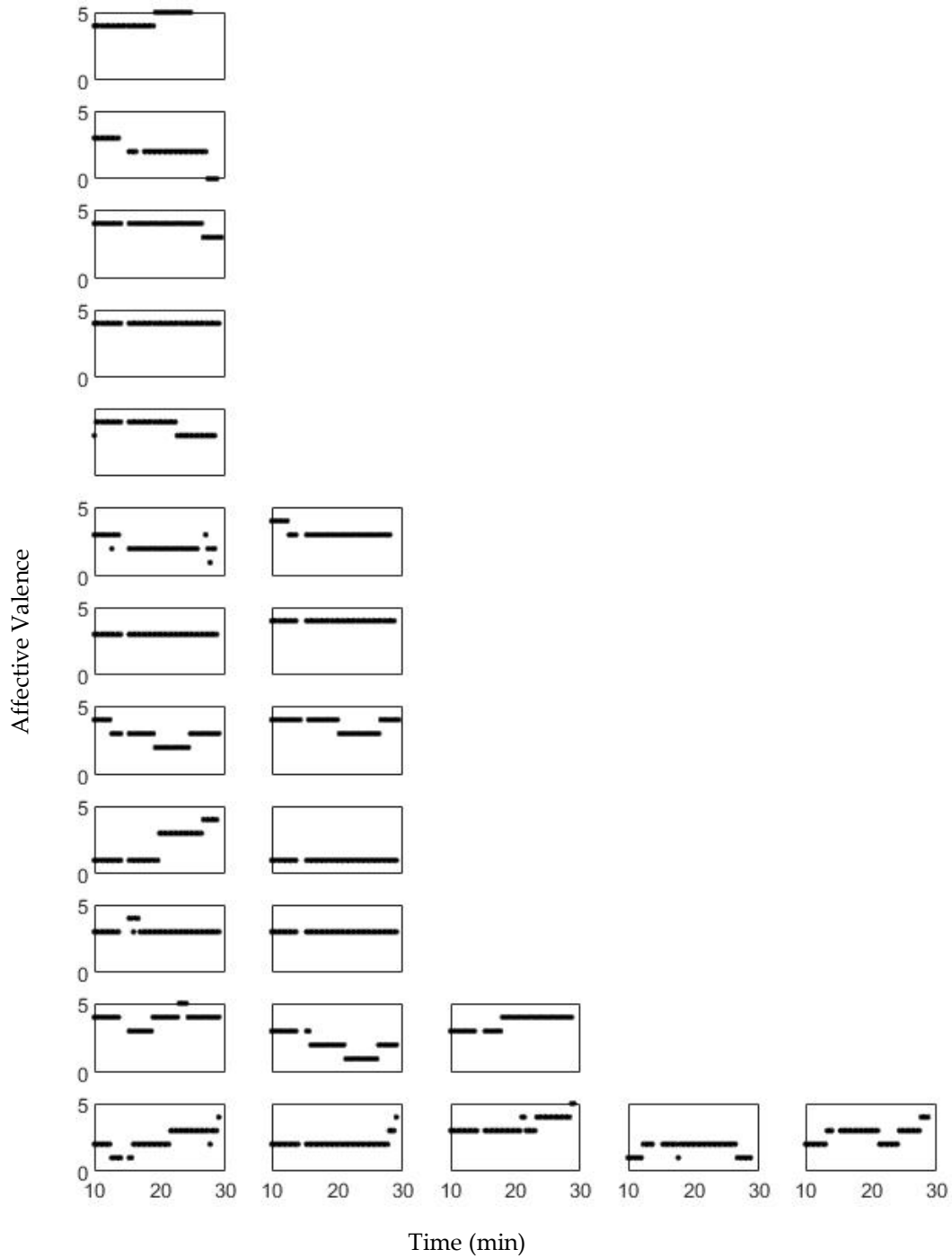
Figure 5.4: Affective valence (i.e., FS rating) time series where each row is a different participant (n=12 participants) and each column is a different run for the given participant. Participants provided between 2 and 14 ratings per run (average: 8), reporting affective valence between 0: neutral and 5: very good. The number, range, and variability of ratings differed between participants and runs.

PACES, and flow scale ratings are shown in Figure 5.5 and 5.6. PACES scores ranged from 70

to 114 (median: 97, mean: 94) relative to possible scores ranging from 18 to 126, and FSS scores

119

ranged from 57 to 86 (median: 72, mean: 71) relative to possible scores ranging from 13 to 97.

FSS and PACES scores were moderately correlated (R = 0.439, p = 0.036) while FS scores were

not correlated with either the FSS or PACES (average FS and FSS: R = -0.172, p = 0.433;

average FS and PACES: R = -0.033, p = 0.880).
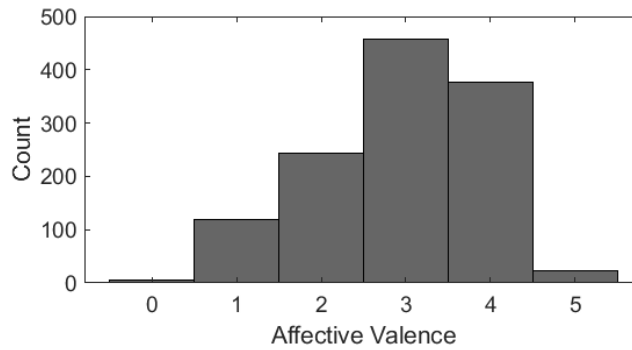
Figure 5.5: Distribution of affective valence (i.e., FS) ratings across all participants, runs, and time points. The runners experienced similar affective valence (i.e., FS) to those previously reported during moderate intensity running [348,388–390].
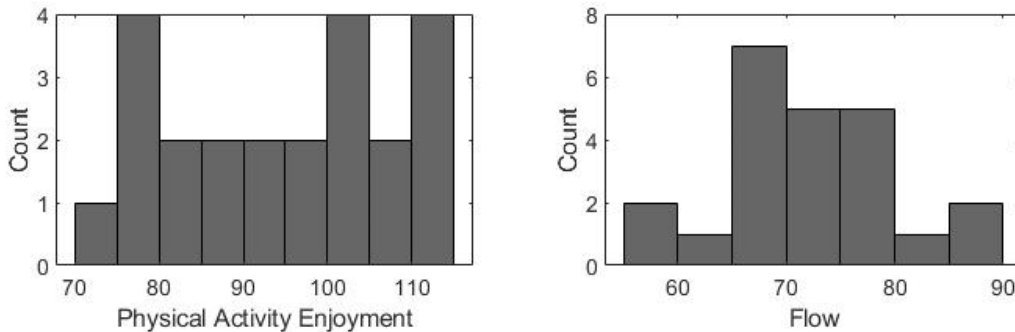
Figure 5.6: Distribution of physical activity enjoyment (i.e., PACES) and flow (i.e., FSS) ratings across all participants and runs. PACES scores ranged from 70 to 114 (median: 97, mean: 94) relative to possible scores ranging from 18 to 126, and FSS scores ranged from 57 to 86 (median: 72, mean: 71) relative to possible scores ranging from 13 to 97. The runners experienced similar activity enjoyment (i.e., PACES) and flow (i.e., FSS) to those previously reported during physical activity [358,391–393].

5.4.2 Inter-run associations between running kinematics and psychological states

The inter-run associations between the heart rate or kinematic measure and affective

valence, activity enjoyment, and flow are shown in Figure 5.7 and Table 5.3 and 5.4. When

grouping runs by global running pattern, 18 runs were aerial while only 5 were terrestrial.

Resultantly, only aerial runs were analyzed as a subgroup.

Figure 5.7: A summary of the significant inter-run associations between kinematic measures and runner psychology. PTA, peak tibial acceleration; BW, body weight; RMS, root mean square; AP, anterior/posterior; ROM, range of motion; ES, early stance; MS, mid stance; LS, late stance.

Table 5.3: Inter-run associations between kinematic measures and runner psychology (n = 23 runs). R is the Pearson correlation, and β is the regression coefficient where $\beta = 1$ reflects that a difference of one in the psychological rating was associated with a difference of one standard deviation in the given kinematic measure. * denotes significance (p ≤ 0.05). BW, body weight; RMS, root mean square; AP, anterior/posterior; ML, medial-lateral; ROM, range of motion; ES, early stance; MS, mid stance; LS, late stance; TS, terminal swing.

	Affective Valence			Activity Enjoyment			Flow		
	R	*β*	*p-Value*	*R*	*β*	*p-Value*	*R*	*β*	*p-Value*
Heart Rate	0.17	0.15	0.465	-0.37	-5.25	0.095	-0.38	-2.86	0.092
Speed	-0.24	-0.21	0.267	-0.36	-5.02	0.092	-0.01	-0.07	0.968
Stride Length	-0.24	-0.21	0.271	-0.30	-4.22	0.161	-0.02	-0.17	0.920
Stride Time	-0.07	-0.06	0.743	0.09	1.23	0.690	-0.07	-0.51	0.767
Contact Time	0.15	0.13	0.509	0.11	1.52	0.621	-0.37	-2.85	0.085
Flight Time	-0.17	-0.15	0.436	-0.09	-1.33	0.667	0.37	2.91	0.079
Duty Factor	0.16	0.15	0.453	0.11	1.49	0.629	-0.37	-2.89	0.080
Peak Tibial Acceleration	-0.36	-0.32	0.087	-0.27	-3.81	0.207	0.22	1.74	0.304
Peak Pelvic Acceleration	0.28	0.24	0.200	-0.18	-2.51	0.412	0.01	0.07	0.969
Peak Head Acceleration	-0.36	-0.32	0.107	0.07	0.97	0.765	**0.52**	**4.18**	**0.016***
Peak Tibial Acceleration Per BW	**-0.50**	**-0.44**	**0.016***	-0.09	-1.26	0.683	0.28	2.15	0.201
Peak Pelvic Acceleration Per BW	0.34	0.30	0.109	-0.05	-0.72	0.816	0.01	0.04	0.980
Peak Head Acceleration Per BW	-0.26	-0.23	0.262	0.41	5.78	0.062	0.40	3.25	0.069
Shank-to-Head Attenuation	0.33	0.30	0.138	**0.57**	**7.91**	**0.007***	-0.07	-0.53	0.775
Shank-to-Pelvis Attenuation	**0.65**	**0.57**	**<0.001***	0.10	1.34	0.664	-0.20	-1.52	0.372
Pelvis-to-Head Attenuation	-0.35	-0.31	0.119	0.31	4.29	0.176	0.19	1.55	0.403
Vertical Ratio of Pelvis Acceleration RMS	0.30	0.26	0.170	-0.05	-0.74	0.810	0.01	0.05	0.979
ML Ratio of Pelvis Acceleration RMS	-0.12	-0.10	0.596	-0.06	-0.84	0.786	-0.22	-1.70	0.316
AP Ratio of Pelvis Acceleration RMS	-0.41	-0.36	0.055	0.13	1.88	0.540	0.33	2.58	0.122
Hip ROM	-0.27	-0.24	0.204	0.09	3.07	0.314	0.38	2.96	0.073
Knee ROM	0.00	0.00	0.983	-0.22	-3.11	0.306	0.07	0.56	0.743
Foot Peak Roll Rate	-0.32	-0.28	0.134	0.22	1.31	0.670	**0.48**	**3.73**	**0.020***
Foot-Shank ES Coordination Variability	0.00	0.00	0.999	-0.03	-0.41	0.894	-0.26	-1.98	0.240
Foot-Shank MS Coordination Variability	-0.16	-0.14	0.461	-0.03	-0.35	0.909	-0.28	-2.17	0.197
Foot-Shank LS Coordination Variability	-0.04	-0.03	0.869	-0.04	-0.51	0.868	-0.10	-0.80	0.639
Foot-Shank TS Coordination Variability	-0.04	-0.04	0.854	-0.13	-1.76	0.567	-0.07	-0.54	0.753
Shank-Thigh ES Coordination Variability	-0.14	-0.12	0.525	-0.10	-1.40	0.649	-0.23	-1.80	0.287
Shank-Thigh MS Coordination Variability	**-0.44**	**-0.38**	**0.038***	0.05	0.77	0.803	0.10	0.74	0.666

Shank-Thigh LS Coordination Variability	-0.10	-0.09	0.657	0.04	0.60	0.845	-0.24	-1.89	0.264
Shank-Thigh TS Coordination Variability	0.00	0.00	0.988	-0.11	-1.50	0.625	-0.05	-0.36	0.834
Thigh-Pelvis ES Coordination Variability	-0.06	-0.05	0.788	0.05	0.70	0.821	-0.12	-0.96	0.574
Thigh-Pelvis MS Coordination Variability	-0.05	-0.04	0.826	0.09	1.29	0.676	0.12	0.93	0.589
Thigh-Pelvis LS Coordination Variability	0.15	0.13	0.508	-0.02	-0.23	0.940	-0.17	-1.30	0.444
Thigh-Pelvis TS Coordination Variability	0.14	0.13	0.515	-0.05	-0.72	0.816	-0.16	-1.22	0.476
Arm Vertical Acceleration RMS	-0.28	-0.25	0.191	0.12	1.61	0.599	**0.49**	**3.84**	**0.017***
Arm ML Acceleration RMS	-0.20	-0.17	0.367	0.37	5.16	0.083	0.17	1.32	0.439
Arm AP Acceleration RMS	0.07	0.06	0.741	0.17	2.33	0.447	-0.02	-0.18	0.919

Table 5.4: Inter-run associations between kinematic measures and runner psychology in aerial type runs (n = 18 runs). R is the Pearson correlation, and β is the regression coefficient where $\beta = 1$ reflects that a difference of one in the psychological rating was associated with a difference of one standard deviation in the given kinematic measure. * denotes significance (p ≤ 0.05). BW, body weight; RMS, root mean square; AP, anterior/posterior; ML, medial-lateral; ROM, range of motion; ES, early stance; MS, mid stance; LS, late stance; TS, terminal swing.

	Affective Valence			Activity Enjoyment			Flow		
	R	*β*	*p-Value*	*R*	*β*	*p-Value*	*R*	*β*	*p-Value*
Heart Rate	0.13	0.11	0.640	-0.37	-5.46	0.158	-0.45	-3.45	0.079
Speed	**-0.50**	**-0.41**	**0.036***	-0.40	-5.91	0.096	-0.03	-0.20	0.920
Stride Length	-0.46	-0.38	0.053	-0.33	-4.82	0.181	-0.01	-0.08	0.969
Stride Time	-0.04	-0.03	0.889	0.11	1.60	0.666	0.04	0.27	0.889
Contact Time	0.37	0.31	0.131	0.32	4.75	0.188	-0.41	-3.22	0.087
Flight Time	-0.44	-0.37	0.065	-0.29	-4.18	0.250	**0.49**	**3.84**	**0.037***
Duty Factor	0.43	0.36	0.074	0.33	4.79	0.184	**-0.48**	**-3.70**	**0.046***
Peak Tibial Acceleration	**-0.49**	**-0.40**	**0.040***	-0.27	-3.92	0.282	0.24	1.83	0.347
Peak Pelvic Acceleration	0.31	0.26	0.210	-0.12	-1.75	0.635	-0.07	-0.52	0.790
Peak Head Acceleration	-0.47	-0.39	0.067	0.06	0.81	0.840	**0.53**	**4.31**	**0.033***
Peak Tibial Acceleration Per BW	**-0.61**	**-0.51**	**0.007***	-0.04	-0.53	0.887	0.35	2.70	0.158
Peak Pelvic Acceleration Per BW	0.44	0.36	0.071	0.06	0.86	0.817	-0.07	-0.52	0.791
Peak Head Acceleration Per BW	-0.26	-0.22	0.322	0.42	6.20	0.104	0.47	3.77	0.068
Shank-to-Head Attenuation	0.42	0.34	0.107	**0.63**	**9.31**	**0.008***	-0.05	-0.37	0.866
Shank-to-Pelvis Attenuation	**0.75**	**0.62**	**< 0.001***	0.17	2.46	0.504	-0.28	-2.19	0.256
Pelvis-to-Head Attenuation	**-0.55**	**-0.45**	**0.029***	0.29	4.26	0.277	0.37	3.02	0.154
Vertical Ratio of Pelvis Acceleration RMS	**0.48**	**0.40**	**0.042***	-0.04	-0.64	0.863	-0.03	-0.20	0.918
ML Ratio of Pelvis Acceleration RMS	-0.23	-0.19	0.351	-0.12	-1.76	0.635	-0.22	-1.70	0.383
AP Ratio of Pelvis Acceleration RMS	**-0.62**	**-0.51**	**0.006***	0.20	2.89	0.431	0.41	3.21	0.088
Hip ROM	**-0.55**	**-0.46**	**0.018***	0.18	2.58	0.484	0.42	3.27	0.082
Knee ROM	-0.12	-0.10	0.635	-0.21	-3.08	0.401	0.02	0.14	0.942
Foot Peak Roll Rate	**-0.57**	**-0.47**	**0.014***	0.25	3.70	0.310	**0.55**	**4.31**	**0.017***
Foot-Shank ES Coordination Variability	-0.23	-0.19	0.362	0.03	0.42	0.909	-0.18	-1.39	0.478
Foot-Shank MS Coordination Variability	-0.09	-0.07	0.733	0.02	0.36	0.922	-0.35	-2.69	0.158

Foot-Shank LS Coordination Variability	-0.28	-0.23	0.257	0.02	0.22	0.953	0.15	1.20	0.542
Foot-Shank TS Coordination Variability	-0.08	-0.07	0.754	-0.11	-1.66	0.654	-0.30	-2.33	0.227
Shank-Thigh ES Coordination Variability	-0.42	-0.35	0.083	0.00	0.02	0.995	-0.22	-1.72	0.378
Shank-Thigh MS Coordination Variability	-0.46	-0.38	0.054	0.07	1.08	0.771	-0.01	-0.06	0.975
Shank-Thigh LS Coordination Variability	-0.38	-0.31	0.121	0.14	2.01	0.586	0.06	0.48	0.809
Shank-Thigh TS Coordination Variability	0.03	0.03	0.892	-0.15	-2.14	0.562	-0.38	-2.95	0.120
Thigh-Pelvis ES Coordination Variability	-0.14	-0.12	0.578	0.18	2.63	0.475	-0.28	-2.17	0.260
Thigh-Pelvis MS Coordination Variability	0.00	0.00	0.992	0.12	1.74	0.638	0.12	0.94	0.633
Thigh-Pelvis LS Coordination Variability	0.14	0.11	0.592	0.05	0.79	0.832	0.04	0.32	0.871
Thigh-Pelvis TS Coordination Variability	-0.07	-0.06	0.784	0.07	0.98	0.792	-0.40	-3.07	0.105
Arm Vertical Acceleration RMS	-0.46	-0.38	0.056	0.08	1.17	0.752	**0.47**	**3.64**	**0.050***
Arm ML Acceleration RMS	-0.35	-0.29	0.159	0.40	5.85	0.100	0.27	2.09	0.279
Arm AP Acceleration RMS	0.00	0.00	0.986	0.11	1.62	0.661	-0.05	-0.38	0.849

5.4.3 Intra-run associations between running kinematics and psychological states

For all kinematic measures, significant intra-run correlations occurred for one or more runs. However, no kinematic measures exhibited consistent intra-run correlations across the majority of all runs, all aerial runs, or all terrestrial runs (see Figure 5.8). Many of the significant intra-run correlations were also strongly confounded with time (see Figure 5.9).
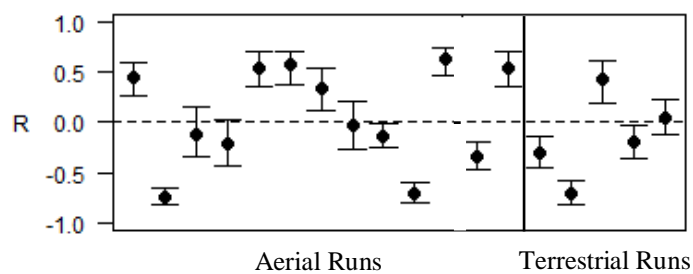
Figure 5.8: Intra-run correlation coefficients between affective valence and contact time in aerial (n = 18) and terrestrial (n = 5) runs where each data point and corresponding 95% confidence interval is associated with an individual run.
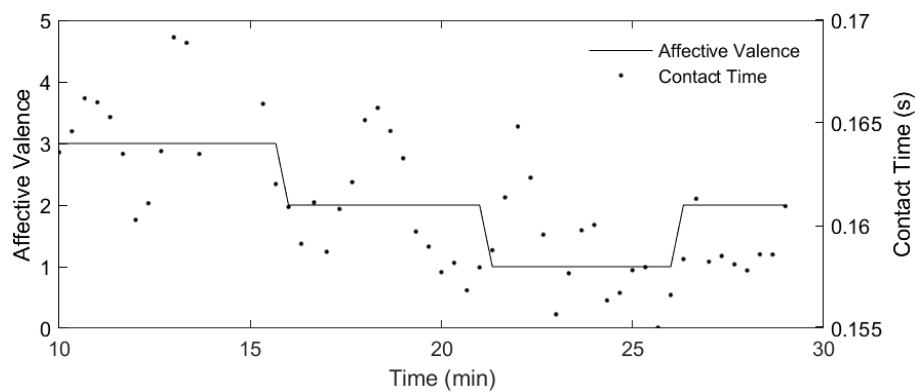
Figure 5.9: Exemplar contact time and affective valence time series in which the combined linear effects of time result in a significant positive correlation between contact time and affective valence.

5.5 Discussion

Numerous biomechanical measures exhibited significant inter-run associations with a positive running experience. Grouping the runs by global running pattern (to our knowledge for the first time in outdoor, long distance runs) resulted in increased significant associations in aerial runs, potentially due to the difference in average biomechanics observed in the two groups [155,345,346,394]. Terrestrial and aerial runs may also exhibit different underlying relationships between running biomechanics and positive running experiences. However, these comparisons are limited by the small number (n=5) of terrestrial runs included in the dataset.

Importantly, different biomechanical measures were associated with each psychological measure. The pursuit of different aspects or types of positive experience may require unique adaptations and skills. Next, we discuss the primary findings for each of the three psychological measures.

5.5.1 Inter-run associations with affective valence

Heart rate, a measure of aerobic exertion, was not significantly associated with affective valence in the group of all runs or the group of aerial runs. While this finding suggests that higher levels of exertion may not be associated with lower affect in experienced runners, participants ran at a moderate and constant effort (heart rate first quartile: 152 bpm, third quartile: 165 bpm). Conclusions about the relationship with aerobic exertion are limited.

Reduced running speed was associated with higher affective valence in aerial runs (R = -0.50; see Table 5.4). Potentially due to their association with running speed [273,395,396], reduced hip ROM and reduced peak foot roll rate (strongly and positively correlated with ankle frontal plane ROM [379]) were also associated with higher affective valence (R = -0.55 and -0.57, respectively; see Table 5.4). However, knee ROM and various spatiotemporal measures

were similarly correlated with running speed but were not significantly correlated with affective valence. For example, stride length and/or stride time must change in order to achieve a change in speed. Some associations may be weaker than what could be identified in this study.

Reduced PTA was associated with increased affective valence in both the group of all runs (R = -0.50; see Table 5.3) and the group of aerial runs (absolute: R = -0.49, per BW: R = -0.61; see Table 5.4). Reduced PTA has been associated with reduced instantaneous vertical force loading [252] and reduced overall workload. Reduced PTA has also been associated with a non-rear foot strike pattern [336], shortened stride length, and lower running speeds [252,397]; however, correlations between affective valence and stride length or running speed were insignificant.

Associations between affective valence and acceleration attenuation differed between the group of all runs and the group of aerial runs. In both the group of all runs and the group of aerial runs, increased shank-to-pelvis attenuation (achieved via active and passive systems in the lower-body) was associated with increased affective valence (R = 0.65 and 0.75, respectively; see Table 5.3 and 5.4). Aerial runs also exhibited a significant association between increased affective valence and decreased pelvis-to-head attenuation (R = -0.55; see Table 5.4). The same association was insignificant in the group of all runs. Note that while it may intuitively appear that correlations between affective valence and PTA or shank-to-pelvis attenuation would result in a similar correlation with PPA, recall that the kinematic measures were averaged over many strides and that $mean(A/B) \neq mean(A)/mean(B)$ when A and B are correlated. In fact, both the pelvis and head mean peak vertical accelerations were not significantly correlated with affective valence.

Increased stability (i.e., increased vertical ratio of pelvis acceleration RMS) was associated with improved affective valence in aerial runs (R = 0.48; see Table 5.4). Increased stability has been associated with more highly trained runners, lower levels of fatigue, stable running surfaces, and decreased running economy [248,377,398,399]. While the running surface was the same for the group of all runs and the level of fatigue was expected to be minimal, the participants' level of training varied from recreational running without prior coaching to a retired professional runner (see Table 5.1). The observed association with stability may be a reflection of differing levels of training and/or running economy.

Coordination variability was primarily uncorrelated with affective valence. This study suggests that correlations between affective valence and head stability demands [400] or injury prevention due to decreased repetitive loading [401], if existent, are smaller than could be detected in the current study. Because only one association was significant (shank-thigh coordination variability during mid-stance in the group of all runs; R = -0.44; see Table 5.3), it may be the product of multiple comparison testing and should be further studied before use. Finally, arm movement intensity (i.e., arm acceleration RMS) was not correlated with affective valence.

The finding that affective valence was positively correlated with lower-body attenuation and not significantly correlated with flight time in aerial runners is in agreement with findings reported by Lussiana and Gindre [155]. While Lussiana and Gindre reported leg stiffness rather than attenuation, leg stiffness has been related to impact magnitude and impact attenuation [402,403]. The finding that contact time was not significantly correlated with affective valence differs from that of Lussiana and Gindre who reported significant negative correlation [155]. Additionally, the finding that arm movement intensity was not correlated with affective valence

differs from that of van der Bie and Kröse who reported significant negative correlation for arm ML and AP acceleration variances [156]. Because numerous kinematic measures including contact time differ between treadmill and overground running [132], these differences in findings may be the result of differing running contexts, which underscores the need for studies such as this for overground running.

5.5.2 Inter-run associations with enjoyment

Increased physical activity enjoyment was moderately correlated with only increased shank-to-head attenuation in both the group of all runs (R = 0.57; see Table 5.3) and the group of aerial runs (R = 0.63; see Table 5.4). Increased whole-body attenuation has been associated with a non-rearfoot strike pattern [336], higher running speed [404], longer stride length [403–405], and lower stride frequency [397,404]. Because associations with running speed, stride length, and stride time were insignificant, differences in attenuation may have resulted from the combination of many small or perhaps inconsistent biomechanical changes.

5.5.3 Inter-run associations with flow

An increased level of flow was moderately correlated with decreased head stability (i.e., increased PHA), increased ankle roll (i.e., greater peak ankle roll rate), increased intensity of vertical arm movement (i.e., increased arm vertical acceleration RMS), and, within aerial runs, an increased degree of aerial running (i.e., longer flight times, lower duty factor). Level of flow was not significantly correlated with measures of heart rate, speed, lower-body peak acceleration, acceleration attenuation, stability, or coordination variability.

Similar to affective valence, flow was not significantly associated with aerobic exertion (i.e., heart rate) in the group of all runs or the group of aerial runs. While no spatiotemporal

parameters were associated with flow in the group of all runs, aerial runs exhibited significant associations between higher levels of flow and an increased degree of aerial running as characterized by increased flight time (R = 0.49; see Table 5.4) and decreased duty factor (R = -0.48; see Table 5.4).

Unlike affective valence, flow was not significantly associated with PTA or attenuation, despite their association with workload [252] and with the work done by active and passive attenuation systems. However, greater levels of flow were associated with increased PHA in all runs as well as aerial runs (R = 0.52 and 0.53, respectively; see Table 5.3 and 5.4). Increased PHA has also been associated with reduced head and gaze stabilization [406]. The level of gaze stabilization required for safe running may have been low as the path was smooth and paved. Low stabilization may have been possible at times when the runner was absorbed in the running task and was not simultaneously completing secondary tasks that required a stable gaze (e.g., observation of passerby or other surroundings). Because absorption is a hallmark of flow [347,361], an increased level of flow may have been accompanied by lower gaze stabilization.

Flow was not significantly associated with stability (i.e., pelvis acceleration RMS ratios) or coordination variability. Any associations may be weaker than what could be identified in this study. However, increased levels of flow were associated with increased foot peak roll rate within the group of all runs and within the group of aerial runs (R = 0.48 and 0.55, respectively; see Table 5.3 and 5.4). Peak foot roll rate has been strongly and positively correlated with ankle frontal plane ROM [379]; increased levels of flow may be associated with reduced ankle stability. Similarly, greater levels of flow were associated with increased arm vertical acceleration RMS within the group of all runs and within the group of aerial runs (R = 0.49 and R = 0.47; see Table 5.3 and 5.4). Because flow is associated with sensation of being in control

131

and with the balance of challenge and skill, participants may have been less worried about safety and more relaxed, leading to reduced ankle stability and increased arm movement when in flow.

5.5.4 Intra-run associations between running kinematics and psychological states

While significant intra-run associations were identified between affective valence and each kinematic measure, the associations were strongly confounded with the effect of time (see Figure 5.9). Additionally, the narrow range of affective valence observed within many runs (see Figure 5.4) severely limits the assessment of intra-run associations. Some participants reported a greater intra-run range or number of affective valence ratings; future studies may identify and target runners who experience a greater range of affect or who are better able to self-report these changes. Future studies may also explore running conditions which could produce more variable affective valence (e.g., fartlek running). However, such modifications may also limit the applicability of findings to the average experienced runner during a typical training run.

5.5.5 Limitations

Limitations of this study include a relatively small sample size, the use of highly cushioned footwear, the inclusion of a limited category of runners and a single run type, and the inclusion of limited terrestrial runs. Additionally, the use of many sensors and data collection methods may have affected the running experience. Some participants expressed discomfort with wearing many visible sensors and audibly rating affective valence while running in public. The task of reporting affective valence throughout the run may have also influenced both enjoyment and flow. Future studies should examine additional runners and running contexts (e.g., intensity, surface, shoes, surroundings, competitive season). They may opt to seek participants less cognizant of their appearance, reduce the number of sensors (and the resulting breadth of data),

132

and/or complete the runs in a less populated location. They may also opt to seek participants with high self-awareness and increased ability to self-report psychological changes during a run. Future work should also investigate causal relationships between the identified biomechanical measures and positive running experiences.

5.6 Conclusion

This study identified numerous inter-run correlations between running biomechanics and positive running experiences during long, outdoor training runs. However, different biomechanical measures were correlated with each measure of positive experience, suggesting that no single running technique is associated with all three measures of positive experience. Higher affective valence was associated with reduced peak accelerations and improved acceleration attenuation in certain parts of the body (i.e., PTA, lower-body attenuation). During aerial runs, higher affective valence was also associated with slower running speeds, less attenuation in the upper-body, and increased stability. In contrast, increased physical activity enjoyment was associated with increased lower-body attenuation. Finally, an increased level of flow was associated with decreased head and ankle stabilization and, in aerial runs, an increased degree of aerial running. Intra-run correlations were often significant; however, they differed between runs and may have simply been the result of aligned temporal trends.

These findings suggest that there are significant inter-run associations between positive running experiences and biomechanics during typical training runs in well-trained runners. The findings importantly differ from those of prior treadmill or track-based studies, demonstrating the need to study running biomechanics and psychology in "real-world" running settings. The associations identified here during "real-world" training runs should be considered when

examining psychological and biomechanical determinants of performance, and they may be explored as a means to support positive running experiences.

5.7 Appendix: Psychological scales

Appendix Figure 5.10: The Feeling Scale used to quantify affective valence.

FEELING SCALE	
+5	Very Good
+4	
+3	Good
+2	
+1	Fairly Good
0	Neutral
-1	Fairly Bad
-2	
-3	Bad
-4	
-5	Very Bad

Appendix Figure 5.11: The Flow Short Scale used to quantify flow.

	not at all	partly	very much
I feel just the right amount of challenge.	O—O—O—O—O—O—O		
My thoughts/activities run fluidly and smoothly.	O—O—O—O—O—O—O		
I don't notice time passing.	O—O—O—O—O—O—O		
I have no difficulty concentrating.	O—O—O—O—O—O—O		
My mind is completely clear.	O—O—O—O—O—O—O		
I am totally absorbed in what I am doing.	O—O—O—O—O—O—O		
The right thoughts/movements occur of their own accord.	O—O—O—O—O—O—O		
I know what I have to do each step of the way.	O—O—O—O—O—O—O		
I feel that I have everything under control.	O—O—O—O—O—O—O		
I am completely lost in thought.	O—O—O—O—O—O—O		

	easy		difficult
Compared to all other activities which I partake in, this one is …	O—O—O—O—O—O—O—O—O		

	low		high
I think that my competence in this area is …	O—O—O—O—O—O—O—O—O		

	too low	just right	too high
For me personally, the current demands are …	O—O—O—O—O—O—O—O—O		

Appendix Figure 5.12: The Physical Activity Enjoyment Scale used to quantify running enjoyment.

Physical Activity Enjoyment Scale

Please rate how you feel *at the moment* about the physical activity you have been doing.

*	1	2	3	4	5	6	7	
I enjoy it								I hate it

	1	2	3	4	5	6	7	
I feel bored								I feel interested

	1	2	3	4	5	6	7	
I dislike it								I like it

*	1	2	3	4	5	6	7	
I find it pleasurable								I find it unpleasurable

*	1	2	3	4	5	6	7	
I am very absorbed in this activity								I am not at all absorbed in this activity

	1	2	3	4	5	6	7	
It's no fun at all								It's a lot of fun

*	1	2	3	4	5	6	7	
I find it energizing								I find it tiring

	1	2	3	4	5	6	7	
It makes me depressed								It makes me happy

*	1	2	3	4	5	6	7	
It's very pleasant								It's very unpleasant

*	1	2	3	4	5	6	7	
I feel good physically while doing it								I feel bad physically while doing it

*	1	2	3	4	5	6	7	
It's very invigorating								It's not at all invigorating

	1	2	3	4	5	6	7	
I am very frustrated by it								I am not at all frustrated by it

*	1	2	3	4	5	6	7	
It's very gratifying								It's not at all gratifying

*	1	2	3	4	5	6	7	
It's very exhilarating								It's not at all exhilarating

	1	2	3	4	5	6	7	
It's not at all stimulating								It's very stimulating

*	1	2	3	4	5	6	7	
It gives me a strong sense of accomplishment								It does not give me any sense of accomplishment at all

*	1	2	3	4	5	6	7	
It's very refreshing								It's not at all refreshing

	1	2	3	4	5	6	7	
I felt as though I would rather be doing something else								I felt as though there was nothing else I would rather be doing

*Item is reversed scored (i.e., 1=7, 2=6, . . . 6=2, 7=1).

Chapter 6 Summary and Future Work

6.1 Major contributions and overview of dissertation

Through a collection of four studies, this dissertation demonstrates both the challenges in quantifying human movement via wearable sensors and the unique opportunities presented for "real-world" assessment and feedback. The specific contributions are in two application areas: balance rehabilitation, and distance running. In Part I on balance rehabilitation, two studies demonstrated that inertial sensors can be used to make high-quality balance rehabilitation more accessible. Chapter 2 identified an accessible alternative to existing feedback methods and demonstrated its promise for improving the efficacy of home-based balance training. Chapter 3 suggested that both self-assessments and wearable sensor data can further support home-based balance training by enabling remote assessments of intensity and therefore dosage. Next, in Part II on distance running, two studies demonstrated that wearable sensors can provide meaningful measures of running performance, supporting the study of "real-world" outdoor distance running. Chapter 4 illustrated that, with advanced algorithms, inertial sensors can be used to estimate traditional and interpretable kinematic measures such as three-dimensional lower-body joint angles. Chapter 5 then associated IMU-based biomechanical measurements with positive running experiences, suggesting that running technique and runner psychology may be interrelated. Collectively, these studies advance each of the primary objectives in human performance quantification (see Figure 6.1).

Performance Quantification via Inertial Sensors		
HOME–BASED BALANCE REHABILITATION	**OBJECTIVES**	**"REAL – WORLD" DISTANCE RUNNING**
	Calculation of accurate metrics	IMUs and ErKFs should be further developed for lower-body kinematic estimation during 'real-world' running.
Terminal feedback may be an effective and more accessible alternative to concurrent feedback during standing balance training.	*Association of metrics with outcomes*	Associations between positive experiences and biomechanics should be further explored as means to improve running experiences.
Patient self-ratings and sway kinematics may support assessments of balance exercise intensity during remote training.	*Delivery of augmented feedback*	

Figure 6.1: Dissertation contributions that support each of the primary objectives in the quantification of home-based standing balance and "real-world" distance running.

This dissertation also demonstrates that wearable inertial sensors can be applied to a variety of human movements, ranging from low to very high dynamics. However, a number of challenges to the use of wearable sensors are evidenced, including the complexity of signal processing, algorithm development, and the relation of calculated metrics with outcome measures. The remainder of this chapter further describes the implications of this dissertation and explores areas for future work.

6.2 The use of IMUs to support balance telerehabilitation

In Part I of this dissertation, two studies supported that inertial sensors can make high-quality balance rehabilitation more accessible. Telerehabilitation and home-based balance training have become prevalent as methods to improve access [205,206] and to mitigate public health risks such as those posed by COVID-19 [207–210]. However, training without a professional's guidance is less effective than supervised training [86,87], and only 29% of PTs in

a 2022 vestibular rehabilitation study expressed that telerehabilitation was as effective as in-person care [207]. Chapters 2 and 3 provide evidence that smart phone-based systems can improve the quality of home-based care without requiring specialized equipment. Multifunctional systems may incorporate various supports for remote training including automated progress monitoring via the scoring of clinical balance tests [106–110], increased engagement and increased improvement rates via feedback (see Chapter 2), and well-informed remote exercise progression supported by intensity assessments (see Chapter 3). Additional research should examine the longitudinal benefits of multifunctional smart phone-based systems that support key aspects of balance rehabilitation.

6.3 The use of IMUs to support evaluations of "real-world" running

In Part II of this dissertation, two studies demonstrated that IMUs can support the study of "real-world" distance running. However, both studies leveraged constraints on the environment and task in order to ensure the accuracy and interpretability of calculated metrics. In Chapter 4, a single set of noise parameters governing the ErKF algorithm were selected in part because each participant completed the same task (i.e., level treadmill running at a given speed). If the task were more variable between (e.g., differing speeds) or within (e.g., variable inclination or surface) participants, the optimal noise parameters may vary and therefore be more difficult to approximate. In Chapter 5, a relatively smooth and flat path was selected in order to minimize sources of variability in running kinematics and psychology that were not the focus of the study. Even so, because speed during extended over ground runs is not as easily controlled as it is during treadmill runs, interpretation of the kinematic measures is complicated by fluctuations in running speed. Because few studies have examined near "real-world" running, methods have yet to be established for the control of variability and reduction of confounders when studying real-

world distance running [146]. Over time and with the development of increasingly robust algorithms, studies may require less constraints on the running task and environment.

While the two parts of this dissertation advanced different application areas, studies in both parts employed a range of data types including inertial data, traditional laboratory-based measures, and self-assessments. We therefore next discuss the advantages of each and some considerations for data collection and processing.

6.4 Inertial sensors as one of many sensing options: Choose the right tool for the job

This dissertation focuses on the advancement of IMU-driven systems because, unlike traditional sensing technologies, they can be used in a variety of environments (e.g., Chapters 2, 3, and 5), can easily record long trials (e.g., Chapter 5), and can require less time for post-processing (e.g., Chapters 2, 3, and 5). They are also relatively accessible, enabling widespread and longitudinal use of IMU-based training support and feedback systems. Finally, they are in their relative infancy and require additional study in order to fully capitalize on these benefits.

However, as with any tool, wearable sensors are not ideal for every task. Rather than replacing traditional, laboratory-based sensor technologies such as marker-based motion capture, new technology options such as inertial and markerless motion capture should be considered as additional options during the design of an experiment. While both marker-based and markerless motion capture are limited to restricted capture volumes, markerless motion capture can be performed without attaching any equipment to the body. It is also relatively fast and accessible, and it may provide sufficiently accurate lower-body sagittal plane joint angles [249,321]. Marker-based motion capture additionally supports the study of joint moments and work [294], off-sagittal plane joint angles [249,321], complex movements within the feet and hands, and soft-tissue (e.g., breast tissue [407,408]) movement. Finally, as seen in Chapter 5, both markerless

and marker-based motion capture may require less bespoke algorithms when estimating joint angles and may be preferable within laboratory settings.

Similarly, in some experiments, self-assessments may complement or even be preferable to sensor-based measurements. In Chapter 3, both self-assessments and sensor data were similarly correlated to expert physical therapist assessments. Both options may support home-based training, and the decision between the two should include numerous factors including accessibility, ease of use, engagement, and compliance. These factors will depend on needs of the end user, as well as other incorporated features (e.g., feedback as seen in Chapter 2).

Ultimately, deep understanding of the relationships between various data, as pursued in Chapters 3 and 4, are needed so that researchers and designers can intelligently select combinations of wearable sensors, traditional laboratory-based sensors, and/or self-assessment tools.

6.5 Determinants for the accuracy of inertial motion capture

When using inertial sensors, careful methodology should be followed in order to ensure accuracy and interpretability of the data. The accuracy of inertial motion capture is determined by 1) sensor specifications, 2) attachment methods, and 3) calibration, signal processing, and metric calculation methods (see Figure 6.2). Appropriate selections will differ based on the movement and application; the data collection methods used in Parts I and II therefore necessarily differed. A summary of each of these three determinates follows.
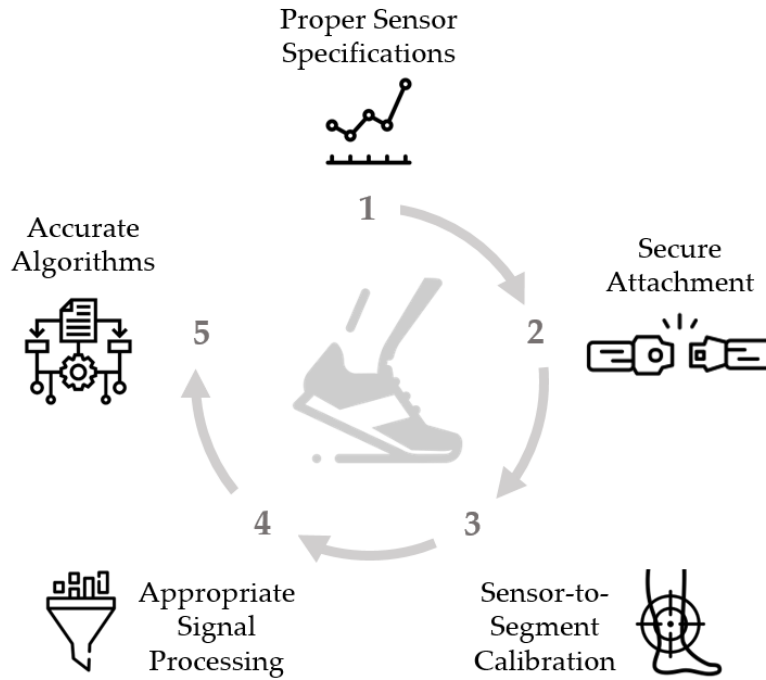
Figure 6.2: The steps required for accurate measurement of human movement using inertial sensors.

6.5.1 IMU sensor specifications

IMU selection involves the balancing of numerous sensor specifications, including sensor ranges, resolutions, sampling frequencies, battery life, data storage or transmission capacity, weight, and cost and availability.

Accelerometer and gyroscope ranges must be large enough to avoid saturation while being small enough to avoid poor resolution. Sampling frequencies must also be high enough to accurately capture the frequency content of a given movement. Sensor range, resolution, and sampling frequency requirements should also be balanced against the cost and availability of the sensor, the battery required to power the sensor for a given duration, and the data storage or transmission rate needed in order to record the data. Lastly, the total sensor mass should be low so as to avoid encumbrance and reduce the effects of soft tissue movement [252,350,409].

142

As a result, different IMUs are optimal for applications with low or high dynamics (e.g., balance or running, respectively). Small sensor ranges and low sampling frequencies are often preferable in applications with low dynamics such as balance rehabilitation due to their improved resolution and lower cost. Additionally, depending on the expected end user, longer battery lives may improve adoption. Because of the low dynamics, the additional mass of a larger battery will likely increase soft tissue movement by a negligible amount. In contrast, in highly dynamic applications such as running, larger sensor ranges and high sampling frequencies are often necessary due to the large and high frequency acceleration peaks [252,276,349]. Similarly, a low mass IMU is needed to reduce the effects of soft-tissue movement.

In order to make a single IMU well-suited to a variety of movements, research-grade IMUs often combine multiple sensors such that higher resolution data are available within a small range, and lower resolution data are available for a large range. Additionally, commercially available IMUs often sample data at a high frequency and then intelligently down sample prior to transmission or storage in order to reduce power use and improve battery life. Note, however, that the downsampling method may have a large effect on accuracy [349]. While these methods may result in a single IMU that can be used for a variety of purposes during research and development, the cost of these IMUs is much higher than for their simpler counterparts.

6.5.2 Sensor attachment

In order to minimize movement between the IMU and the body, the IMU should be securely attached [409]. Straps such as those used in Chapters 2, 3, and 5 may be sufficient when recording movements characterized by low dynamics (e.g., balance) or on parts of the body experiencing lower dynamics (e.g., the head when running). Elastic tapes like the one used in

Chapter 5 may provide more secure attachment during highly dynamic movements and endurance activities during which participants sweat considerably.

6.5.3 Calibration, signal processing, and metric calculation methods

As illustrated throughout this dissertation, inertial data analysis methods must be carefully selected so that resulting metrics are accurate. As seen in Chapter 5, analysis methods that derive metrics directly from acceleration and angular rate data are similar in both complexity and specificity to optical motion capture analysis methods. However, algorithms for position-domain kinematics benefit from assumptions about movement characteristics and perform best when highly specialized to the task. In Chapters 2 and 3, the algorithm for sway angle estimation relied heavily upon the identification of periods with low dynamics during which the gravitational acceleration vector could be used to correct errors in the pitch and roll estimates. Because standing balance requires a relatively low level of dynamic movement, there were many periods of low dynamics, and this single correction method was sufficient for arresting drift. However, as seen in Chapter 4, running is a much more dynamic movement that requires additional correction methods in order to successfully arrest drift in the position-domain estimates.

6.6 Considerations when using self-assessments

While inertial data capture requires specialized methodology in order to be accurate and can therefore be seen as prohibitively challenging to novices, the use of self-assessments also presents a unique set of challenges. Firstly, the scale should be granular enough to support the quantification of even small effects but not so granular as to be confusing to participants. In Chapter 3, the appropriate level of granularity in the balance intensity scale was suggested to be

144

different between balance and physical therapist participants. While physical therapist participants were able to effectively use the entirety of the 5-point scale, balance participants could best distinguish between two levels of intensity.

The specificity of a scale should also be carefully chosen so as to capture the effect of interest, avoid undue variation in the participants' interpretations, and be practical to use. In Chapter 3, the intensity scale was specific to standing balance and successfully limited the variability of expert ratings. However, it also referenced level of sway, while people with balance impairments may exhibit increased or decreased sway [184–187]. Balance participants may have also incorporated both task intenstiy and balance confidence. In Chapter 5, multiple scales of varying specificity and various target constructs were employed. Participants expressed discomfort with the level of generality of the Feeling Scale, asking what factors should be incorporated into a rating. However, unlike the Physical Activity Enjoyment Scale and Flow Short Scale, it was simple enough to be remembered and used verbally throughout a training run. Regardless of the scale specifics, people may differ in their ability to self-assess and self-report due to differences in their (1) ability to perceive the movement of their body, (2) ability to recall their experience throughout the task upon its completing, and (3) willingness to report extreme values. In Chapter 3, the acuity of a participants' sensory systems may directly limit the perception of movement. Various patient populations may be more of less able to assess their own balance performance. In Chapter 5, all participants had full use of their sensory systems; however, various aspects of runner psychology (e.g., attentional focus) may affect a participant's awareness of their state. In both Chapters 3 and 5, participants may have had opinions of what ratings were acceptable. No runner participant rated their affective valence as below neutral (i.e., 0) despite some runners commenting on their high level of fatigue and stress that day. Different

balance participants were more or less reticent to rate intensity at either extreme. Some participants commented that they felt it would be too harsh on themselves to give a rating of 5 (I lost my balance). As a result of these inter-person differences, study populations may be selected in part due to their ability to provide self-assessments.

6.7 Implications

This dissertation explored a broad range of applications for inertial sensors, all of which aimed at the advancement of "real-world" performance assessment and feedback systems. Chapters 2 and 3 demonstrated that IMUs found ubiquitously in smart phones and other devices can support balance training by yielding increased rates of improvement and by enabling the remote assessment of dosage. These approaches may be particularly beneficial during telerehabilitation, when the expert assessments and recommendations of a physical therapist are limited by poor visibility. Chapters 4 and 5 examined distance running applications and illustrated that, despite the much higher level of dynamics, wearable sensors can still be effective at capturing a variety of relevant metrics. Wearable inertial sensors may be particularly advantageous when studying "real-world" running, as done in Chapter 5, or when "gold-standard" laboratory-based equipment is not available. Inertial sensors may therefore support the democratization of personalized, data-driven decision making and training in a variety of contexts spanning both healthcare and athletics.

However, Chapters 2 through 5 also demonstrated a variety of challenges in the use of IMUs including the need for known constraints on the movement and task-specific algorithms. Continued development of robust algorithms may alleviate some of these challenges and allow for use in increasingly "real-world" environments.

6.8 Limitations

While the findings of this dissertation contribute to the development of IMU-based performance quantification, these studies precede the design of devices that are ready for "real-world" use. As such, Chapters 2, 3, and 4 were based on data collected in laboratory environments. Doing so allowed for comparisons to established methods such as marker-based motion capture or concurrent visual feedback. It also reduced the variability of sensor placement, task completion, etc. which allowed for better examination of the underlying phenomena. However, allowances for increased variability are necessary prior to widespread use. Similarly, as is expected in research discoveries, all chapters employed bespoke algorithms which required standardized and hand-cleaned data. Finally, the studies employed relatively small sample sizes and relevant but restricted participant populations. Additional participants may exhibit variable responses, further elucidating both group and individual effects.

6.9 Future work

In addition to the immediate work suggested in Chapters 3 through 5, future work should continue to advance the three primary objectives of wearable assessment and feedback systems for balance telerehabilitation or distance running as outlined in Figure 6.1. Longitudinal studies should examine the effects of terminal visual feedback and intensity-based exercise progression during home-based balance training on both balance ability and fall risk. Studies should also explore diverse patient populations and consider varying levels of physical therapist involvement. Wearable systems for distance running are nascent and consequently are less developed than those for balance rehabilitation. Chapters 4 and 5 demonstrated the potential for inertial sensors to provide meaningful insight into "real-world" running experiences. Future work should continue to develop filter-based algorithms for lower-body running kinematic estimation

147

that are robust to experimental protocol including sensor characteristics, running speed, surface and surface regularity, etc. Additional studies may also explore relationships between running biomechanics, physiology, and psychology in various running populations and in differing environments.

Within the broader context of balance rehabilitation, the quantification of balance intensity and the relation of various data sources (see Chapter 3) may support increasingly complete reports of balance training dosage. Future work should consider training intensity when identifying dosage effects, comparing between training programs, and optimizing physical therapist training [201,202]. In addition, the majority of studies focused on the development and evaluation of IMU-driven wearable systems have historically focused on a single element of balance training (e.g., augmented feedback). Because substantial developments have occurred in various areas; future studies may consider the combined effects of automated balance assessment tools, feedback devices, and automated or remote progression systems. Finally, as inertial systems near widespread availability to physical therapists and their patients, the relevant contextual factors and user needs should be deliberately studied in order to optimize adoption and compliance [410–412].

While there is an abundance of future work for the advancement of inertial sensors in balance rehabilitation, there is arguably even more to be done in the field of running biomechanics. As previously discussed, research on running biomechanics has historically been limited to laboratory environments, while the vast majority of running takes place in importantly different contexts. Researchers have begun to use IMUs and other wearables in studies of running biomechanics; however, the majority of these studies still differ notably from "real-world" running[146]. Chapter 5 demonstrated that it is possible to study running biomechanics in

an environment that more nearly approximates a typical training run. Others have successfully studied biomechanical changes during marathon races [413], the effects of elevation change during trail running [414], and the effects of medial tibial stress syndrome [415]. Additional work should continue to explore near "real-world" running conditions, re-examining phenomena previously observed in laboratory settings and extending our knowledge of topics previously unstudied. Relatedly, the development of cost effective, user-friendly IMUs suitable to running (e.g., large sensor ranges and high sampling frequencies) would further support the widespread use of IMUs in running research.

Bibliography

[1] Lee R, James C, Edwards S, Skinner G, Young JL, Snodgrass SJ. Evidence for the effectiveness of feedback from wearable inertial sensors during work-related activities: A scoping review. Sensors 2021;21:1–37. https://doi.org/10.3390/s21196377.

[2] Radhakrishnan U, Koumaditis K, Chinello F. A systematic review of immersive virtual reality for industrial skills training. Behav Inf Technol 2021;40:1310–39. https://doi.org/10.1080/0144929X.2021.1954693.

[3] Sienko KH, Seidler RD, Carender WJ, Goodworth AD, Whitney SL, Peterka RJ. Potential mechanisms of sensory augmentation systems on human balance control. Front Neurol 2018;9:944. https://doi.org/10.3389/fneur.2018.00944.

[4] Gordt K, Gerhardy T, Najafi B, Schwenk M. Effects of wearable sensor-based balance and gait training on balance, gait, and functional performance in healthy and patient populations: A systematic review and meta-analysis of randomized controlled trials. Gerontology 2017;64:74–89. https://doi.org/10.1159/000481454.

[5] De Angelis S, Princi AA, Dal Farra F, Morone G, Caltagirone C, Tramontano M. Vibrotactile-based rehabilitation on balance and gait in patients with neurological diseases: A systematic review and metanalysis. Brain Sci 2021;11:518. https://doi.org/10.3390/brainsci11040518.

[6] Karasinski JA, Torron Valverde IC, Brosnahan HL, Gale JW, Kim R, Yashar M, et al. Designing procedure execution tools with emerging technologies for future astronauts. Appl Sci 2021;11:1607. https://doi.org/10.3390/app11041607.

[7] Welch KC, Harnett C, Lee YC. A review on measuring affect with practical sensors to monitor driver behavior. Safety 2019;5:72. https://doi.org/10.3390/safety5040072.

[8] Van Hooren B, Goudsmit J, Restrepo J, Vos S. Real-time feedback by wearables in running: Current approaches, challenges and suggestions for improvements. J Sports Sci 2020;38:214–30. https://doi.org/10.1080/02640414.2019.1690960.

[9] Neumann DL, Moffitt RL, Thomas PR, Loveday K, Watling DP, Lombard CL, et al. A systematic review of the application of interactive virtual reality to sport. Virtual Real 2018;22:183–98. https://doi.org/10.1007/s10055-017-0320-5.

[10] Lauber B, Keller M. Improving motor performance: Selected aspects of augmented feedback in exercise and health. Eur J Sport Sci 2014;14:36–43. https://doi.org/10.1080/17461391.2012.725104.

[11] Bangaru SS, Wang C, Aghazadeh F. Automated and continuous fatigue monitoring in construction workers using forearm EMG and IMU wearable sensors and recurrent neural network. Sensors 2022;22:9729. https://doi.org/10.3390/s22249729.

[12] Clermont CA, Pohl AJ, Ferber R. Fatigue-related changes in running gait patterns persist in the days following a marathon race. J Sport Rehabil 2020;29:934–41. https://doi.org/10.1123/JSR.2019-0206.

[13] Marotta L, Scheltinga BL, van Middelaar R, Bramer WM, van Beijnum BJF, Reenalda J,

et al. Accelerometer-based identification of fatigue in the lower limbs during cyclical physical exercise: A systematic review. Sensors 2022;22:3008. https://doi.org/10.3390/s22083008.

[14] Ibrahim AA, Küderle A, Gaßner H, Klucken J, Eskofier BM, Kluge F. Inertial sensor-based gait parameters reflect patient-reported fatigue in multiple sclerosis. J Neuroeng Rehabil 2020;17:165. https://doi.org/10.1186/s12984-020-00798-9.

[15] Karvekar S, Abdollahi M, Rashedi E. Smartphone-based human fatigue level detection using machine learning approaches. Ergonomics 2021;64:600–12. https://doi.org/10.1080/00140139.2020.1858185.

[16] Arlotti JS, Carroll WO, Afifi Y, Talegaonkar P, Albuquerque L, Burch RFV, et al. Benefits of IMU-based wearables in sports medicine: narrative review. Int J Kinesiol Sport Sci 2022;10:36–43. https://doi.org/10.7575/aiac.ijkss.v.10n.1p.36.

[17] Aroganam G, Manivannan N, Harrison D. Review on wearable technology sensors used in consumer sport applications. Sensors 2019;19:1983. https://doi.org/10.3390/s19091983.

[18] Preatoni E, Bergamini E, Fantozzi S, Giraud LI, Orejel Bustos AS, Vannozzi G, et al. The use of wearable sensors for preventing, assessing, and informing recovery from sport-related musculoskeletal injuries: A systematic scoping review. Sensors 2022;22:3225. https://doi.org/10.3390/s22093225.

[19] Zhao J, Obonyo E, Bilén SG. Wearable inertial measurement unit sensing system for musculoskeletal disorders prevention in construction. Sensors 2021;21:1324. https://doi.org/10.3390/s21041324.

[20] Usmani S, Saboor A, Haris M, Khan MA, Park H. Latest research trends in fall detection and prevention using machine learning: A systematic review. Sensors 2021;21:5134. https://doi.org/10.3390/s21155134.

[21] Hu X, Qu X. Pre-impact fall detection. Biomed Eng Online 2016;15:61. https://doi.org/10.1186/s12938-016-0194-x.

[22] Kumar VCV, Ha S, Sawicki G, Liu CK. Learning a control policy for fall prevention on an assistive walking device. Proc. - IEEE Int. Conf. Robot. Autom., 2020, p. 4833–40. https://doi.org/10.1109/ICRA40945.2020.9196798.

[23] Camomilla V, Bergamini E, Fantozzi S, Vannozzi G. Trends supporting the in-field use of wearable inertial sensors for sport performance evaluation: A systematic review. Sensors 2018;18:873. https://doi.org/10.3390/s18030873.

[24] Giraldo-Pedroza A, Lee WCC, Lam WK, Coman R, Alici G. Effects of wearable devices with biofeedback on biomechanical performance of running—a systematic review. Sensors 2020;20:6637. https://doi.org/10.3390/s20226637.

[25] Picerno P, Iosa M, D'Souza C, Benedetti MG, Paolucci S, Morone G. Wearable inertial sensors for human movement analysis: a five-year update. Expert Rev Med Devices 2021;18:79–94. https://doi.org/10.1080/17434440.2021.1988849.

[26] Gawronska A, Pajor A, Zamyslowska-Szmytke E, Rosiak O, Jozefowicz-Korczynska M. Usefulness of mobile devices in the diagnosis and rehabilitation of patients with dizziness and balance disorders: A state of the art review. Clin Interv Aging 2020;15:2397–406. https://doi.org/10.2147/CIA.S289861.

[27] Vitali R V., Barone VJ, Ferris J, Stirling LA, Sienko KH. Effects of concurrent and terminal visual feedback on ankle co-contraction in older adults during standing balance. Sensors 2021;21:7305. https://doi.org/10.3390/s21217305.

[28] Seshadri DR, Li RT, Voos JE, Rowbottom JR, Alfes CM, Zorman CA, et al. Wearable

sensors for monitoring the physiological and biochemical profile of the athlete. Npj Digit Med 2019;2. https://doi.org/10.1038/s41746-019-0150-9.

[29] Prieto TE, Myklebust JB, Hoffmann RG, Lovett EG, Myklebust BM. Measures of postural steadiness: Differences between healthy young and elderly adults. IEEE Trans Biomed Eng 1996;43:956–66. https://doi.org/10.1109/10.532130.

[30] Ghislieri M, Gastaldi L, Pastorelli S, Tadano S, Agostini V. Wearable inertial sensors to assess standing balance: a systematic review. Sensors (Switzerland) 2019;19:1–25. https://doi.org/10.3390/s19194075.

[31] Benson LC, Clermont CA, Bošnjak E, Ferber R. The use of wearable devices for walking and running gait analysis outside of the lab: A systematic review. Gait Posture 2018;63:124–38. https://doi.org/10.1016/j.gaitpost.2018.04.047.

[32] Mason R, Pearson LT, Barry G, Young F, Lennon O, Godfrey A, et al. Wearables for running gait analysis: A systematic review. Sport Med 2023;53:241–68. https://doi.org/10.1007/s40279-022-01760-6.

[33] Siqueira CM, Lahoz Moya GB, Caffaro RR, Fu C, Kohn AF, Amorim CF, et al. Misalignment of the knees: Does it affect human stance stability. J Bodyw Mov Ther 2011;15:235–41. https://doi.org/10.1016/j.jbmt.2009.08.005.

[34] dos Anjos F, Lemos T, Imbiriba LA. Does the type of visual feedback information change the control of standing balance? Eur J Appl Physiol 2016;116:1771–9. https://doi.org/10.1007/s00421-016-3434-7.

[35] Hirjaková Z, Lobotková J, Bučková K, Bzdúšková D, Hlavačka F. Age-related differences in efficiency of visual and vibrotactile biofeedback for balance improvement. Act Nerv Super Rediviva 2015;57:63–71.

[36] Luczak T, Burch R, Lewis E, Chander H, Ball J. State-of-the-art review of athletic wearable technology: What 113 strength and conditioning coaches and athletic trainers from the USA said about technology in sports. Int J Sport Sci Coach 2020;15:26–40. https://doi.org/10.1177/1747954119885244.

[37] Muniz-Pardos B, Sutehall S, Gellaerts J, Falbriard ; Mathieu, Mariani B, Bosch A, et al. Integration of wearable sensors into the evaluation of running economy and foot mechanics in elite Rrunners. Wearable Sensors Compet Sport 2018;17:480–8.

[38] Willy RW. Innovations and pitfalls in the use of wearable devices in the prevention and rehabilitation of running related injuries. Phys Ther Sport 2018;29:26–33. https://doi.org/10.1016/j.ptsp.2017.10.003.

[39] Norris M, Anderson R, Kenny IC. Method analysis of accelerometers and gyroscopes in running gait: A systematic review. Proc. Inst. Mech. Eng. Part P J. Sport. Eng. Technol., vol. 228, 2014, p. 3–15. https://doi.org/10.1177/1754337113502472.

[40] Winstein CJ. Knowledge of results and motor learning—Implications for physical therapy. Phys Ther 1991;71:140–9. https://doi.org/10.1093/ptj/71.2.140.

[41] Oppici L, Dix A, Narciss S. When is knowledge of performance (KP) superior to knowledge of results (KR) in promoting motor skill learning? A systematic review. Int Rev Sport Exerc Psychol 2021. https://doi.org/10.1080/1750984X.2021.1986849.

[42] Zhang X, Shan G, Wang Y, Wan B, Li H. Wearables, biomechanical feedback, and human motor-skills' learning & optimization. Appl Sci 2019;9:226. https://doi.org/10.3390/app9020226.

[43] Ranakoti S, Arora S, Chaudhary S, Beetan S, Sandhu AS, Khandnor P, et al. Human fall detection system over IMU sensors using triaxial accelerometer. In: Verma NK, Ghosh

AK, editors. Adv. Intell. Syst. Comput. 799 Comput. Intell. Theor. , Appl. Futur. Dir., vol. II, Springer Nature Singapore; 2018, p. 495–507.

[44] Li P, Meziane R, Otis MJD, Ezzaidi H, Cardou P. A smart safety helmet using IMU and EEG sensors for worker fatigue detection. ROSE 2014 - 2014 IEEE Int. Symp. Robot. SEnsors Environ. Proc., 2014. https://doi.org/10.1109/ROSE.2014.6952983.

[45] Petropoulos A, Sikeridis D, Antonakopoulos T. Wearable Smart Health Advisors: An IMU-Enabled Posture Monitor. IEEE Consum Electron Mag 2020;9:20–7. https://doi.org/10.1109/MCE.2019.2956205.

[46] Choi A, Kim TH, Yuhai O, Jeong S, Kim K, Kim H, et al. Deep learning-based near-fall detection algorithm for fall risk monitoring system using a single inertial measurement unit. IEEE Trans Neural Syst Rehabil Eng 2022;30:2385–94. https://doi.org/10.1109/TNSRE.2022.3199068.

[47] Sigrist R, Rauter G, Riener R, Wolf P. Augmented visual, auditory, haptic, and multimodal feedback in motor learning: A review. Psychon Bull Rev 2013;20:21–53. https://doi.org/10.3758/s13423-012-0333-8.

[48] Wulf G, Shea C, Lewthwaite R. Motor skill learning and performance: A review of influential factors. Med Educ 2010;44:75–84. https://doi.org/10.1111/j.1365-2923.2009.03421.x.

[49] Shull PB, Damian DD. Haptic wearables as sensory replacement, sensory augmentation and trainer - A review. J Neuroeng Rehabil 2015;12:59. https://doi.org/10.1186/s12984-015-0055-z.

[50] Lee JD, Wickens CD, Liu Y, Boyle LN. Designing for people: An introduction to human factors engineering. 3rd ed. CreateSpace, Charleston, SC, USA,; 2017.

[51] Ma CZH, Wong DWC, Lam WK, Wan AHP, Lee WCC. Balance improvement effects of biofeedback systems with state-of-the-art wearable sensors: A systematic review. Sensors 2016;16:434. https://doi.org/10.3390/s16040434.

[52] Patel M, Pavic A, Goodwin VA. Wearable inertial sensors to measure gait and posture characteristic differences in older adult fallers and non-fallers: A scoping review. Gait Posture 2020;76:110–21. https://doi.org/10.1016/j.gaitpost.2019.10.039.

[53] Montesinos L, Castaldo R, Pecchia L. Wearable inertial sensors for fall risk assessment and prediction in older adults: A systematic review and meta-analysis. IEEE Trans Neural Syst Rehabil Eng 2018;26:573–82. https://doi.org/10.1109/TNSRE.2017.2771383.

[54] Horsley BJ, Tofari PJ, Halson SL, Kemp JG, Dickson J, Maniar N, et al. Does site matter? Impact of inertial measurement unit placement on the validity and reliability of stride variables during running: A systematic review and meta-analysis. Sport Med 2021;51:1449–89. https://doi.org/10.1007/s40279-021-01443-8.

[55] Ahmad N, Ghazilla RAR, Khairi NM, Kasi V. Reviews on various inertial measurement unit (IMU) sensor applications. Int J Signal Process Syst 2013;1:256–62. https://doi.org/10.12720/ijsps.1.2.256-262.

[56] McGinnis RS, Perkins NC. A highly miniaturized, wireless inertial measurement unit for characterizing the dynamics of pitched baseballs and softballs. Sensors 2012;12:11933–45. https://doi.org/10.3390/s120911933.

[57] Straeten M, Rajai P, Ahamed MJ. Method and implementation of micro inertial measurement unit (IMU) in sensing basketball dynamics. Sensors Actuators, A Phys 2019;293:7–13. https://doi.org/10.1016/j.sna.2019.03.042.

[58] Lapinski M, Feldmeier M, Paradiso JA. Wearable wireless sensing for sports and

ubiquitous interactivity. Proc IEEE Sensors 2011:1425–8.
https://doi.org/10.1109/ICSENS.2011.6126902.

[59]   Canavan PK, Suderman B, Sklar A, Yang N. A novel approach for baseball pitch analysis using a full-body motion analysis system: A descriptive case study. Baseb Res J 2021;50:109–15.

[60]   Wang Z, Ramamoorthy V, Gal U, Guez A. Possible life saver: A review on human fall detection technology. Robotics 2020;9:55. https://doi.org/10.3390/ROBOTICS9030055.

[61]   Hauth J, Jabri S, Kamran F, Feleke EW, Nigusie K, Ojeda L V., et al. Automated loss-of-balance event identification in older adults at risk of falls during real-world walking using wearable inertial measurement units. Sensors 2021;21:4661. https://doi.org/10.3390/s21144661.

[62]   Ahn S, Kim J, Koo B, Kim Y. Evaluation of inertial sensor-based pre-impact fall detection algorithms using public dataset. Sensors 2019;19:774. https://doi.org/10.3390/s19040774.

[63]   Vitali R V., Perkins NC. Determining anatomical frames via inertial motion capture: A survey of methods. J Biomech 2020;106:109832. https://doi.org/10.1016/j.jbiomech.2020.109832.

[64]   Potter M V, Cain SM, Ojeda L V, Gurchiek RD, Mcginnis RS, Perkins NC. Evaluation of error-state kalman filter method for estimating human lower-limb kinematics during various walking Ggaits. Sensors 2022;22:8398. https://doi.org/10.3390/s22218398.

[65]   Wahlstrom J, Skog I. Fifteen years of progress at zero velocity: A review. IEEE Sens J 2021;21:1139–51. https://doi.org/10.1109/JSEN.2020.3018880.

[66]   Gałecki A, Burzykowski T. Mixed-effects models: Theory. Linear Mix. Model. using R, New York, NY: Springer; 2013, p. 245–73. https://doi.org/10.4127/ch.2012.0065.

[67]   Winter DA. Human balance and posture control during standing and walking. Gait Posture 1995;3:193–214. https://doi.org/10.1016/0966-6362(96)82849-9.

[68]   Konrad HR, Girardi M, Helfert R. Balance and aging. Laryngoscope 1999;109:1454–60. https://doi.org/10.1097/00005537-199909000-00019.

[69]   Laughton CA, Slavin M, Katdare K, Nolan L, Bean JF, Kerrigan DC, et al. Aging, muscle activity, and balance control: Physiologic changes associated with balance impairment. Gait Posture 2003;18:101–8. https://doi.org/10.1016/S0966-6362(02)00200-X.

[70]   Anson E, Studenski S, Sparto PJ, Agrawal Y. Community-dwelling adults with a history of falling report lower perceived postural stability during a foam eyes closed test than non-fallers. Exp Brain Res 2019;237:769–76. https://doi.org/10.1007/s00221-018-5458-1.

[71]   L. Sturnieks D, St George R, R. Lord S. Balance disorders in the elderly. Neurophysiol Clin 2008;38:467–78. https://doi.org/10.1016/j.neucli.2008.09.001.

[72]   Agrawal Y, Carey JP, Della Santina CC, Schubert MC, Minor LB. Disorders of balance and vestibular function in US adults. Arch Intern Med 2009;169:938. https://doi.org/10.1001/archinternmed.2009.66.

[73]   Dunlap PM, Holmberg JM, Whitney SL. Vestibular rehabilitation: Advances in peripheral and central vestibular disorders. Curr Opin Neurol 2019;32:137–44. https://doi.org/10.1097/WCO.0000000000000632.

[74]   Soyuer F, Mirza M, Erkorkmaz Ü. Balance performance in three forms of multiple sclerosis. Neurol Res 2006;28:555–62. https://doi.org/10.1179/016164105X49373.

[75]   Gunn H, Markevics S, Haas B, Marsden J, Freeman J. Systematic review: The effectiveness of interventions to reduce falls and improve balance in adults with multiple sclerosis. Arch Phys Med Rehabil 2015;96:1898–912.

https://doi.org/10.1016/j.apmr.2015.05.018.

[76] Cameron MH, Nilsagard Y. Balance, gait, and falls in multiple sclerosis. Handb. Clin. Neurol. 159, 2018, p. 237–50.

[77] Lendraitienė E, Tamošauskaitė A, Petruševičienė D, Savickas R. Balance evaluation techniques and physical therapy in post-stroke patients: A literature review. Neurol Neurochir Pol 2017;51:92–100. https://doi.org/10.1016/j.pjnns.2016.11.003.

[78] Bland DC, Zampieri C, Damiano DL. Effectiveness of physical therapy for improving gait and balance in individuals with traumatic brain injury: A systematic review. Brain Inj 2011;25:664–79. https://doi.org/10.3109/02699052.2011.576306.

[79] Harrell RG, Manetta CJ, Gorgacz MP. Dizziness and balance disorders in a traumatic brain injury population: Current clinical approaches. Curr Phys Med Rehabil Reports 2021;9:41–6. https://doi.org/10.1007/s40141-021-00308-5.

[80] Park J-H, Kang Y-J, Horak FB. What is wrong with balance in Parkinson's Disease? J Mov Disord 2015;8:109–14. https://doi.org/10.14802/jmd.15018.

[81] Rinalduzzi S, Trompetto C, Marinelli L, Alibardi A, Missori P, Fattapposta F, et al. Balance dysfunction in Parkinson's Disease 2015;2015.

[82] Lesinski M, Hortobágyi T, Muehlbauer T, Gollhofer A, Granacher U. Effects of balance training on balance performance in healthy older adults: A systematic review and meta-analysis. Sport Med 2015;45:1721–38. https://doi.org/10.1007/s40279-015-0375-y.

[83] Kümmel J, Kramer A, Giboin LS, Gruber M. Specificity of balance training in healthy individuals: A systematic review and meta-analysis. Sport Med 2016;46:1261–71. https://doi.org/10.1007/s40279-016-0515-z.

[84] Zimbelman JL, Juraschek SP, Zhang X, Lin VWH. Physical Therapy Workforce in the United States: Forecasting Nationwide Shortages. PM R 2010;2:1021–9. https://doi.org/10.1016/j.pmrj.2010.06.015.

[85] Landry MD, Hack LM, Coulson E, Freburger J, Johnson MP, Katz R, et al. Workforce projections 2010–2020: Annual supply and demand forecasting models for physical therapists across the united states. Phys Ther 2016;96:71–80. https://doi.org/10.2522/ptj.20150010.

[86] Lacroix A, Hortobágyi T, Beurskens R, Granacher U. Effects of supervised vs. unsupervised training programs on balance and muscle strength in older adults: A systematic review and meta-analysis. Sport Med 2017;47:2341–61. https://doi.org/10.1007/s40279-017-0747-6.

[87] Sherrington C, Fairhall N, Wallbank G, Tiedemann A, Michaleff ZA, Howard K, et al. Exercise for preventing falls in older people living in the community: An abridged Cochrane systematic review. Br J Sports Med 2020;54:885–91. https://doi.org/10.1136/bjsports-2019-101512.

[88] Kinnaird C, Lee J, Carender WJ, Kabeto M, Martin B, Sienko KH. The effects of attractive vs. repulsive instructional cuing on balance performance. J Neuroeng Rehabil 2016;13:1–5. https://doi.org/10.1186/s12984-016-0131-z.

[89] Halická Z, Lobotková J, Bučková K, Bzdúšková D, Hlavačka F. Age-related effect of visual biofeedback on human balance control. Act Nerv Super Rediviva 2011;53:67–71.

[90] Dozza M, Chiari L, Peterka RJ, Wall C, Horak FB. What is the most effective type of audio-biofeedback for postural motor learning? Gait Posture 2011;34:313–9. https://doi.org/10.1016/j.gaitpost.2011.05.016.

[91] Taube W, Leukel C, Gollhofer A. Influence of enhanced visual feedback on postural

control and spinal reflex modulation during stance. Exp Brain Res 2008;188:353–61. https://doi.org/10.1007/s00221-008-1370-4.

[92] Davis JR, Carpenter MG, Tschanz R, Meyes S, Debrunner D, Burger J, et al. Trunk sway reductions in young and older adults using multi-modal biofeedback. Gait Posture 2010;31:465–72. https://doi.org/10.1016/j.gaitpost.2010.02.002.

[93] Lee BC, Sienko KH. Design and assessment of vibrotactile biofeedback and instructional systems for balance rehabilitation applications. University of Michigan, 2012.

[94] Bechly KE, Carender WJ, Myles JD, Sienko KH. Determining the preferred modality for real-time biofeedback during balance training. Gait Posture 2013;37:391–6. https://doi.org/10.1016/j.gaitpost.2012.08.007.

[95] Ma CZH, Lee WCC. A wearable vibrotactile biofeedback system improves balance control of healthy young adults following perturbations from quiet stance. Hum Mov Sci 2017;55:54–60. https://doi.org/10.1016/j.humov.2017.07.006.

[96] Grewal GS, Schwenk M, Lee-Eng J, Parvaneh S, Bharara M, Menzies RA, et al. Sensor-based interactive balance training with visual joint movement feedback for improving postural stability in diabetics with peripheral neuropathy: A randomized controlled trial. Gerontology 2015;61:567–74. https://doi.org/10.1159/000371846.

[97] Alhasan H, Hood V, Mainwaring F. The effect of visual biofeedback on balance in elderly population: a systematic review. Clin Interv Aging 2017;12:487–97. https://doi.org/10.2147/CIA.S127023.

[98] Mak TCT, Wong TWL, Ng SSM. Visual-related training to improve balance and walking ability in older adults: A systematic review. Exp Gerontol 2021;156:111612. https://doi.org/10.1016/j.exger.2021.111612.

[99] Zijlstra A, Mancini M, Chiari L, Zijlstra W. Biofeedback for training balance and mobility tasks in older populations: A systematic review. J Neuroeng Rehabil 2010;7:58. https://doi.org/10.1186/1743-0003-7-58.

[100] Bao T, Carender WJ, Kinnaird C, Barone VJ, Peethambaran G, Whitney SL, et al. Effects of long-term balance training with vibrotactile sensory augmentation among community-dwelling healthy older adults: A randomized preliminary study. J Neuroeng Rehabil 2018;15:5. https://doi.org/10.1186/s12984-017-0339-6.

[101] Basta D, Rossi-Izquierdo M, Soto-Varela A, Greters ME, Bittar RS, Steinhagen-Thiessen E, et al. Efficacy of a vibrotactile neurofeedback training in stance and gait conditions for the treatment of balance deficits: A double-blind, placebo-controlled multicenter study. Otol Neurotol 2011;32:1492–9. https://doi.org/10.1097/MAO.0b013e31823827ec.

[102] Rossi-Izquierdo M, Ernst A, Soto-Varela A, Santos-Pérez S, Faraldo-García A, Sesar-Ignacio ángel, et al. Vibrotactile neurofeedback balance training in patients with Parkinson's disease: Reducing the number of falls. Gait Posture 2013;37:195–200. https://doi.org/10.1016/j.gaitpost.2012.07.002.

[103] Brugnera C, Bittar RSM, Greters ME, Basta D. Effects of vibrotactile vestibular substitution on vestibular rehabilitation - preliminary study. Braz J Otorhinolaryngol 2015;81:616–21. https://doi.org/10.1016/j.bjorl.2015.08.013.

[104] Barry G, van Schaik P, MacSween A, Dixon J, Martin D. Exergaming (XBOX Kinect[TM]) versus traditional gym-based exercise for postural control, flow and technology acceptance in healthy adults: A randomised controlled trial. BMC Sports Sci Med Rehabil 2016;8:25. https://doi.org/10.1186/s13102-016-0050-0.

[105] Yang CM, Chen Hsieh JS, Chen YC, Yang SY, Lin HCK. Effects of Kinect exergames on

balance training among community older adults: A randomized controlled trial. Medicine (Baltimore) 2020;99:e21228. https://doi.org/10.1097/MD.0000000000021228.

[106] Senden R, Savelberg HHCM, Grimm B, Heyligers IC, Meijer K. Accelerometry-based gait analysis, an additional objective approach to screen subjects at risk for falling. Gait Posture 2012;36:296–300. https://doi.org/10.1016/j.gaitpost.2012.03.015.

[107] Rivolta MW, Aktaruzzaman M, Rizzo G, Lafortuna CL, Ferrarin M, Bovi G, et al. Evaluation of the Tinetti score and fall risk assessment via accelerometry-based movement analysis. Artif Intell Med 2019;95:38–47. https://doi.org/10.1016/j.artmed.2018.08.005.

[108] O'sullivan M, Blake C, Cunningham C, Boyle G, Finucane C. Correlation of accelerometry with clinical balance tests in older fallers and non-fallers. Age Ageing 2009;38:308–13. https://doi.org/10.1093/ageing/afp009.

[109] Tang W, Fulk G, Zeigler S, Zhang T, Sazonov E. Estimating berg balance scale and mini balance evaluation system test scores by using wearable shoe sensors. 2019 IEEE EMBS Int. Conf. Biomed. Heal. Informatics, Chicago: 2019.

[110] Weiss A, Herman T, Plotnik M, Brozgol M, Maidan I, Giladi N, et al. Can an accelerometer enhance the utility of the Timed Up & Go Test when evaluating patients with Parkinson's disease? Med Eng Phys 2010;32:119–25. https://doi.org/10.1016/j.medengphy.2009.10.015.

[111] Alsubaie SF, Whitney SL, Furman JM, Marchetti GF, Sienko KH, Klatt BN, et al. Reliability and validity of ratings of perceived difficulty during performance of static standing balance exercises. J Phys Ther 2019;99:1381–93.

[112] Alsubaie SF, Whitney SL, Furman JM, Marchetti GF, Sienko KH, Sparto PJ. Rating of perceived difficulty scale for measuring intensity of standing balance exercises in individuals with vestibular disorders. J Vestib Res 2022;32:529–40.

[113] Winter DA. ABC (Anatomy, Balance, and Control) of Balance during Standing and Walking 1995.

[114] Mancini M, Salarian A, Carlson-Kuhta P, Zampieri C, King L, Chiari L, et al. ISway: A sensitive, valid and reliable measure of postural control. J Neuroeng Rehabil 2012;9:59. https://doi.org/10.1186/1743-0003-9-59.

[115] Roeing KL, Hsieh KL, Sosnoff JJ. A systematic review of balance and fall risk assessments with mobile phone technology. Arch Gerontol Geriatr 2017;73:222–6. https://doi.org/10.1016/j.archger.2017.08.002.

[116] Bao T, Klatt BN, Carender WJ, Kinnaird C, Alsubaie S, Whitney SL, et al. Effects of long-term vestibular rehabilitation therapy with vibrotactile sensory augmentation for people with unilateral vestibular disorders-A randomized preliminary study. J Vestib Res Equilib Orientat 2020;29:323–34. https://doi.org/10.3233/VES-190683.

[117] Ozinga SJ, Alberts JL. Quantification of postural stability in older adults using mobile technology. Exp Brain Res 2014;232:3861–72. https://doi.org/10.1007/s00221-014-4069-8.

[118] Mak TCT, Wong TWL, Ng SSM. Visual-related training to improve balance and walking ability in older adults: A systematic review. Exp Gerontol 2021;156:111612. https://doi.org/10.1016/j.exger.2021.111612.

[119] Halvorsen S, Vøllestad NK, Fongen C, Provan SA, Semb AG, Hagen KB, et al. Physical fitness in patients with ankylosing spondylitis: Comparison with population controls. Phys Ther 2012;92:298–309. https://doi.org/10.2522/ptj.20110137.

[120] McGinnis PQ, Hack LM, Nixon-Cave K, Michlovitz SL. Factors that influence the clincal decision making of physical therapists in choosing a balance assessment approach. Phys Ther 2009;89:233–47. https://doi.org/10.2522/ptj.20080131.

[121] Wainwright SF, Shepard KF, Harman LB. Factors that influence the clinical decision making of novice and experienced physical therapists. Phys Ther 2011;91:87–101. https://doi.org/10.2522/ptj.20100161.

[122] Bao T, Klatt BN, Whitney SL, Sienko KH, Wiens J. Automatically evaluating balance: A machine learning approach. IEEE Trans Neural Syst Rehabil Eng 2019;27:179–86. https://doi.org/10.1109/TNSRE.2019.2891000.

[123] Kamran F, Harrold K, Zwier J, Carender W, Bao T, Sienko K, et al. Automatically evaluating balance using machine learning and data from a single inertial measurement unit. J Neuroeng Rehabil 2021;18:114. https://doi.org/10.1186/s12984-021-00894-4.

[124] Browne J, O'Hare N, O'Hare G, Finn A, Colin J. Clinical assessment of the quantitative posturography system. Physiotherapy 2002;88:217–23. https://doi.org/10.1016/S0031-9406(05)60413-0.

[125] Browne JE, O'Hare NJ. Review of the different methods for assessing standing balance. Physiotherapy 2001;87:489–95. https://doi.org/10.1016/S0031-9406(05)60696-7.

[126] Blazey P, Michie T V., Napier C. A narrative review of running wearable measurement system accuracy and reliability: can we make running shoe prescription objective? Footwear Sci 2021;13:117–31. https://doi.org/10.1080/19424280.2021.1878287.

[127] Sutherland DH. The evolution of clinical gait analysis: Part II kinematics. Gait Posture 2002;16:159–79. https://doi.org/10.1016/S0966-6362(02)00004-8.

[128] Wang W, Adamczyk PG. Analyzing gait in the real world using wearable movement paths. Sensors 2019;19:1925. https://doi.org/10.3390/s19081925.

[129] Sun D, Song Y, Cen X, Zheng Z, Istvan B, Gu Y. The implications of sports biomechanics studies on the research and development of running shoes: A systematic review. Bioengineering 2022;9:497. https://doi.org/10.2139/ssrn.4031261.

[130] Darch L, Chalmers S, Wiltshire J, Causby R, Arnold J. Running-induced fatigue and impact loading in runners: A systematic review and meta-analysis. J Sports Sci 2022;40:1512–31. https://doi.org/10.1080/02640414.2022.2089803.

[131] Ceyssens L, Vanelderen R, Barton C, Malliaras P, Dingenen B. Biomechanical risk factors associated with running-related injuries: A systematic review. Sport Med 2019;49:1095–115. https://doi.org/10.1007/s40279-019-01110-z.

[132] Van Hooren B, Fuller JT, Buckley JD, Miller JR, Sewell K. Is motorized treadmill running biomechanically comparable to overground running? A systematic review and meta-analysis of cross-over studies. Sport Med 2020;50:785–813. https://doi.org/10.1007/s40279-019-01237-z.

[133] Miller JR, Van Hooren B, Bishop C, Buckley JD, Willy RW, Fuller JT. A systematic review and meta-analysis of crossover studies comparing physiological, perceptual and performance measures between treadmill and overground running. Sport Med 2019;49:763–82. https://doi.org/10.1007/s40279-019-01087-9.

[134] Clansey AC, Hanlon M, Wallace ES, Lake MJ. Effects of fatigue on running mechanics associated with tibial stress fracture risk. Med Sci Sports Exerc 2012;44:1917–23. https://doi.org/10.1249/MSS.0b013e318259480d.

[135] Derrick TR, Dereu D, Mclean SP. Impacts and kinematic adjustments during an exhaustive run. Med Sci Sports Exerc 2002;34:998–1002.

https://doi.org/10.1097/00005768-200206000-00015.

[136] Ruder M, Jamison ST, Tenforde A, Mulloy F, Davis I. Relationship of footstrike pattern and landing impacts during a marathon. Med Sci Sport Exerc 2019;51:2073–9. https://doi.org/10.1249/MSS.0000000000002032.

[137] Schütte KH, Aeles J, De Beéck TO, van der Zwaard BC, Venter R, Vanwanseele B. Surface effects on dynamic stability and loading during outdoor running using wireless trunk accelerometry. Gait Posture 2016;48:220–5. https://doi.org/10.1016/j.gaitpost.2016.05.017.

[138] Brito HS, Carraça E V., Palmeira AL, Ferreira JP, Vleck V, Araújo D. Benefits to performance and well-being of nature-based exercise: A critical systematic review and meta-analysis. Environ Sci Technol 2022;56:62–77. https://doi.org/10.1021/acs.est.1c05151.

[139] Kerr JH, Fujiyama H, Sugano A, Okamura T, Chang M, Onouha F. Psychological responses to exercising in laboratory and natural environments. Psychol Sport Exerc 2006;7:345–59. https://doi.org/10.1016/j.psychsport.2005.09.002.

[140] Lawton E, Brymer E, Clough P, Denovan A. The relationship between the physical activity environment, nature relatedness, anxiety, and the psychological well-being benefits of regular exercisers. Front Psychol 2017;8. https://doi.org/10.3389/fpsyg.2017.01058.

[141] Harte JL, Eifert GH. The effects of running, environment, and attentional focus on athletes' catecholamine and cortisol levels and mood. Psychophysiology 1995;32:49–54. https://doi.org/10.1111/j.1469-8986.1995.tb03405.x.

[142] Reich AH, Queathem EJ. Setting, age, and intensity influence responses to exercise in young endurance runners. Percept Mot Skills 2020;127:533–54. https://doi.org/10.1177/0031512520903907.

[143] LaCaille RA, Masters KS, Heath EM. Effects of cognitive strategy and exercise setting on running performance, perceived exertion, affect, and satisfaction. Psychol Sport Exerc 2004;5:461–76. https://doi.org/10.1016/S1469-0292(03)00039-6.

[144] Kong PW, Koh TMC, Tan WCR, Wang YS. Unmatched perception of speed when running overground and on a treadmill. Gait Posture 2012;36:46–8. https://doi.org/10.1016/j.gaitpost.2012.01.001.

[145] Halperin I, Pyne DB, Martin DT. Threats to internal validity in exercise science: A review of overlooked confounding variables. Int J Sports Physiol Perform 2015;10:823–9. https://doi.org/10.1123/IJSPP.2014-0566.

[146] Benson LC, Räisänen AM, Clermont CA, Ferber R. Is this the real life, or is this just laboratory? A scoping review of IMU-based running gait analysis. Sensors 2022;22:1722. https://doi.org/10.3390/s22051722.

[147] McDevitt S, Hernandez H, Hicks J, Lowell R, Bentahaikt H, Burch R, et al. Wearables for biomechanical performance optimization and risk assessment in industrial and sports applications. Bioengineering 2022;9:33. https://doi.org/10.3390/bioengineering9010033.

[148] Adelaar RS. The practical biomechanics of running. Am J Sports Med 1986;14:497–500. https://doi.org/10.1177/036354658601400613.

[149] Potter M V., Cain SM, Ojeda L V., Gurchiek RD, McGinnis RS, Perkins NC. Error-state Kalman filter for lower-limb kinematic estimation: Evaluation on a 3-body model. PLoS One 2021;16:e0249577. https://doi.org/10.1371/journal.pone.0249577.

[150] Teufl W, Miezal M, Taetz B, Fröhlich M, Bleser G. Validity, test-retest reliability and

long-term stability of magnetometer free inertial sensor based 3D joint kinematics. Sensors 2018;18:1980. https://doi.org/10.3390/s18071980.

[151] Rapp E, Shin S, Thomsen W, Ferber R, Halilaj E. Estimation of kinematics from inertial measurement units using a combined deep learning and optimization framework. J Biomech 2021;116:110229. https://doi.org/10.1016/j.jbiomech.2021.110229.

[152] Midgley AW, McNaughton LR, Jones AM. Training to enhance the physiological determinants of long-distance running performance: Can valid recommendations be given to runners and coaches based on current scientific knowledge? Sport Med 2007;37:857–80. https://doi.org/10.2165/00007256-200737100-00003.

[153] Boullosa D, Esteve-Lanao J, Casado A, Peyré-Tartaruga LA, Da Rosa RG, Del Coso J. Factors affecting training and physical performance in recreational endurance runners. Sports 2020;8:35. https://doi.org/10.3390/sports8030035.

[154] McCormick A, Meijen C, Marcora S. Psychological determinants of whole-body endurance performance. Sport Med 2015;45:997–1015. https://doi.org/10.1007/s40279-015-0319-6.

[155] Lussiana T, Gindre C. Feel your stride and find your preferred running speed. Biol Open 2016;5:45–8. https://doi.org/10.1242/bio.014886.

[156] van der Bie J, Kröse B. Happy running? Using an accelerometer to predict the affective state of a runner. Lect. Notes Comput. Sci. (including Subser. Lect. Notes Artif. Intell. Lect. Notes Bioinformatics), vol. 9425, Springer Verlag; 2015, p. 357–60. https://doi.org/10.1007/978-3-319-26005-1_26.

[157] World Health Organization. Falls 2018. https://www.who.int/en/news-room/fact-sheets/detail/falls.

[158] Hull SL, Kneebone II, Farquharson L. Anxiety, depression, and fall-related psychological concerns in community-dwelling older people. Am J Geriatr Psychiatry 2013;21:1287–91. https://doi.org/10.1016/j.jagp.2013.01.038.

[159] Hughes CC, Kneebone II, Jones F, Brady B, Pachana NA, Oude Voshaar RC. A theoretical and empirical review of psychological factors associated with falls-related psychological concerns in community-dwelling older people. Int Psychogeriatrics 2015;27:1071–87. https://doi.org/10.1017/S1041610214002701.

[160] Denkinger MD, Lukas A, Nikolaus T, Hauer K. Factors associated with fear of falling and associated activity restriction in community-dwelling older adults: A systematic review. Am J Geriatr Psychiatry 2015;23:72–86. https://doi.org/10.1016/j.jagp.2014.03.002.

[161] Cumming RG, Salkeld G, Thomas M, Szonyi G. Prospective study of the impact of fear of falling on activities of daily living, SF-36 scores, and nursing home admission. J Gerontol Med Sci 2000;55A:M299-305.

[162] Zijlstra GAR, van Haastregt JCM, van Eijk JTM, van Rossum E, Stalenhoef PA, Kempen GIJM. Prevalence and correlates of fear of falling, and associated avoidance of activity in the general population of community-living older people. Age Ageing 2007;36:304–9. https://doi.org/10.1093/ageing/afm021.

[163] Arfken CL, Lach HW, Birge SJ, Miller JP. The prevalence and correlates of fear of falling in elderly persons living in the community. Am J Public Health 1994;84:565–70. https://doi.org/10.2105/AJPH.84.4.565.

[164] Howland J, Peterson EW, Levin WC, Fried L, Pordon D, Bak S. Fear of falling among the community-dwelling elderly. J Aging Health 1993;5:229–43. https://doi.org/10.1177/089826439300500205.

[165]   Dozza M, Chiari L, Chan B, Rocchi L, Horak FB, Cappello A. Influence of a portable audio-biofeedback device on structural properties of postural sway. 2005;2:13. https://doi.org/10.1186/1743-0003-2-13.

[166]   Chiari L, Dozza M, Cappello A, Horak FB, Macellari V, Giansanti D. Audio-biofeedback for balance improvement: An accelerometry-based system. IEEE Trans Biomed Eng 2005;52:2108–11. https://doi.org/10.1109/TBME.2005.857673.

[167]   Alhagbani A, Williams A. Home-based exergames for older adults balance and falls risk: A systematic review. Phys Occup Ther Geriatr 2021;39:241–57. https://doi.org/10.1080/02703181.2020.1867286.

[168]   Sienko KH, Balkwill MD, Oddsson LIE, Wall C. Effects of multi-directional vibrotactile feedback on vestibular-deficient postural performance during continuous multi-directional support surface perturbations. J Vestib Res Equilib Orientat 2008;18:273–85. https://doi.org/10.3233/ves-2008-185-604.

[169]   Yousefi Babadi S, Daneshmandi H. Effects of virtual reality versus conventional balance training on balance of the elderly. Exp Gerontol 2021;153:111498. https://doi.org/10.1016/j.exger.2021.111498.

[170]   Ranganathan R, Newell K. Influence of augmented feedback on coordination strategies. J Mot Behav 2009;41:317–30. https://doi.org/10.3200/JMBR.41.4.317-330.

[171]   Sigrist R, Rauter G, Riener R, Wolf P. Terminal feedback outperforms concurrent visual, auditory, and haptic feedback in learning a complex rowing-type task. J Mot Behav 2013;45:455–72. https://doi.org/10.1080/00222895.2013.826169.

[172]   Yamamoto R, Akizuki K, Kanai Y, Nakano W, Kobayashi Y, Ohashi Y. Differences in skill level influence the effects of visual feedback on motor learning. J Phys Ther Sci 2019;31:939–45. https://doi.org/10.1589/jpts.31.939.

[173]   Winstein CJ, Pohl PS, Lewthwaite R. Effects of physical guidance and knowledge of results on motor learning: Support for the guidance hypothesis. Res Q Exerc Sport 1994;65:316–23. https://doi.org/10.1080/02701367.1994.10607635.

[174]   Goodwin JE, Goggin NL. An older adult study of concurrent visual feedback in learning continuous balance. Percept Mot Skills 2018;125:1160–72. https://doi.org/10.1177/0031512518795758.

[175]   Moe-Nilssen R, Helbostad JL. Trunk accelerometry as a measure of balance control during quiet standing. Gait Posture 2002;16:60–8. https://doi.org/10.1016/S0966-6362(01)00200-4.

[176]   McManus K, Greene BR, Ader LGM, Caulfield B. Development of data-driven metrics for balance impairment and fall risk assessment in older adults. IEEE Trans Biomed Eng 2022;69:2324–32. https://doi.org/10.1109/TBME.2022.3142617.

[177]   Valenciano PJ, Conceição NR, Marcori AJ, Teixeira LA. Use of accelerometry to investigate standing and dynamic body balance in people with cerebral palsy: A systematic review. Gait Posture 2022;96:357–64. https://doi.org/10.1016/j.gaitpost.2022.06.017.

[178]   Sullivan KJ, Kantak SS, Burtner PA. Motor learning in children: Feedback effects on skill acquisition. Phys Ther 2008;88:720–32. https://doi.org/10.1111/dmcn.12364.

[179]   Wulf G, Schmidt RA. The learning of generalized motor programs: Reducing the relative frequency of knowledge of results enhances memory. J Exp Psychol Learn Mem Cogn 1989;15:748–57. https://doi.org/10.1037//0278-7393.15.4.748.

[180]   Thomas DM. The effects of relative frequency of knowledge of results on brain injured

and neurologically normal individuals learning a linear positioning task. Grand Valley State University, 1995.

[181] Gandía J, García-Massó X, Marco-Ahulló A, Estevan I. Adolescents' postural control learning according to the frequency of knowledge of process. J Mot Learn Dev 2019;7:204–14. https://doi.org/10.1123/jmld.2017-0042.

[182] Marco-Ahulló A, Sánchez-Tormo A, García-Pérez JA, Villarrasa-Sapiña I, González LM, García-Massó X. Effect of concurrent visual feedback frequency on postural control learning in adolescents. J Mot Behav 2019;51:193–8. https://doi.org/10.1080/00222895.2018.1454397.

[183] Huffman JL, Norton LE, Adkin AL, Allum JHJ. Directional effects of biofeedback on trunk sway during stance tasks in healthy young adults. Gait Posture 2010;32:62–6. https://doi.org/10.1016/j.gaitpost.2010.03.009.

[184] Horak FB, Shupert CL, Mirka A. Components of postural dyscontrol in the elderly: A review. Neurobiol Aging 1989;10:727–38. https://doi.org/10.1016/0197-4580(89)90010-9.

[185] Carpenter MG, Frank JS, Silcher CP. Surface height effects on postural control: A hypothesis for a stiffness strategy for stance. J Vestib Res Equilib Orientat 1999;9:277–86. https://doi.org/10.3233/ves-1999-9405.

[186] Adkin AL, Frank JS, Carpenter MG, Peysar GW. Postural control is scaled to level of postural threat. Gait Posture 2000;12:87–93. https://doi.org/10.1016/S0966-6362(00)00057-6.

[187] Melzer I, Benjuya N, Kaplanski J. Age-related changes of postural control: Effect of cognitive tasks. Gerontology 2001;47:189–94. https://doi.org/10.1159/000052797.

[188] Dault MC, de Haart M, Geurts ACH, Arts IMP, Nienhuis B. Effects of visual center of pressure feedback on postural control in young and elderly healthy adults and in stroke patients. Hum Mov Sci 2003;22:221–36. https://doi.org/10.1016/S0167-9457(03)00034-4.

[189] Wiesmeier IK, Dalin D, Wehrle A, Granacher U, Muehlbauer T, Dietterle J, et al. Balance training enhances vestibular function and reduces overactive proprioceptive feedback in elderly. Front Aging Neurosci 2017;9:273. https://doi.org/10.3389/fnagi.2017.00273.

[190] Chang J-Y, Chang G-L, Chien C-JC, Chung K-C, Hsu A-T. Effectiveness of two forms of feedback on training of a joint mobilization skill by using a joint translation simulator. Phys Ther 2007;87:418–30. https://doi.org/10.2522/ptj.20060154.

[191] Krpič A, Savanović A, Cikajlo I. Telerehabilitation: Remote multimedia-supported assistance and mobile monitoring of balance training outcomes can facilitate the clinical staff's effort. Int J Rehabil Res 2013;36:162–71. https://doi.org/10.1097/MRR.0b013e32835dd63b.

[192] Walker C, Brouwer BJ, Culham EG. Use of visual feedback in retraining balance following acute stroke. Phys Ther 2000;80:886–95. https://doi.org/10.1093/ptj/80.9.886.

[193] Yang WC, Wang HK, Wu RM, Lo CS, Lin KH. Home-based virtual reality balance training and conventional balance training in Parkinson's disease: A randomized controlled trial. J Formos Med Assoc 2016;115:734–43. https://doi.org/10.1016/j.jfma.2015.07.012.

[194] Yen CY, Lin KH, Hu MH, Wu RM, Lu TW, Lin CH. Effects of virtual reality-augmented balance training on sensory organization and attentional demand for postural control in people with Parkinson disease: A randomized controlled trial. Phys Ther 2011;91:862–74. https://doi.org/10.2522/ptj.20100050.

[195] Vereeck L, Wuyts F, Truijen S, Van De Heyning P. Clinical assessment of balance: Normative data, and gender and age effects. Int J Audiol 2008;47:67–75. https://doi.org/10.1080/14992020701689688.

[196] Drew JAR, Xu D. Trends in fatal and nonfatal injuries among older americans, 2004-2017. Am J Prev Med 2020;59:3–11. https://doi.org/10.1016/j.amepre.2020.01.008.

[197] Hadjistavropoulos T, Delbaere K, Fitzgerald TD. Reconceptualizing the role of fear of falling and balance confidence in fall risk. J Aging Health 2011;23:3–23. https://doi.org/10.1177/0898264310378039.

[198] Landers MR, Oscar S, Sasaoka J, Vaughn K. Balance confidence and fear of falling avoidance behavior are most predictive of falling in older adults: Prospective analysis. Phys Ther 2016;96:433–42. https://doi.org/10.2522/ptj.20150184.

[199] Burzynski J, Sulway S, Rutka JA. Vestibular rehabilitation: Review of indications, treatments, advances, and limitations. Curr Otorhinolaryngol Rep 2017;5:160–6. https://doi.org/10.1007/s40136-017-0157-1.

[200] Farlie MK, Molloy E, Keating JL, Haines TP. Clinical markers of the intensity of balance challenge: Observational study of older adult responses to balance tasks. Phys Ther 2016;96:313–23. https://doi.org/10.2522/ptj.20140524.

[201] Farlie MK, Robins L, Keating JL, Molloy E, Haines TP. Intensity of challenge to the balance system is not reported in the prescription of balance exercises in randomised trials: A systematic review. J Physiother 2013;59:227–35. https://doi.org/10.1016/S1836-9553(13)70199-1.

[202] Reinthal A. Getting the dosage right in balance exercise prescription: The intensity problem. J Nov Physiother 2017;7. https://doi.org/10.4172/2165-7025.1000e147.

[203] Espy D, Reinthal A, Meisel S. Intensity of balance task intensity, as measured by the Rate of Perceived Stability, is independent of physical exertion as measured by heart rate. J Nov Physiother 2017;7. https://doi.org/10.4172/2165-7025.1000343.

[204] Pescatello LS, American College of Sports Medicine. ACSM's guidelines for exercise testing and prescription. 9th ed. Philadelphia: Wolters Kluwer/Lippincott Williams & Wilkins Health; 2014.

[205] Jesus TS, Landry MD, Dussault G, Fronteira I. Human resources for health (and rehabilitation): Six Rehab-Workforce Challenges for the century. Hum Resour Health 2017;15:1–12. https://doi.org/10.1186/s12960-017-0182-7.

[206] Horsley S, Schock G, Grona SL, Montieth K, Mowat B, Stasiuk K, et al. Use of real-time videoconferencing to deliver physical therapy services: A scoping review of published and emerging evidence. J Telemed Telecare 2020;26:581–9. https://doi.org/10.1177/1357633X19854647.

[207] Harrell RG, Schubert MC, Oxborough S, Whitney SL. Vestibular rehabilitation telehealth during the SAEA-CoV-2 (COVID-19) pandemic. Front Neurol 2022;12:781482. https://doi.org/10.3389/fneur.2021.781482.

[208] Signal N, Martin T, Leys A, Maloney R, Bright F. Implementation of telerehabilitation in response to COVID-19: Lessons learnt from neurorehabilitation clinical practice and education. New Zeal J Physiother 2020;48:117–26. https://doi.org/10.15619/NZJP/48.3.03.

[209] Buabbas AJ, Albahrouh SE, Alrowayeh HN, Alshawaf H. Telerehabilitation during the COVID-19 Pandemic: Patients and Physical Therapists' Experiences. Med Princ Pract 2022;31:156–64. https://doi.org/10.1159/000523775.

[210] Werneke MW, Deutscher D, Grigsby D, Tucker CA, Mioduski JE, Hayes D. Telerehabilitation during the COVID-19 pandemic in outpatient rehabilitation settings: A descriptive study. Phys Ther 2021;101:1–11. https://doi.org/10.1093/ptj/pzab110.

[211] Zhang X, Lin D, Pforsich H, Lin VW. Physician workforce in the United States of America: Forecasting nationwide shortages. Hum Resour Health 2020;18:1–9. https://doi.org/10.1186/s12960-020-0448-3.

[212] Jesus TS, Koh G, Landry M, Ong PH, Lopes AMF, Green PL, et al. Finding the "right-size" physical therapy workforce: International perspective across 4 countries. Phys Ther 2016;96:1597–609. https://doi.org/10.2522/ptj.20160014.

[213] Conradie T, Berner K, Louw Q. Rehabilitation workforce descriptors: a scoping review. BMC Health Serv Res 2022;22:1169. https://doi.org/10.1186/s12913-022-08531-z.

[214] Saaei F, Klappa SG. Rethinking telerehabilitation: attitudes of physical therapists and patients. J Patient Exp 2021;8:1–7. https://doi.org/10.1177/23743735211034335.

[215] Klatt BN, Carender WJ, Lin CC, Alsubaie SF, Kinnaird CR, Sienko KH, et al. A conceptual framework for the progression of balance exercises in persons with balance and vestibular disorders. Phys Med Rehabil Int 2015;2:1044.

[216] Borg GAV. Psychophysical bases of perceived exertion. Med Sci Sports Exerc 1982;14:377–81.

[217] Robertson RJ, Goss FL, Rutkowski J, Lenz B, Dixon C, Timmer J, et al. Concurrent validation of the OMNI perceived exertion scale for resistance exercise. Med Sci Sports Exerc 2003;35:333–41. https://doi.org/10.1249/01.MSS.0000048831.15016.2A.

[218] Lagally KM, Robertson RJ. Construct validity of the OMNI Resistance Exercise Scale. J Strength Cond Res 2006;20:252–6. https://doi.org/10.1519/R-17224.1.

[219] Shenoy A, Peng TH, Todd RM, Eng JJ, Silverberg ND, Tembo T, et al. Rate of perceived stability as a measure of balance exercise intensity in people post-stroke. Disabil Rehabil 2022. https://doi.org/10.1080/09638288.2021.2022777.

[220] Farlie MK, Keating JL, Molloy E, Bowles KA, Neave B, Yamin J, et al. The balance intensity scales for therapists and exercisers measure balance exercise intensity in older adults: Initial validation using Rasch analysis. Phys Ther 2019;99:1394–404. https://doi.org/10.1093/ptj/pzz092.

[221] Wong CK. Interrater reliability of the Berg Balance Scale when used by clinicians of various experience levels to assess people with lower limb amputations. Phys Ther 2014;94:371–8. https://doi.org/10.2522/ptj.20130182.

[222] Krebs DE, Edelstein JE, Fishman S. Reliability of observational kinematic gait analysis. Phys Ther 1985;7:1027–1033. https://doi.org/10.1093/ptj/65.7.1027.

[223] Choi YM, Dobson F, Martin J, Bennell KL, Hinman RS. Interrater and intrarater reliability of common clinical standing balance tests for people with hip osteoarthritis. Phys Ther 2014;94:696–704. https://doi.org/10.2522/ptj.20130266.

[224] Stratford PW, Kennedy DM. A comparison study of KOOS-PS and KOOS function and sport scores. Phys Ther 2014;94:1614–21. https://doi.org/10.2522/ptj.20140086.

[225] Hansen C, Beckbauer M, Romijnders R, Warmerdam E, Welzel J, Geritz J, et al. Reliability of IMU-derived static balance parameters in neurological diseases. Int J Environ Health Res 2021;18:3644. https://doi.org/10.3390/s22062304.

[226] Lee BC, Martin BJ, Sienko KH. Directional postural responses induced by vibrotactile stimulations applied to the torso. Exp Brain Res 2012;222:471–82. https://doi.org/10.1007/s00221-012-3233-2.

[227] Lee B-C, Kim JH, Chen S, Sienko KH. Cell phone based balance trainer. J Neuroeng Rehabil 2012;9. https://doi.org/10.1115/1.3135151.

[228] Johnson DR, Creech JC. Ordinal measures in multiple indicator models: A simulation study of categorization error. Am Sociol Rev 1983;48:398–407. https://doi.org/10.2307/2095231.

[229] Norris CM, Ghali WA, Saunders LD, Brant R, Galbraith D, Faris P, et al. Ordinal regression model and the linear regression model were superior to the logistic regression models. J Clin Epidemiol 2006;59:448–56. https://doi.org/10.1016/j.jclinepi.2005.09.007.

[230] Norman G. Likert scales, levels of measurement and the "laws" of statistics. Adv Heal Sci Educ 2010;15:625–32. https://doi.org/10.1007/s10459-010-9222-y.

[231] Rhemtulla M, Brosseau-Liard PÉ, Savalei V. When can categorical variables be treated as continuous? A comparison of robust continuous and categorical SEM estimation methods under suboptimal conditions. Psychol Methods 2012;17:354–73. https://doi.org/10.1037/a0029315.

[232] Robitzsch A. Why ordinal variables can (almost) always be treated as continuous variables: Clarifying assumptions of robust continuous and ordinal factor analysis estimation methods. Front Educ 2020;5:589965. https://doi.org/10.3389/feduc.2020.589965.

[233] Cook DA, Beckman TJ. Current concepts in validity and reliability for psychometric instruments: Theory and application. Am J Med 2006;119:166.e7-166.e16. https://doi.org/10.1016/j.amjmed.2005.10.036.

[234] Jeyaraman MM, Al-Yousif N, Robson RC, Copstein L, Balijepalli C, Hofer K, et al. Inter-rater reliability and validity of risk of bias instrument for non-randomized studies of exposures: A study protocol. Syst Rev 2020;9. https://doi.org/10.1186/s13643-020-01291-z.

[235] Mchugh ML. Interrater reliability: the kappa statistic. Biochem Medica 2012;22:276–82.

[236] Asendorpf JB, Conner M, Fruyt F De, Houwer J De, Denissen JJA, Fiedler K, et al. Recommendations for increasing replicability in psychology. In: A. E. Kazdin, editor. Methodol. issues Strateg. Clin. Res., American Psychological Association; 2012, p. 607–622. https://doi.org/https://doi.org/10.1037/14805-038.

[237] Hallgren KA. Computing inter-rater reliability for observational data: An overview and tutorial. Tutor Quant Methods Psychol 2012;8:23–34. https://doi.org/10.20982/tqmp.08.1.p023.

[238] Liljequist D, Elfving B, Roaldsen KS. Intraclass correlation – A discussion and demonstration of basic features. PLoS One 2019;14:e0219854. https://doi.org/10.1371/journal.pone.0219854.

[239] Koo TK, Li MY. A guideline of selecting and reporting intraclass correlation coefficients for reliability research. J Chiropr Med 2016;15:155–63. https://doi.org/10.1016/j.jcm.2016.02.012.

[240] O'brien MK, Hidalgo-Araya MD, Mummidisetty CK, Vallery H, Ghaffari R, Rogers JA, et al. Augmenting clinical outcome measures of gait and balance with a single inertial sensor in age-ranged healthy adults. Sensors 2019;19:4537. https://doi.org/10.3390/s19204537.

[241] Schieppati M, Tacchini E, Nardone A, Tarantola J, Corna S. Subjective perception of body sway. J Neurol Neurosurg Psychiatry 1999;66:313–22. https://doi.org/10.1136/jnnp.66.3.313.

[242] Nakagawa S, Schielzeth H. A general and simple method for obtaining R2 from generalized linear mixed-effects models. Methods Ecol Evol 2013;4:133–42. https://doi.org/10.1111/j.2041-210x.2012.00261.x.

[243] Allum JHJ, Carpenter MG, Honegger F, Adkin AL, Bloem BR. Age-dependent variations in the directional sensitivity of balance corrections and compensatory arm movements in man. J Physiol 2002;542:643–63. https://doi.org/10.1113/jphysiol.2001.015644.

[244] Guillory JJ, Blankson AN. Using recently acquired knowledge to self-assess understanding in the classroom. Scholarsh Teach Learn Psychol 2017;3:77–89. https://doi.org/10.1037/stl0000079.

[245] Srikumaran D, Tian J, Ramulu P, Boland M V., Woreta F, Wang KM, et al. Ability of ophthalmology residents to self-assess their performance through established milestones. J Surg Educ 2019;76:1076–87. https://doi.org/10.1016/j.jsurg.2018.12.004.

[246] Hastie P, Brock S, Mowling C, Eiler K. Third grade students' self-assessment of basketball dribbling tasks. J Phys Educ Sport 2012;12:427–30. https://doi.org/10.7752/jpes.2012.04063.

[247] Klatt BN, Carender WJ, Lin C, Alsubaie S, Kinnaird C, Sienko KH, et al. A conceptual framework for the progression of balance exercises in persons with balance and vestibular disorders. Physiol Behav 2015;2:1044.

[248] Schütte KH, Aeles J, Op T, Beéck D, Zwaard BC Van Der, Venter R, et al. Surface effects on dynamic stability and loading during outdoor running using wireless trunk accelerometry. Gait Posture 2016;48:220–5. https://doi.org/10.1016/j.gaitpost.2016.05.017.

[249] Kanko RM, Laende EK, Davis EM, Selbie WS, Deluzio KJ. Concurrent assessment of gait kinematics using marker-based and markerless motion capture. J Biomech 2021;127:110665. https://doi.org/10.1016/j.jbiomech.2021.110665.

[250] Needham L, Evans M, Wade L, Cosker DP, McGuigan MP, Bilzon JL, et al. The development and evaluation of a fully automated markerless motion capture workflow. J Biomech 2022;144:111338. https://doi.org/10.1016/j.jbiomech.2022.111338.

[251] Kanko RM, Laende E, Selbie WS, Deluzio KJ. Inter-session repeatability of markerless motion capture gait kinematics. J Biomech 2021;121:110422. https://doi.org/10.1016/j.jbiomech.2021.110422.

[252] Sheerin KR, Reid D, Besier TF. The measurement of tibial acceleration in runners—A review of the factors that can affect tibial acceleration during running and evidence-based guidelines for its use. Gait Posture 2019;67:12–24. https://doi.org/10.1016/j.gaitpost.2018.09.017.

[253] Moore IS, Willy RW. Use of wearables: tracking and retraining in endurance runners. Curr Sports Med Rep 2019;18:437–44. https://doi.org/10.1249/JSR.0000000000000667.

[254] Gallow A, Heiderscheit B. Clinical aspects of running gait analysis. In: Miller TL, editor. Endur. Sport. Med., Switzerland: Springer; 216AD, p. 201–14.

[255] Weygers I, Kok M, Konings M, Hallez H, De Vroey H, Claeys K. Inertial sensor-based lower limb joint kinematics: A methodological systematic review. Sensors 2020;20:673. https://doi.org/10.3390/s20030673.

[256] Xiang L, Wang A, Gu Y, Zhao L, Shim V, Fernandez J. Recent machine learning progress in lower limb running biomechanics with wearable technology: A systematic review. Front Neurorobot 2022;16:913052. https://doi.org/10.3389/fnbot.2022.913052.

[257] Ahmadi A, Destelle F, Unzueta L, Monaghan DS, Linaza MT, Moran K, et al. 3D Human

Gait Reconstruction and Monitoring Using Body-Worn Inertial Sensors and Kinematic Modeling. IEEE Sens J 2016;16:8823–31. https://doi.org/10.1109/JSEN.2016.2593011.

[258] Nüesch C, Roos E, Pagenstert G, Mündermann A. Measuring joint kinematics of treadmill walking and running: Comparison between an inertial sensor based system and a camera-based system. J Biomech 2017;57:32–8. https://doi.org/10.1016/j.jbiomech.2017.03.015.

[259] Al-Amri M, Nicholas K, Button K, Sparkes V, Sheeran L, Davies JL. Inertial measurement units for clinical movement analysis: Reliability and concurrent validity. Sensors 2018;18:719. https://doi.org/10.3390/s18030719.

[260] Zhang JT, Novak AC, Brouwer B, Li Q. Concurrent validation of Xsens MVN measurement of lower limb joint angular kinematics. Physiol Meas 2013;34. https://doi.org/10.1088/0967-3334/34/8/N63.

[261] Wouda FJ, Giuberti M, Bellusci G, Maartens E, Reenalda J, van Beijnum BJF, et al. Estimation of vertical ground reaction forces and sagittal knee kinematics during running using three inertial sensors. Front Physiol 2018;9:218. https://doi.org/10.3389/fphys.2018.00218.

[262] Dorschky E, Nitschke M, Seifer AK, van den Bogert AJ, Eskofier BM. Estimation of gait kinematics and kinetics from inertial sensor data using optimal control of musculoskeletal models. J Biomech 2019;95:109278. https://doi.org/10.1016/j.jbiomech.2019.07.022.

[263] Slade P, Habib A, Hicks JL, Delp SL. An open-source and wearable system for measuring 3D human motion in real-time. IEEE Trans Biomed Eng 2022;69:678–88. https://doi.org/10.1109/TBME.2021.3103201.

[264] Bennett CL, Odom C, Ben-Asher M. Knee angle estimation based on imu data and artificial neural networks. Proc. - 29th South. Biomed. Eng. Conf. SBEC 2013, IEEE; 2013, p. 111–2. https://doi.org/10.1109/SBEC.2013.64.

[265] Gholami M, Napier C, Menon C. Estimating lower extremity running gait kinematics with a single accelerometer: A deep learning approach. Sensors 2020;20:2939. https://doi.org/10.3390/s20102939.

[266] Hernandez V, Dadkhah D, Babakeshizadeh V, Kulić D. Lower body kinematics estimation from wearable sensors for walking and running: A deep learning approach. Gait Posture 2021;83:185–93. https://doi.org/10.1016/j.gaitpost.2020.10.026.

[267] Cooper G, Sheret I, McMillian L, Siliverdis K, Sha N, Hodgins D, et al. Inertial sensor-based knee flexion/extension angle estimation. J Biomech 2009;42:2678–85. https://doi.org/10.1016/j.jbiomech.2009.08.004.

[268] Kim BH, Hong SH, Oh IW, Lee YW, Kee IH, Lee SY. Measurement of ankle joint movements using IMUs during running. Sensors 2021;21:4240. https://doi.org/10.3390/s21124240.

[269] Dorschky E, Nitschke M, Martindale CF, van den Bogert AJ, Koelewijn AD, Eskofier BM. CNN-based estimation of sagittal plane walking and running biomechanics from measured and simulated inertial sensor data. Front Bioeng Biotechnol 2020;8:604. https://doi.org/10.3389/fbioe.2020.00604.

[270] Potter M V. Advancing human lower-limb kinematic estimation using inertial measurement units. University of Michigan, 2021.

[271] Joukov V, Bonnet V, Karg M, Venture G, Kulić D. Rhythmic extended Kalman filter for gait rehabilitation motion estimation and segmentation. IEEE Trans Neural Syst Rehabil Eng 2018;26:407–18. https://doi.org/10.1109/TNSRE.2017.2659730.

[272] Poitras I, Dupuis F, Bielmann M, Campeau-Lecours A, Mercier C, Bouyer LJ, et al.

Validity and reliability ofwearable sensors for joint angle estimation: A systematic review. Sensors 2019;19:1555. https://doi.org/10.3390/s19071555.

[273] Fukuchi RK, Fukuchi CA, Duarte M. A public dataset of running biomechanics and the effects of running speed on lower extremity kinematics and kinetics. PeerJ 2017;2017:3298. https://doi.org/10.7717/peerj.3298.

[274] Hoitz F, Mohr M, Asmussen M, Lam WK, Nigg S, Nigg B. The effects of systematically altered footwear features on biomechanics, injury, performance, and preference in runners of different skill level: a systematic review. Footwear Sci 2020;12:193–215. https://doi.org/10.1080/19424280.2020.1773936.

[275] Kadaba MP, Ramakrishnan HK, Wootten ME. Measurement of lower extremity kinematics during level walking. J Orthop Res 1990;8:383–92. https://doi.org/10.1007/978-1-4471-5451-8_100.

[276] Mitschke C, Zaumseil F, Milani TL. The influence of inertial sensor sampling frequency on the accuracy of measurement parameters in rearfoot running. Comput Methods Biomech Biomed Engin 2017;20:1502–11. https://doi.org/10.1080/10255842.2017.1382482.

[277] Ancillao A, Tedesco S, Barton J, O'flynn B. Indirect measurement of ground reaction forces and moments by means of wearable inertial sensors: A systematic review. Sensors 2018;18:2564. https://doi.org/10.3390/s18082564.

[278] Tavares JE. Can changing running shoes immediately reduce the risk of tibial stress fractures? Baylor University, 2018.

[279] Drewelow GA. Conservative intervention through changing shoe type to reduce injury risk factors in walking and running. Baylor University, 2019.

[280] Schaefbauer A. The effect of good form running gait retraining on lower extremity kinematics and ground reaction forces. Grand Valley State University, 2017.

[281] Dever D. Interactive effects of load carriage magnitude and marching velocity on kinetic, kinematic, and spatiotemporal gait characteristics in recruit-aged, physically active females. University of Pittsburgh, 2016.

[282] Murphy SP. The influence of asymmetry on the metabolic cost of locomotion. University of Northern Colorado, 2019.

[283] Wiggins C. Rearfoot eversion pilot study. Baylor University, 2020.

[284] Kessler SE, Rainbow MJ, Lichtwark GA, Cresswell AG, D'andrea SE, Konow N, et al. A direct comparison of biplanar videoradiography and optical motion capture for foot and ankle kinematics. Front Bioeng Biotechnol 2019;7:199. https://doi.org/10.3389/fbioe.2019.00199.

[285] Kristianslund E, Krosshaug T, Van den Bogert AJ. Effect of low pass filtering on joint moments from inverse dynamics: Implications for injury prevention. J Biomech 2012;45:666–71. https://doi.org/10.1016/j.jbiomech.2011.12.011.

[286] Wu G, Siegler S, Allard P, Kirtley C, Leardini A, Rosenbaum D, et al. ISB recommendation on definitions of joint coordinate system of various joints for the reporting of human joint motion—part I: ankle, hip, and spine. J Biomech 2002;35:543–8. https://doi.org/10.1300/J237v07n01_02.

[287] Cockcroft J, Louw Q, Baker R. Proximal placement of lateral thigh skin markers reduces soft tissue artefact during normal gait using the Conventional Gait Model. Comput Methods Biomech Biomed Engin 2016;19:1497–504. https://doi.org/10.1080/10255842.2016.1157865.

[288] Hara R, McGinley J, Briggs C, Baker R, Sangeux M. Predicting the location of the hip joint centres, impact of age group and sex. Sci Rep 2016;6:37707. https://doi.org/10.1038/srep37707.

[289] Skog I, Peter H, Rantakokko J, Nilsson J. Zero-velocity detection — an algorithm evaluation. IEEE Trans Biomed Eng 2010;57:2657–66. https://doi.org/10.1109/TBME.2010.2060723.

[290] Zrenner M, Gradl S, Jensen U, Ullrich M, Eskofier BM. Comparison of different algorithms for calculating velocity and stride length in running using inertial measurement units. Sensors 2018;18:4194. https://doi.org/10.3390/s18124194.

[291] Lora-Millan JS, Hidalgo AF, Rocon E. An IMUs-based extended Kalman filter to estimate gait lower limb sagittal kinematics for the control of wearable robotic devices. IEEE Access 2021;9:144550–4. https://doi.org/10.1109/access.2021.3122160.

[292] Berner K, Cockcroft J, Morris LD, Louw Q. Concurrent validity and within-session reliability of gait kinematics measured using an inertial motion capture system with repeated calibration. J Bodyw Mov Ther 2020;24:251–60. https://doi.org/10.1016/j.jbmt.2020.06.008.

[293] Fleisig GS, Slowik JS, Wassom D, Yanagita Y, Bishop J, Diffendaffer A. Comparison of marker-less and marker-based motion capture for baseball pitching kinematics. Sport Biomech 2022. https://doi.org/10.1080/14763141.2022.2076608.

[294] Tang H, Pan J, Munkasy B, Duffy K, Li L. Comparison of lower extremity joint moment and power estimated by markerless and marker-based systems during treadmill running. Bioengineering 2022;9:574. https://doi.org/10.3390/bioengineering9100574.

[295] Mcgrath T, Stirling L. Body-worn IMU-based human hip and knee kinematics estimation during treadmill walking. Sensors 2022;22:2544. https://doi.org/10.3390/s22072544.

[296] Dugan SA, Bhat KP. Biomechanics and analysis of running gait. Phys Med Rehabil Clin N Am 2005;16:603–21. https://doi.org/10.1016/j.pmr.2005.02.007.

[297] Christopher SM, McCullough J, Snodgrass SJ, Cook C. Do alterations in muscle strength, flexibility, range of motion, and alignment predict lower extremity injury in runners: a systematic review. Arch Physiother 2019;9:2. https://doi.org/10.1186/s40945-019-0054-7.

[298] Newman P, Witchalls J, Waddington G, Adams R. Risk factors associated with medial tibial stress syndrome in runners: a systematic review and meta-analysis. Open Access J Sport Med 2013:229. https://doi.org/10.2147/oajsm.s39331.

[299] Almeida MO, Davis IS, Lopes AD. Biomechanical differences of foot-strike patterns during running: A systematic review with meta-analysis. J Orthop Sports Phys Ther 2015;45:738–55. https://doi.org/10.2519/jospt.2015.6019.

[300] Franz JR, Paylo KW, Dicharry J, Riley PO, Kerrigan DC. Changes in the coordination of hip and pelvis kinematics with mode of locomotion. Gait Posture 2009;29:494–8. https://doi.org/10.1016/j.gaitpost.2008.11.011.

[301] Mentiplay BF, Kemp JL, Crossley KM, Scholes MJ, Coburn SL, Jones DM, et al. Relationship between hip muscle strength and hip biomechanics during running in people with femoroacetabular impingement syndrome. Clin Biomech 2022;92:105587. https://doi.org/10.1016/j.clinbiomech.2022.105587.

[302] Jacobsen JS, Nielsen DB, Sorensen H, Soballe K, Mechlenburg I. Changes in walking and running in patients with hip dysplasia. Acta Orthop 2013;84:265–70. https://doi.org/10.3109/17453674.2013.792030.

[303] Edwards WB, Derrick TR, Hamill J. Musculoskeletal attenuation of impact shock in

response to knee angle manipulation. J Appl Biomech 2012;28:502–10. https://doi.org/10.1123/jab.28.5.502.

[304] Xu Y, Yuan P, Wang R, Wang D, Liu J, Zhou H. Effects of foot strike techniques on running biomechanics: A systematic review and meta-analysis. Sports Health 2021;13:71–7. https://doi.org/10.1177/1941738120934715.

[305] Reinschmidt C, Van Den Bogert AJ, Murphy N, Lundberg A, Nigg BM. Tibiocalcaneal motion during running, measured with external and bone markers. Clin Biomech 1997;12:8–16. https://doi.org/10.1016/S0268-0033(96)00046-0.

[306] Reinschmidt C, Van Den Bogert AJ, Nigg BM, Lundberg A, Murphy N. Effect of skin movement on the analysis of skeletal knee joint motion during running. J Biomech 1997;30:729–32. https://doi.org/10.1016/S0021-9290(97)00001-8.

[307] Barré A, Jolles BM, Theumann N, Aminian K. Soft tissue artifact distribution on lower limbs during treadmill gait: Influence of skin markers' location on cluster design. J Biomech 2015;48:1965–71. https://doi.org/10.1016/j.jbiomech.2015.04.007.

[308] Leardini A, Chiari A, Della Croce U, Cappozzo A. Human movement analysis using stereophotogrammetry Part 3. Soft tissue artifact assessment and compensation. Gait Posture 2005;21:212–25. https://doi.org/10.1016/j.gaitpost.2004.05.002.

[309] Cappozzo A, Cappello A, Croce UD, Pensalfini F. Surface-marker cluster design criteria for 3-d bone movement reconstruction. IEEE Trans Biomed Eng 1997;44:1165–74. https://doi.org/10.1109/10.649988.

[310] McGinley JL, Baker R, Wolfe R, Morris ME. The reliability of three-dimensional kinematic gait measurements: A systematic review. Gait Posture 2009;29:360–9. https://doi.org/10.1016/j.gaitpost.2008.09.003.

[311] Okahisa T, Matsuura T, Tomonari K, Komatsu K, Yokoyama K, Iwase J, et al. Between-day reliability and minimum detectable change of the Conventional Gait Model 2 and Plug-in Gait Model during running. Gait Posture 2023;100:171–8. https://doi.org/10.1016/j.gaitpost.2022.12.006.

[312] Meldrum D, Shouldice C, Conroy R, Jones K, Forward M. Test-retest reliability of three dimensional gait analysis: Including a novel approach to visualising agreement of gait cycle waveforms with Bland and Altman plots. Gait Posture 2014;39:265–71. https://doi.org/10.1016/j.gaitpost.2013.07.130.

[313] Gorton GE, Hebert DA, Gannotti ME. Assessment of the kinematic variability among 12 motion analysis laboratories. Gait Posture 2009;29:398–402. https://doi.org/10.1016/j.gaitpost.2008.10.060.

[314] Leboeuf F, Sangeux M. Wand-mounted lateral markers are less prone to misplacement and soft-tissue artefacts than skin-mounted markers when using the conventional gait model. Gait Posture 2023;100:243–6. https://doi.org/10.1016/j.gaitpost.2022.12.013.

[315] Collins TD, Ghoussayni SN, Ewins DJ, Kent JA. A six degrees-of-freedom marker set for gait analysis: Repeatability and comparison with a modified Helen Hayes set. Gait Posture 2009;30:173–80. https://doi.org/10.1016/j.gaitpost.2009.04.004.

[316] Ferrari A, Benedetti MG, Pavan E, Frigo C, Bettinelli D, Rabuffetti M, et al. Quantitative comparison of five current protocols in gait analysis. Gait Posture 2008;28:207–16. https://doi.org/10.1016/j.gaitpost.2007.11.009.

[317] Wouda FJ, Giuberti M, Bellusci G, Maartens E, Reenalda J, Van Beijnum BJF, et al. On the validity of different motion capture technologies for the analysis of running. Proc. IEEE RAS EMBS Int. Conf. Biomed. Robot. Biomechatronics, The Netherlands: IEEE;

2018, p. 1175–80. https://doi.org/10.1109/BIOROB.2018.8487210.

[318] Song K, Hullfish TJ, Silva RS, Silbernagel KG, Baxter JR. Markerless motion capture estimates of lower extremity kinematics and kinetics are comparable to marker-based across 8 movements. BioRxiv (Preprint) 2023:2023.02.21.526496.

[319] Molina-Molina A, Mercado-Palomino E, Delgado-García G, Millán-Sánchez A, Ureña Espa A, Soto-Hermoso VM. Concurrent validity of lower limb kinematics between markerless and marker-based motion capture systems in gait and running. ISBS Proc. Arch., Cologne: 2017, p. 809–12.

[320] Van Hooren B, Pecasse N, Meijer K, Essers JMN. The accuracy of markerless motion capture combined with computer vision techniques for measuring running kinematics. Scand J Med Sci Sport 2023:966–78. https://doi.org/10.1111/sms.14319.

[321] Kanko RM, Outerleys JB, Laende EK, Silbie WS, Deluzio KJ. Comparison of concurrent and asynchronous running kinematics and kinetics from marker-based motion capture and markerless motion capture under two clothing conditions. BioRxiv (Preprint) 2023:1–35.

[322] Coll I. Validation of markerless motion capture for the assessment of soldier movement patterns under varying body-borne loads. University of Ottawa, 2023.

[323] Smirmaul BPC, Dantas JL, Nakamura FY, Pereira G. The psychobiological model: a new explanation to intensity regulation and (in)tolerance in endurance exercise. Rev Bras Educ Física e Esporte 2013;27:333–40. https://doi.org/10.1590/s1807-55092013005000008.

[324] Barwood MJ, Corbett J, Wagstaff CRD, McVeigh D, Thelwell RC. Improvement of 10-km time-trial cycling with motivational self-talk compared with neutral self-talk. Int J Sports Physiol Perform 2015;10:166–71. https://doi.org/10.1123/ijspp.2014-0059.

[325] Díaz-Ocejo J, Kuitunnen S, Mora-Mérida JA. An intervention to enhance the performance of a 3000 metre steeplechase athlete, using segmentation and self-talk. Rev Psicol Del Deport 2013;22:87–92.

[326] Wolframm IA, Micklewright D. The effect of a mental training program on state anxiety and competitive dressage performance. J Vet Behav Clin Appl Res 2011;6:267–75. https://doi.org/10.1016/j.jveb.2011.03.003.

[327] Zetou E, Vernadakis N, Bebetsos E, Makraki E. The effect of self-talk in learning the volleyball service skill and self-efficacy improvement. J Hum Sport Exerc 2012;7:794–805. https://doi.org/10.4100/jhse.2012.74.07.

[328] Blanchfield AW, Hardy J, De Morree HM, Staiano W, Marcora SM. Talking yourself out of exhaustion: The effects of self-talk on endurance performance. Med Sci Sports Exerc 2014;46:998–1007. https://doi.org/10.1249/MSS.0000000000000184.

[329] Hatzigeorgiadis A, Bartura K, Argiropoulos C, Comoutos N, Galanis E, D. Flouris A. Beat the heat: Effects of a motivational self-talk intervention on endurance performance. J Appl Sport Psychol 2018;30:388–401. https://doi.org/10.1080/10413200.2017.1395930.

[330] Van Raalte JL, Vincent A, Brewer BW. Self-talk: Review and sport-specific model. Psychol Sport Exerc 2016;22:139–48. https://doi.org/10.1016/j.psychsport.2015.08.004.

[331] Brick N, MacIntyre T, Campbell M. Attentional focus in endurance activity: new paradigms and future directions. Int Rev Sport Exerc Psychol 2014;7:106–34. https://doi.org/10.1080/1750984X.2014.885554.

[332] Noakes TD, Myburgh KH, Schall R. Peak treadmill running velocity during the vo2 max test predicts running performance. J Sports Sci 1990;8:35–45. https://doi.org/10.1080/02640419008732129.

[333] Foster C. Vo2max and training indices as determinants of competitive running

performance. J Sports Sci 1983;1:13–22. https://doi.org/10.1080/02640418308729657.

[334] Moore IS. Is there an economical running technique? A review of modifiable biomechanical factors affecting running economy. Sport Med 2016;46:793–807. https://doi.org/10.1007/s40279-016-0474-4.

[335] Barnes KR, Kilding AE. Running economy: measurement, norms, and determining factors. Sport Med - Open 2015;1:8. https://doi.org/10.1186/s40798-015-0007-y.

[336] Delgado TL, Kubera-Shelton E, Robb RR, Hickman R, Wallmann HW, Dufek JS. Effects of foot strike on low back posture, shock attenuation, and comfort in running. Med Sci Sports Exerc 2013;45:490–6. https://doi.org/10.1249/MSS.0b013e3182781b2c.

[337] Masumoto K, Mercer JA. The combined influence of body weight support and running direction on self-selected movement patterns. Hum Mov Sci 2023;88:103065. https://doi.org/10.1016/j.humov.2023.103065.

[338] Soylu Y, Arslan E. Effects of mental fatigue on psychophysiological, cognitive responses, and technical skills in small-sided soccer games in amateur players. Balt J Heal Phys Act 2021;13:43–50. https://doi.org/10.29359/BJHPA.2021.Suppl.2.05.

[339] Casado A, Renfree A, Jaenes-Sánchez JC, Cuadrado-Peñafiel V, Jiménez-Reyes P. Differentiating endurance-and speed-adapted types of elite and world class milers according to biomechanical, pacing and perceptual responses during a sprint interval session. Int J Environ Res Public Health 2021;18:2448. https://doi.org/10.3390/ijerph18052448.

[340] Jebabli N, Khlifi M, Ouerghi N, Boujabli M, Bouassida A, Abderrahman A Ben, et al. Single and combined effects of preferred music and endpoint knowledge on jump performance in basketball players. Sports 2023;11:105. https://doi.org/10.3390/sports11050105.

[341] Wilson PB, Ingraham SJ. Effects of glucose–fructose versus glucose ingestion on stride characteristics during prolonged treadmill running. Sport Biomech 2016;15:270–82. https://doi.org/10.1080/14763141.2016.1159726.

[342] Philippen P, Bakker FC, Oudejans R, Canal-Bruland R, Exercise IN. The Effects of Smiling and Frowning on Perceived Affect. J Sport Behav 2012;35:337–53.

[343] Brick NE, McElhinney MJ, Metcalfe RS. The effects of facial expression and relaxation cues on movement economy, physiological, and perceptual responses during running. Psychol Sport Exerc 2018;34:20–8. https://doi.org/10.1016/j.psychsport.2017.09.009.

[344] McCormick A. Psychologically-informed methods of enhancing endurance performance. University of Kent, 2016.

[345] Lussiana T, Gindre C, Mourot L, Hébert-Losier K. Do subjective assessments of running patterns reflect objective parameters? Eur J Sport Sci 2017;17:847–57. https://doi.org/10.1080/17461391.2017.1325072.

[346] Patoz A, Gindre C, Thouvenot A, Mourot L, Hébert-Losier K, Lussiana T. Duty factor is a viable measure to classify spontaneous running forms. Sports 2019;7:233. https://doi.org/10.3390/sports7110233.

[347] Swann C, Keegan RJ, Piggott D, Crust L. A systematic review of the experience, occurrence, and controllability of flow states in elite sport. Psychol Sport Exerc 2012;13:807–19. https://doi.org/10.1016/j.psychsport.2012.05.006.

[348] Kendzierski D, DeCarlo KJ. Physical Activity Enjoyment Scale: Two validation studies. J Sport Exerc Psychol 1991;13:50–64. https://doi.org/10.1123/jsep.13.1.50.

[349] Potter M V., Ojeda L V., Perkins NC, Cain SM. Effect of imu design on imu-derived

stride metrics for running. Sensors 2019;19:2601. https://doi.org/10.3390/s19112601.

[350] Pacher L, Chatellier C, Vauzelle R, Fradet L. Sensor-to-segment calibration methodologies for lower-body kinematic analysis with inertial sensors: A systematic review. Sensors 2020;20:3322. https://doi.org/10.3390/s20113322.

[351] Bouvier B, Duprey S, Claudon L, Dumas R, Savescu A. Upper limb kinematics using inertial and magnetic sensors: Comparison of sensor-to-segment calibrations. Sensors 2015;15:18813. https://doi.org/10.3390/s150818813.

[352] Kothandapani V. Validation of feeling, belief, and intention to act as three components of attitude and their contribution to prediction of contraceptive behavior. J Pers Soc Psychol 1971;19:321–33. https://doi.org/10.1037/h0031448.

[353] Tavares VD de O, Schuch FB, Tempest G, Parfitt G, Oliveira Neto L, Galvão-Coelho NL, et al. Exercisers' affective and enjoyment responses: A meta-analytic and meta-regression review. Percept Mot Skills 2021;128:2211–36. https://doi.org/10.1177/00315125211024212.

[354] Acevedo EO, Rinehardt KF, Kraemer RR. Perceived exertion and affect at varying intensities of running. Res Q Exerc Sport 1994;65:372–5. https://doi.org/10.1080/02701367.1994.10607643.

[355] Hardy CJ, Rejeski WJ. Not what, but how one feels: The measurement of affect during exercise. J Sport Excercise Psychol 1989;11:304–17. https://doi.org/10.1123/jsep.11.3.304.

[356] Russel J. A circumplex model of affect. J Pers Soc Psychol 1980;39:1161–78. https://doi.org/10.1037/h0077714.

[357] Ekkekakis P, Hartman ME, Ladwig MA. Affective responses to exercise. In: Tenenbaum G, Eklund RC, editors. Handb. Sport Psychol. Fourth Edi, Hoboken, NJ: Wiley; 2020, p. 233–53. https://doi.org/10.1002/9781118270011.

[358] Murrock CJ, Bekhet A, Zauszniewski JA. Psychometric evaluation of the Physical Activity Enjoyment Scale in adults with functional limitations. Issues Ment Health Nurs 2016;37:164–71. https://doi.org/10.3109/01612840.2015.1088904.

[359] Kimiecik JC, Harris AT. What is enjoyment? A conceptual/definitional analysis with implications for sport and exercise psychology. J Sport Exerc Psychol 1996;18:247–63. https://doi.org/10.1123/jsep.18.3.247.

[360] Chen C, Weyland S, Fritsch J, Woll A, Niessner C, Burchartz A, et al. A short version of the physical activity enjoyment scale: Development and psychometric properties. Int J Environ Res Public Health 2021;18:11035. https://doi.org/10.3390/ijerph182111035.

[361] Csikszentmihalyi M. Flow: The psychology of optimal experience 1990:303.

[362] Rheinberg F, Vollmeyer R, Engeser S. Die erfassung des flow-erlebens. Diagnostik von Motiv. und Selstkonzept (Tests und Trends N.F. 2), Göttingen: Hogrefe; 2003, p. 261–79.

[363] Rheinberg F, Vollmeyer R. Flow-erleben in einem computerspiel unter experimentell variierten bedingungen. Z Psychol 2003;4:161–70. https://doi.org/10.1026//0044-3409.211.4.161.

[364] Stoll O, Pithan JM. Running and flow: Does controlled running lead to flow-states? Testing the transient hypofontality theory. In: Harmat L, Ørsted Andersen F, Ullén F, Wright J, Sadlo G, editors. Flow Exp., Cham: Springer; 2016, p. 65–75. https://doi.org/10.1007/978-3-319-28634-1.

[365] Stoll O, Lau A. Flow-erleben beim marathonlauf. Zeitschrift Für Sport 2005;12:75–82. https://doi.org/10.1026/1612-5010.12.3.75.

[366] McGowan CJ, Pyne DB, Thompson KG, Rattray B. Warm-up strategies for sport and exercise: Mechanisms and applications. Sport Med 2015;45:1523–46. https://doi.org/10.1007/s40279-015-0376-x.

[367] Riazati S, Caplan N, Hayes PR. The number of strides required for treadmill running gait analysis is unaffected by either speed or run duration. J Biomech 2019;97:109366. https://doi.org/10.1016/j.jbiomech.2019.109366.

[368] Timme S, Brand R. Affect and exertion during incremental physical exercise: Examining changes using automated facial action analysis and experiential self-report. PLoS One 2020;15:e0228739. https://doi.org/10.1371/journal.pone.0228739.

[369] Ekkekakis P, Hall EE, Petruzzello SJ. The relationship between exercise intensity and affective responses demystified: To crack the 40-year-old nut, replace the 40-year-old nutcracker! Ann Behav Med 2008;35:136–49. https://doi.org/10.1007/s12160-008-9025-z.

[370] Williams DM, Dunsiger S, Jennings EG, Marcus BH. Does affective valence during and immediately following a 10-min walk predict concurrent and future physical activity? Ann Behav Med 2012;44:43–51. https://doi.org/10.1007/s12160-012-9362-9.

[371] Haines M, Broom D, Gillibrand W, Stephenson J. Effects of three low-volume, high-intensity exercise conditions on affective valence. J Sports Sci 2020;38:121–9. https://doi.org/10.1080/02640414.2019.1684779.

[372] Rose EA, Parfitt G. Exercise experience influences affective and motivational outcomes of prescribed and self-selected intensity exercise. Scand J Med Sci Sport 2012;22:265–77. https://doi.org/10.1111/j.1600-0838.2010.01161.x.

[373] Gurchiek RD, Choquette RH, Beynnon BD, Slauterbeck JR, Tourville TW, Toth MJ, et al. Open-Source Remote Gait Analysis: A post-surgery patient monitoring application. Sci Rep 2019;9:17966. https://doi.org/10.1038/s41598-019-54399-1.

[374] Mo S, Chow DHK. Accuracy of three methods in gait event detection during overground running. Gait Posture 2018;59:93–8. https://doi.org/10.1016/j.gaitpost.2017.10.009.

[375] Lussiana T, Patoz A, Gindre C, Mourot L, Hébert-Losier K. The implications of time on the ground on running economy: Less is not always better. J Exp Biol 2019;222:jeb192047. https://doi.org/10.1242/jeb.192047.

[376] Patoz A, Lussiana T, Thouvenot A, Mourot L, Gindre C. Duty factor reflects lower limb kinematics of running. Appl Sci 2020;10:8818. https://doi.org/10.3390/app10248818.

[377] Schütte KH, Sackey S, Venter R, Vanwanseele B. Energy cost of running instability evaluated with wearable trunk accelerometry. J Appl Physiol 2018;124:462–72. https://doi.org/10.1152/japplphysiol.00429.2017.

[378] Clermont CA, Benson LC, Osis ST, Kobsar D, Ferber R. Running patterns for male and female competitive and recreational runners based on accelerometer data. J Sports Sci 2019;37:204–11. https://doi.org/10.1080/02640414.2018.1488518.

[379] Shih Y, Ho CS, Shiang TY. Measuring kinematic changes of the foot using a gyro sensor during intense running. J Sports Sci 2014;32:550–6. https://doi.org/10.1080/02640414.2013.843013.

[380] Needham RA, Naemi R, Chockalingam N. A new coordination pattern classification to assess gait kinematics when utilising a modified vector coding technique. J Biomech 2015;48:3506–11. https://doi.org/10.1016/j.jbiomech.2015.07.023.

[381] Hafer JF, Peacock J, Zernicke RF, Agresta CE. Segment coordination variability differs by years of running experience. Med Sci Sport Exerc 2019;51:1438–43. https://doi.org/10.1249/MSS.0000000000001913.Segment.

[382] Toro IS, Weir G, Amado A, Emmerik R van, Ervilha U, Hamill J. Is coordination variability using vector coding different in overground and treadmill walking and running? Gait Posture 2022;92:413–20. https://doi.org/10.1016/j.gaitpost.2021.12.016.

[383] Team RC. R: A language and environment for statistical computing. R Foundation for Statistical Computing 2023.

[384] Wickham H, François R, Henry L, Müller K, Vaughan D. _dplyr: A grammar of data manipulation_ 2023.

[385] Armstrong RA. When to use the Bonferroni correction. Ophthalmic Physiol Opt 2014;34:502–8. https://doi.org/10.1111/opo.12131.

[386] Kim J, Bang H. Three common misuses of P values. Dent Hypotheses 2016;7:73–80. https://doi.org/10.4103/2155-8213.190481.

[387] Dancey C, Reidy J. Statistics without maths for psychology: using SPSS for windows. London, England: Pearson Education; 2004.

[388] dos Santos Ferreira S, Neto ALB, Follador L, de Abreu Garcia EDS, dos Santos Andrade VF, da Silva SG. Effects of different verbal commands on perceptual, affective, and physiological responses during running. Motriz Rev Educ Fis 2021;27. https://doi.org/10.1590/S1980-65742021006521.

[389] Hutchinson JC, Jones L, Vitti SN, Moore A, Dalton PC, O'Neil BJ. The influence of self-selected music on affect-regulated exercise intensity and remembered pleasure during treadmill running. Sport Exerc Perform Psychol 2018;7:80–92. https://doi.org/10.1037/spy0000115.

[390] Bok D, Rakovac M, Foster C. An examination and critique of subjective methods to determine exercise intensity: The Talk Test, Feeling Scale, and Rating of Perceived Exertion. Sport Med 2022;52:2085–109. https://doi.org/10.1007/s40279-022-01690-3.

[391] Crocker PRE, Bouffard M, Gessaroli ME. Measuring enjoyment in youth sport settings: A confirmatory factor analysis of the Physical Activity Enjoyment Scale. J Sport Exerc Psychol 1995;17:200–5.

[392] Jekauc D, Voelkle M, Wagner MO, Mewes N, Woll A. Reliability, validity, and measurement invariance of the german version of the physical activity enjoyment scale. J Pediatr Psychol 2013;38:104–15. https://doi.org/10.1093/jpepsy/jss088.

[393] Engeser S, Rheinberg F. Flow, performance and moderators of challenge-skill balance. Motiv Emot 2008;32:158–72. https://doi.org/10.1007/s11031-008-9102-4.

[394] Davis S, Fox A, Bonacci J, Davis F. Mechanics, energetics and implementation of grounded running technique: A narrative review. BMJ Open Sport Exerc Med 2020;6:1–7. https://doi.org/10.1136/bmjsem-2020-000963.

[395] Thordarson DB. Running biomechanics. Clin Sports Med 1997;16:239–47. https://doi.org/10.1016/S0278-5919(05)70019-3.

[396] Kuhman D, Melcher D, Paquette MR. Ankle and knee kinetics between strike patterns at common training speeds in competitive male runners. Eur J Sport Sci 2016;16:433–40. https://doi.org/10.1080/17461391.2015.1086818.

[397] Schubert AG, Kempf J, Heiderscheit BC. Influence of stride frequency and length on running mechanics: A systematic review. Sports Health 2014;6:210–7. https://doi.org/10.1177/1941738113508544.

[398] McGregor SJ, Busa MA, Yagie JA, Bollt EM. High resolution MEMS accelerometers to estimate VO2 and compare running mechanics between highly trained inter-collegiate and untrained runners. PLoS One 2009;4:e7355.

https://doi.org/10.1371/journal.pone.0007355.

[399] Schütte KH, Maas EA, Exadaktylos V, Berckmans D, Venter RE, Vanwanseele B. Wireless tri-axial trunk accelerometry detects deviations in dynamic center of mass motion due to running-induced fatigue. PLoS One 2015;10:e0141957. https://doi.org/10.1371/journal.pone.0141957.

[400] Lim J, Hamill J, Busa MA, van Emmerik REA. Changes in coordination and variability during running as a function of head stability demands. Hum Mov Sci 2020;73:102673. https://doi.org/10.1016/j.humov.2020.102673.

[401] Stock H, van Emmerik R, Wilson C, Preatoni E. Applying circular statistics can cause artefacts in the calculation of vector coding variability: A bivariate solution. Gait Posture 2018;65:51–6. https://doi.org/10.1016/j.gaitpost.2018.06.169.

[402] Derrick TR, Caldwell GE, Hamill J. Modeling the stiffness characteristics of the human body while running with various stride lengths. J Appl Biomech 2000;16:36–51. https://doi.org/10.1123/jab.16.1.36.

[403] Derrick TR, Hamill J, Caldwell GE. Energy absorption of impacts during running at various stride lengths. Med Sci Sports Exerc 1998;30:128–35. https://doi.org/10.1097/00005768-199801000-00018.

[404] Mercer JA, Vance J, Hreljac A, Hamill J. Relationship between shock attenuation and stride length during running at different velocities. Eur J Appl Physiol 2002;87:403–8. https://doi.org/10.1007/s00421-002-0646-9.

[405] Mercer JA, Devita P, Derrick TR, Bates BT. Individual effects of stride length and frequency on shock attenuation during running. Med Sci Sports Exerc 2003;35:307–13. https://doi.org/10.1249/01.MSS.0000048837.81430.E7.

[406] Hamill J, Lim J, van Emmerik R. Locomotor coordination, visual perception and head stability during running. Brain Sci 2020;10:174. https://doi.org/10.3390/brainsci10030174.

[407] McGhee DE, Steele JR. Biomechanics of breast support for active women. Exerc Sport Sci Rev 2020;48:99–109. https://doi.org/10.1249/JES.0000000000000221.

[408] McGhee DE, Steele JR. Breast biomechanics: What do we really know? Physiology 2020;35:144–56. https://doi.org/10.1152/physiol.00024.2019.

[409] Hughes GTG, Camomilla V, Vanwanseele B, Harrison AJ, Fong DTP, Bradshaw EJ. Novel technology in sports biomechanics: some words of caution. Sport Biomech 2021. https://doi.org/10.1080/14763141.2020.1869453.

[410] Mabogunje A, Sonalkar N, Leifer L. Design thinking: A new foundational science for engineering. Int J Eng Educ 2016;32:1540–56.

[411] Aranda-Jan CB, Jagtap S, Moultrie J. Towards a framework for holistic contextual design for low-resource settings. Int J Des 2016;10:43–63. https://doi.org/10.17863/CAM.7254.

[412] Bombard Y, Baker GR, Orlando E, Fancott C, Bhatia P, Casalino S, et al. Engaging patients to improve quality of care: A systematic review. Implement Sci 2018;13:98. https://doi.org/10.1186/s13012-018-0784-z.

[413] Clermont CA, Benson LC, Edwards WB, Hettinga BA, Ferber R. New considerations for wearable technology data: Changes in running biomechanics during a marathon. J Appl Biomech 2019;35:401–9. https://doi.org/10.1123/jab.2018-0453.

[414] Perrotin N, Gardan N, Lesprillier A, Le Goff C, Seigneur JM, Abdi E, et al. Biomechanics of trail running performance: Quantification of spatio-temporal parameters by using low cost sensors in ecological conditions. Appl Sci 2021;11:1–14.

https://doi.org/10.3390/app11052093.

[415] Schütte KH, Seerden S, Venter R, Vanwanseele B. Influence of outdoor running fatigue and medial tibial stress syndrome on accelerometer-based loading and stability. Gait Posture 2018;59:222–8. https://doi.org/10.1016/j.gaitpost.2017.10.021.